

# **Synthesis, characterization and *in vitro* analyses of lumefantrine-based pharmacologically active polymer for the treatment of severe malaria**

by

William Morwa Reagile Matshe

A dissertation submitted in partial fulfilment of the requirements for the degree

**Master of Science**

in

**Pharmacology**

in the

**Faculty of Health Sciences**

at the

**University of Pretoria**

**Supervisor**

Prof Duncan A. Cromarty

**Co-supervisor**

Dr Mohammed O. Balogun

(Functional Polymers group, Chemicals cluster, CSIR)

March 2022

## Declaration

I declare that the dissertation, which I hereby submit for the degree MSc (Pharmacology) at the University of Pretoria, is my own work and has not previously been submitted by me for a degree at this or any other tertiary institution.



**Signature:** .....

**Date:** .....22/03/2022.....

## Plagiarism Declaration

I, *William Morwa Reagile Matshe*, student number 12215237, declare that:

1. I understand what plagiarism is and am aware of the University's policy in this regard.
2. I declare that this dissertation is my own original work. Where other people's work has been used (either from a printed source, internet, or any other source), this has been properly acknowledged and referenced in accordance with Departmental requirements.
3. I have not used work previously produced by another student or any other person to hand in as my own.
4. I have not allowed and will not allow anyone to copy my work with the intention of passing it off as his or her own work.



**Signature:** .....

## Ethics

This study was conducted under the guiding ethical principles as stipulated in the Declaration of Helsinki and the amendments thereof. Ethical clearances to conduct the research study were obtained from the University of Pretoria's Research Ethics committee (ref. no.: 202/2019) as well as the Council for Scientific and Industrial's Research Ethics committee (ref. no.: 308/2020).

Approval was also obtained from Masters' committee, Faculty of Health Sciences, University of Pretoria.

## Outputs

Research results obtained from this study have been included into a draft manuscript planned for publication in a peer-reviewed journal.

## Acknowledgements

I would firstly like to give a special and warm-hearted gratitude to my supervisors Prof Duncan Cromarty and Dr Mohammed Balogun, for the opportunity to learn under their mentorship. It has been an exceptionally tough learning period not only within the time frame of the MSc and BSc honours programmes with the Department of Pharmacology (University of Pretoria) but also since joining the CSIR as an intern 2015. I sincerely appreciate you both for taking me up as your student and through the facets of conducting research, which have expanded beyond the laboratory setting.

Conducting the research work would not have been possible without the funding and laboratory resources granted by World Health Organization, Medical Research Council, National Research Foundation and not least the CSIR. Special thanks to my CSIR colleagues, particularly Dr Lesego Tshweu and Dr Sindisiwe Mvango for assisting with the derivation of PEG polymer used in this study.

Thank you to Dr Anjo Theron of the CSIR's Next Generation Health Pharmacology research group for providing training and guidance on parasite cultivation and antiplasmodial testing.

I would also like to thank Dr Ibukun Famuyide of the Onderstepoort Veterinary institute (University of Pretoria) for his assistance in conducting cytotoxicity studies of the conjugates developed in these studies.

Thank you to Dr Joaquin Sanchez of Monash University (Australia) for graciously donating their synthetic polymer which was used in this study.

A very special thanks to THE MAC4 (Abdulmalik, Aliyah, Aisha and Abdulbasit Balogun) for their assistance in drawing the malaria life cycle. My gratitude to all four of you goes beyond the schematic. The Horrible Sciences collection you introduced to me has had an invaluable impact and certainly opened my mind to a great deal of knowledge many take for granted quite often and consistently.

Lastly, my greatest gratitude goes to my family and friends, too many to mention individually but nonetheless your support, well wishes, your prayers and words of encouragement since starting my academic journey, are immeasurably valued.

## Table of Contents

Declaration.....	2
Plagiarism Declaration .....	3
Ethics .....	4
Outputs .....	5
Acknowledgements.....	6
Table of Contents.....	7
List of Figures .....	9
List of Schematics.....	12
List of Tables.....	13
Abbreviations .....	14
Summary.....	17
1. Chapter One: Introduction.....	19
Malaria.....	19
Hypothesis.....	25
Aim .....	26
Objectives.....	26
2. Chapter Two: Chemical synthesis of polymer-lumefantrine conjugates.....	27
Introduction.....	27
Materials and Methods .....	36
Results and Discussion .....	37
Conclusion.....	67
3. Chapter Three: Characterization of polymer-lumefantrine conjugates.....	68
Introduction.....	68
Materials and Methods .....	68
Results and Discussion .....	69

Conclusion.....	76
4. Chapter Four: <i>In vitro</i> biological analyses of polymer-lumefantrine conjugates	77
Introduction.....	77
Materials and Methods .....	79
Results and discussion .....	85
Conclusion.....	91
5. Chapter Five: Final Conclusion.....	92
References.....	94
Appendix.....	100



## List of Figures

Figure 1.1: General categories of the nanomedicine platform. ....	25
Figure 2.1: Schematic illustration of the stereochemical reactivity of ester-activated succinic acid vs succinic anhydride to the secondary alcohol of Lumf.....	32
Figure 2.2: Schematic illustration of the linkage of drugs to (A) mono and (B) multivalent polymers. ....	35
Figure 2.3: Chemical structure of P-N-acryloylmorpholine-stat-p-acrylic acid (PNAM) with the carboxylic acid functional groups shown by green arrow. ....	35
Figure 2.4: The product was purified by A) silica column chromatography. Collected fractions containing Lumf-Suc product were monitored by B) TLC was run using a solvent system of acetone: ethyl acetate at a ratio of 1:1. ....	38
Figure 2.5: Schematic illustration of the interaction of the Lumf-Suc with a silica material. ...	38
Figure 2.6: Free flowing powder of Lumf-Suc.....	39
Figure 2.7: IR spectra of unmodified Lumf and Lumf-Suc purified by precipitation and silica flash chromatography.....	41
Figure 2.8: <sup>1</sup> H-NMR spectra of Lumf and Lumf-Suc both prepared in CDCl <sub>3</sub> . ....	43
Figure 2.9: Radley's ® Carousel 6+ Parallel synthesis unit. ....	45
Figure 2.10: TLC for the chemical synthesis of Lumf-Suc using 3, 2 and 1.5 mol eqv of succinic anhydride. A – All materials spotted; L- lumefantrine. TLC was run using solvent system of ethyl acetate: hexane at a 4:1 ratio. ....	45
Figure 2.11: TLC for the chemical synthesis of a ma-PEG <sub>5000</sub> -Lumf conjugate. A – All materials; R – chemical reaction of ma-PEG <sub>5000</sub> -Lumf synthesis; LS – Lumefantrine-succinic acid (Lumf-Suc); D – dimethylaminopyridine (DMAP). TLC was run using solvent system of ethyl acetate: hexane at 4:1 ratio. ....	47
Figure 2.12: ma-PEG <sub>5000</sub> -Lumf conjugate in phosphate buffer (1.0 M, pH 7.4). ....	48
Figure 2.13: IR spectra for ma-PEG <sub>5000</sub> -Lumf, Lumf-Suc and ma-PEG <sub>5000</sub> .....	49
Figure 2.14: <sup>1</sup> H NMR spectra of ma-PEG <sub>5000</sub> -Lumf and Lumf-Suc prepared in CDCl <sub>3</sub> . Ar-H: proton signals of the aromatic rings of the Lumf drug. ....	51
Figure 2.15: Theoretical calculation of determining the maximum drug loading for ma-PEG <sub>5000</sub> . ....	52
Figure 2.16: A two-step chemical derivation process of dh-PEG <sub>1500</sub> to da-PEG <sub>1500</sub> .....	53
Figure 2.17: IR analysis of chemically derivatized da-PEG <sub>1500</sub> .....	54
Figure 2.18: <sup>1</sup> H-NMR spectra of da-PEG <sub>1500</sub> and dh-PEG <sub>1500</sub> . Polymers were dissolved in CDCl <sub>3</sub> . ....	55
Figure 2.19: TLC for the chemical synthesis of da-PEG <sub>1500</sub> -Lumf conjugate. A – All materials; R – chemical reaction of Lumf conjugation to da-PEG <sub>1500</sub> ; L – lumefantrine; LS – lumefantrine-	

succinate; D – dimethylaminopyridine (DMAP). TLC was run using a solvent system of ethyl acetate: hexane at a ratio of 4:1. .... 57

Figure 2.20: da-PEG<sub>1500</sub>-Lumf conjugate in buffer (pH 7.4). .... 58

Figure 2.21: IR spectra of Lumf-Suc and da-PEG<sub>1500</sub>-Lumf conjugate. .... 60

Figure 2.22: <sup>1</sup>H-NMR spectra of da-PEG<sub>1500</sub>-Lumf and da-PEG<sub>1500</sub> both prepared in D<sub>2</sub>O. .. 61

Figure 2.23: TLC of Lumf conjugation reaction to PNAM. A – All materials; R – chemical reaction of Lumf conjugation to PNAM; L – lumefantrine; D – dimethylaminopyridine (DMAP); H – hydroxybenzotriazole (HoBT). TLC was run using a solvent system of ethyl acetate: hexane at a ratio of 4:1. .... 63

Figure 2.24: Chemical reaction of PNAM and Lumf with the addition of a) No coupling reagents, b) coupling reaction with 24 mol eqv's and c) 2 mol eqv's of Lumf conducted under anhydrous conditions. .... 64

Figure 2.25: IR analysis of PNAM-Lumf, PNAM and Lumf. .... 65

Figure 2.26: <sup>1</sup>H-NMR analysis of PNAM and PNAM-Lumf conjugate prepared in CDCl<sub>3</sub>. .... 66

Figure 3.1: Absorbance spectra of Lumf dissolved in ethyl acetate (25 µg/mL) and measured in a glass cuvette. (1) Absorbance value measured at 335 nm. .... 70

Figure 3.2: Absorbance spectrum of PNAM dissolved in 1.0 M phosphate buffer (1 mg/mL). (1) Absorbance measured at 335 nm. .... 71

Figure 3.3: Absorbance spectra of PNAM-Lumf conjugate dissolved in 1.0 M phosphate buffer. (1) absorbance measured at 335 nm. .... 71

Figure 3.4: UV/Vis analysis of free PNAM. .... 72

Figure 3.5: Total Lumf release from ma-PEG<sub>5000</sub>-Lumf at pH 5.5 (37 °C) conducted at different incubation times extending over a five-day period. .... 74

Figure 3.6: Lumf drug recovered from a small silica column when concentrations of 5 µg/mL to 25 µg/mL Lumf (1.0 mL volume) dissolved in ethyl acetate were passed through the column. n = 3. .... 75

Figure 3.7: Hydrodynamic properties of polymer-Lumf conjugates. .... 76

Figure 4.1: Bright field microscopy image of Giemsa-stained pRBCs. Infected and uninfected RBCs are observed in the yellow and green square grid. The yellow and green grids are used to determine the parasitaemia level. Infected RBCs are counted only within the green grid. 78

Figure 4.2: Plate layout for the antiplasmodial activity screening of ma-PEG<sub>5000</sub>-Lumf compared to lumefantrine (Lumf), chloroquine (CQ, positive control) and ma-PEG<sub>5000</sub>. Infected RBCs (pRBCs) and fresh uninfected RBCs (uRBCs) served as controls. n = 3, ±SD. .... 87

Figure 4.3: Antiplasmodial activity of ma-PEG<sub>5000</sub>-Lumf at concentrations of 1 µg/mL, 5 µg/mL and 10 µg/mL of the Lumf drug from the conjugate. n = 3, ±SD. .... 88

Figure 4.4: Actual haemolysis samples for ma-PEG<sub>5000</sub>-Lumf conjugate after centrifugation step for subsequent haemoglobin analysis. .... 89

Figure 4.5: Haemolytic activity of ma-PEG<sub>5000</sub>-Lumf. .... 90

## List of Schematics

Scheme 1.1: Plasmodium spp. life cycle. Rx general drug targets of the WHO-approved antimalarial drugs.....	21
Scheme 2.1: Conjugation of Lumf to PEG.....	27
Scheme 2.2: Conjugation of Lumf to PNAM.....	28
Scheme 2.3: Activation of succinic acid by carbodiimide chemistry.....	31
Scheme 2.4: Cleavage of PEG-Lumf conjugate linked by ester bonds and its probable degradation products. ....	33
Scheme 2.5: Cleavage of PEG-Lumf conjugate linked by ester and amide bonds and its probable degradation products.....	34
Scheme 2.6: Chemical synthesis of PNAM-Lumf conjugate.....	35
Scheme 2.7: Synthesis of Lumf-Suc using succinic anhydride.....	37
Scheme 2.8: Chemical reactivity of -OH and -NH <sub>2</sub> functional groups as nucleophiles to an activated carboxylic acid. ....	44
Scheme 2.9: Chemical conjugation of Lumf-Suc to ma-PEG <sub>5000</sub> .....	46
Scheme 2.10: Complete conjugation reaction of Lumf-Suc to da-PEG <sub>1500</sub> .....	57

## List of Tables

Table 1.1: WHO-approved antimalarial drug combinations for the treatment of uncomplicated and severe malaria. ....	22
Table 2.1: Commonly used coupling reagents for chemical conjugation and modification... ..	29
Table 3.1: Drug content of polymer-Lumf conjugates determined by UV/Vis analysis at 335 nm.....	70
Table 3.2: UV/Vis absorbance results for PNAM and Lumf. ....	73
Table 4.1: Calculation of the percentage parasitaemia during the cultivation process. ....	78
Table 4.2: Calculation of parasitaemia levels – first cultivation. ....	85
Table 4.3: Calculation of parasitaemia levels – second cultivation. ....	86
Table 4.4: Half maximal cytotoxicity (LC <sub>50</sub> , mg/mL) of ma-PEG <sub>5000</sub> -Lumf and control tested against Vero and Caco-2 cells. ....	91

## Abbreviations

°C	degree Celsius
µm	micrometre
µM	micromolar
ACN	acetonitrile
ACT	artemisinin-based combination therapy
ART	artemether
Caco-2	colorectal adenocarcinoma cell line
CMC	cyclohexyl-(2-morpholinoethyl) carbodiimide
CQ	chloroquine
CSIR	Council for Scientific and Industrial Research
d.nm	diameter in nanometre
Da	Dalton
da-PEG	poly(ethylene glycol) diamine
DCC	dicyclohexyl carbodiimide
DCM	dichloromethane
dH <sub>2</sub> O	deionised water
dh-PEG	poly(ethylene) dihydroxy
DIC	diisopropyl carbodiimide
DIEA	diisopropylethylamine
DLS	dynamic light scattering
DMAP	dimethylaminopyridine
DMF	dimethylformamide
DMSO	dimethyl sulfoxide
DMTMM	N,N-(dimethoxy-triazinyl) methylmorpholinium
EDC	N-ethyl-N-(N-dimethylaminopropyl) carbodiimide
eqv	equivalence
FA	formic acid
FTIR	Fourier-transform infrared spectroscopy
HoBt	hydroxylbenzotriazole

HPLC	high-performance liquid chromatography
IC <sub>50</sub>	half maximal inhibitory concentration
IM	intramuscular
IR	infrared
IV	intravenous
K	Kelvin
kDa	kilodalton
LC <sub>50</sub>	Half maximal cytotoxicity
Lumf	lumefantrine
Lumf-Suc	lumefantrine hemisuccinic acid
ma-PEG	methoxy polyethylene glycol amine
mBar	millibar
MeOH	methanol
mg	milligram
MHz	megahertz
min	minute
mL	millilitres
mmol	millimole
MPa	megapascal
MTT	3-(4,5-dimethylthiazol)-2,5-diphenyl tetrazolium bromide
mV	millivolt
Mw	molecular weight
MWCO	molecular weight cut-off
N/A	not applicable
NaCl	sodium chloride
NaOH	sodium hydroxide
NBT/PES	nitro blue tetrazolium salt/ phenazine ethosulphate
NHS	N-hydroxysuccinimide
nm	nanometre
NMR	nuclear magnetic resonance

PBS	phosphate buffer saline
PDI	polydispersity index
PEG	polyethylene glycol
PEG-Lumf	poly(ethylene glycol) lumefantrine
pH	potential of hydrogen
pLDH	parasite lactate dehydrogenase
PMA	phosphomolybdic acid
PNAM	P-N-acryloylmorpholine-stat-p-acrylic acid
PNAM-Lumf	(P-N-acryloylmorpholine-stat-p-acrylic acid) lumefantrine
PPE	personal protective equipment
PQ	primaquine
RBC	red blood cell
R <sub>f</sub>	retention factor
RPMI	Roswell Park Memorial Institute cell culture medium
SANBS	South African National Blood Services
SD	standard deviations
SOP	standard operating procedure
Sulfo-NHS	sulfo-hydroxysuccinimide
TLC	thin layer chromatography
UV/Vis	ultraviolet-visible
Vero	African green monkey kidney cells
$\rho$	density
WHO	World Health Organization
$\times g$	times gravitational force



## Summary

### Title:

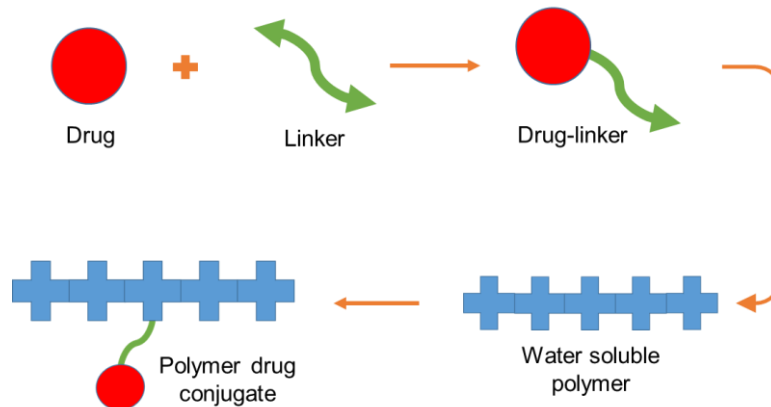
Synthesis, characterization and *in vitro* analyses of lumefantrine-based pharmacologically active polymer for the treatment of severe malaria.

Between 2000 and 2015, new malaria cases dropped by 27% globally. This reduction in the number of reported annual cases could be attributed to the United Nations' Millennium Development Goals (MDGs) and other concerted national and international initiatives that set out to halt the spread of infectious diseases like malaria by the year 2015. Unfortunately, this positive trend has slowed and there are indications of a reversal of the gains made. The last two years of the global COVID-19 have also negatively impacted on the gains made during the MDGs period. At least half of the world's population are still at risk of contracting the disease. To regain the lost ground of 2000-2015, the successor to the MDGs, the Sustainable Development Goals (SDGs), also includes the determination to manage malaria by 2030. Since the adoption of combination therapy in 2001 to treat malaria, treatment outcomes have been highly successful. There is however still a need to improve on the pharmacological properties of the antimalarials for the longevity of the regimen.

Of the current World Health Organization (WHO) approved antimalarial chemotherapy, there are five artemisinin-based drug combinations (ACTs). The artemether/lumefantrine combination has been the most widely administered to treat uncomplicated cases of malaria. The current treatment option for the more complicated cases of malaria requires intravenous (IV) administration of a monotherapy preceding the ACT. This two-part treatment strategy has its disadvantages. The use of a monotherapy, which effectively alleviates the serious clinical symptoms of patients could increase the risk of failure to follow through on the additional full three-day course of ACT. This exposes the artemisinins to a higher risk of drug resistance from the malaria parasites. The partner drug in the ACT, lumefantrine, cannot be used in an IV combination as it is in the oral ACT because of its very low aqueous solubility.

The aim of the project was to improve the aqueous solubility of lumefantrine using nanomedicine delivery systems. In this study, lumefantrine was chemically linked to water-soluble polymers via hydrolysable bonds (Scheme I). This nanomedicine technology of conjugating an active drug molecule to a water-soluble carrier polymer is referred to as polymer therapeutics. While it has been extensively used in the improving cancer chemotherapeutics, the application to parasitic infectious diseases like malaria has been very

limited. There has not been any report in the research literature of conjugation of an antimalarial to a polymer to improve its solubility for the treatment of the disease.



Scheme I

The two polymer types investigated in this project increased the aqueous solubility of the drug by three orders of magnitude. The polymer-lumefantrine conjugate investigated for antiplasmodial activity demonstrated efficacy against the parasite comparable to that of the free drug without introducing any new cytotoxicity. The objectives achieved in this research project pave the way for the potential development of a lumefantrine therapeutic that could be used in combination with artesunate in an IV formulation for the treatment of complicated malaria cases. Some of the findings and data from this project have been contributed to draft manuscripts under preparation for peer-reviewed publications and a conference presentation.

# 1. Chapter One: Introduction

Malaria is an infectious disease often classified into two forms based on the clinical severity of the symptoms: uncomplicated and complicated or severe malaria. Both require different treatment approaches. While the less severe uncomplicated malaria is effectively treated by an oral drug combination only, the treatment of severe malaria consists of two parts, an initial intravenous injection of a single drug, artesunate, followed by an oral drug combination. The initial treatment of severe malaria with the artemisinin derivative artesunate introduces a potential risk of drug resistance against the entire class of artemisinin if patients fail to complete the treatment regimen with the full oral ACT. The most successful ACT to date, the artemether/lumefantrine, has been used for over 30 years and remains the most effective antimalarial chemotherapy particularly on the African continent. This vulnerability is real as, unlike the initial intravenous dosage which is administered at a hospital or other formal health setting, patients are responsible for the oral course of treatment at home. To ensure the continued potency of the artemisinin antimalarials, it would be beneficial to develop a partner drug that could also be administered intravenously. This introductory chapter discusses the disease, and the major current drugs used for chemotherapeutic treatment. The challenges with developing an intravenous combination therapy will also be discussed, followed by the use of the nanotechnology platform as a possible solution. This will be concluded by the aim and objectives of this research project.

## Malaria

Malaria is a highly infectious disease that predominantly occurs in the tropical and sub-tropical regions of the globe. According to the World Health Organization (WHO), over 230 million cases were reported in 2020, with the African continent accounting for over 95% of these.<sup>1</sup> Pregnant women and children up to the age of five years old are the most susceptible groups and at a higher risk for complications of the disease.<sup>2,3</sup>

In humans, the disease is caused by five single-cell parasitic protozoans of the *Plasmodium* genus. These are *P. falciparum*, *P. vivax*, *P. malariae*, *P. ovale* and *P. knowlesi*. *P. falciparum* and *P. vivax* account for majority of infections.

The *Plasmodium* parasite life cycle has several stages shared between two hosts, an infected female mosquito and a human host, each sharing a different segment of the parasite's complex life cycle (Scheme 1.1). The female mosquitoes of the *Anopheles* spp. are the main

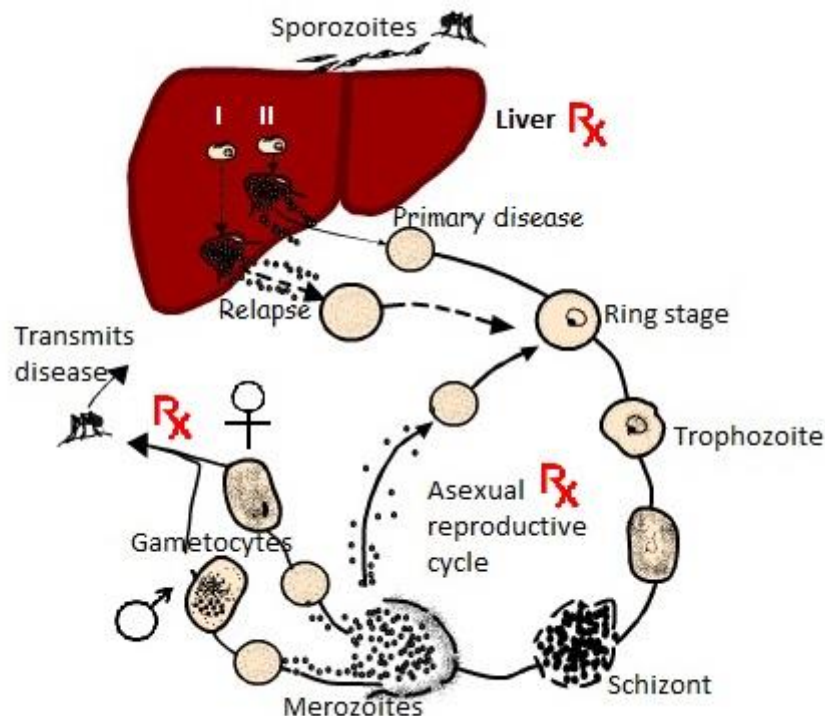
disease-transmitting vectors of malaria. They inoculate a human host with sporozoites when taking a blood meal, which is required for the development of their eggs. The human segment of the parasite's life cycle has three stages that elicit the characteristics of the disease. These three stages, respectively account for the relapse, morbidity, and transmission of the malaria disease.

The pre-erythrocytic or exoerythrocytic liver stage is the first stage in humans. Upon introduction into the human host, the parasites – known at this stage as sporozoites – rapidly move to the liver where they infect hepatocytes. The sporozoites develop into schizonts that divide to form merozoites that are released into the bloodstream, which are then released into the bloodstream to rapidly infect red blood cells (RBCs) and initiate the intraerythrocytic or blood stage. Only the *P. vivax* and *P. ovale* infections have hepatic schizonts that develop into a vegetative form known as hypnozoites. Hypnozoites can stay dormant in the hepatocytes for prolonged periods even after the blood-stage parasites have been cleared and the patient declared “cured”. Spontaneous occurrence or relapse of the disease could occur weeks or even months later.

In the blood stage, the *Plasmodium* parasite goes through 24- to 72-hour developmental cycle.<sup>4</sup> This stage is present in all *Plasmodium* species and is responsible for the characteristic clinical symptoms of the disease that include fever, chills, anaemia, swollen spleen, and muscular aches. These signs and symptoms are commonly associated with parasitaemia as high as 4-5% of the peripheral RBCs. Higher levels of parasitaemia are risk factors for the development of severe malaria and death.<sup>5,6</sup> After several morphological changes and asexual schizogonic replication to form as many as 30 merozoites per RBC, the merozoites emerge by lysis of the host cell. The released merozoites rapidly infect new RBCs, which initiates a new cycle of parasite development. The circadian repetitiveness of the bouts of fever and chills, coincide with the lysis of RBCs and indicates an underlying biochemical or physiological connection. Many of the antimalarial drugs are targeted to and most effective against this asexual stage of the parasite.

The parasite's RBC stage may diverge further, with a fraction of the ring stage parasitaemia, which form after merozoite infection of the RBC, develop to the sexual stage gametocytes. This initiates the third intra-human phase of the malaria disease. Male and female gametocytes are the transmissible forms of the parasite to the mosquito host. This human-mosquito cycle is completed when the gametocytes are taken up by a mosquito during its blood feeding. The *P. vivax* gametocytes can appear a few days post-infection, while the gametocytes for *P. falciparum* infection may take up to two weeks to appear in the blood.<sup>7</sup>

Only a few antimalarial drugs target the gametocytes and inhibit parasite transmission to the mosquito.



Scheme 1.1: *Plasmodium* spp. life cycle. Rx general drug targets of the WHO-approved antimalarial drugs.

Clinically, malaria is classified as uncomplicated or complicated forms. The signs and symptoms of uncomplicated malaria are those generally associated with the disease, i.e., fever, nausea, fatigue, emesis, and muscular pains.<sup>8</sup> They are non-specific, overlapping with other common disease conditions and, although acute and debilitating, are treatable at home. Complicated or severe malaria mainly occurs as a complication of *P. falciparum* infections. The symptoms are noticeably more life-threatening and include cerebral malaria, placental parasite accumulation, pulmonary oedema, hypoglycaemia, severe anaemia, and acidosis. These pathologies can culminate in multiple organ failures and must be treated as a health emergency at a health facility.<sup>9,10</sup>

Development of disease management tools rely on understanding the biology, epidemiology, and clinical presentations of the disease. For malaria, potent antimalarial drugs like chloroquine, primaquine and the artemisinin have been very successful in the treatment of the disease and continue to be used as therapeutics.<sup>11,12</sup> However, the *Plasmodium* parasite

had over time developed resistance to many of the previously effective antimalarial drugs that have become less efficacious in many malaria endemic regions.<sup>13</sup> This has led to a need to develop novel antimalarial drugs and improve on the current treatment regimens to reduce the global prevalence of the disease.<sup>14,15</sup>

### *Current antimalarial chemotherapy*

Combination chemotherapy is currently the WHO's treatment strategy for malaria. The strategy involves the use of at least two antimalarial drugs, often with one being an artemisinin-based compound, with different pharmacokinetics and mode of action.<sup>12,16</sup> There are five WHO-approved artemisinin-based drug combination therapies (ACTs) currently in clinical use for uncomplicated malaria (see Table 1.1).<sup>12</sup> A sixth ACT of artesunate and pyronaridine has recently been approved for clinical use.<sup>17</sup> The combination therapy consists of a very potent, quick-acting artemisinin derivative in combination with a longer-acting antimalarial. The artemisinins typically have a plasma half-life of a few hours while the longer-acting partner drugs have half-lives of the order of days.<sup>18,19</sup> The quick-acting antimalarial rapidly reduces parasitaemia levels with consequent significant symptomatic relief.<sup>20,21</sup> The longer acting agent serves to clear residual or slow maturing parasites that might have been avoided the faster-acting partner drug. This second drug is crucial to the prevention of disease recrudescence and reduces the probability of resistance being developed, especially to the highly effective but short acting artemisinin-based drugs. This complementarity in the pharmacokinetics of the combined drugs has been the key to the antimalarial effectiveness of the ACTs.

Table 1.1: WHO-approved antimalarial drug combinations for the treatment of uncomplicated and severe malaria.

<p><i>WHO-approved ACT's for uncomplicated malaria treatment:</i></p> <ul style="list-style-type: none"> <li>artemether + lumefantrine</li> <li>artesunate + amodiaquine</li> <li>artesunate + mefloquine</li> <li>dihydroartemisinin + piperaquine</li> <li>artesunate + sulfadoxine-pyrimethamine</li> <li><i>(artesunate + pyronaridine)*</i></li> </ul> <p><i>WHO-approved treatment for severe malaria:</i></p> <p>Parenteral administration of artesunate for atleast 24 hours</p> <p>Followed by 3-day ACT course of</p>
---

Artesunate + amodiaquine  
Artemether + lumefantrine or  
Dihydroartemisinin + piperaquine

*\*Recently approved for clinical use.*

The artemether/lumefantrine (Art/Lumf) combination is the most widely distributed and successful ACT used in the treatment of uncomplicated malaria.<sup>22,23</sup> Over 250 million Art/Lumf treatments have been distributed world-wide through collaborative efforts of the WHO, Novartis, Medicines for Malaria Venture as well as a host of private and government organizations and institutions globally.<sup>24</sup> The distribution of the therapy has been mainly to severely affected developing countries, with 75% of the recipients being children. It has contributed to over 95% of successful treatment outcomes.

Although the Art/Lumf combination is an effective combination treatment, it does have its shortcomings. Art has a plasma half-life of about two hours.<sup>18</sup> While Lumf has a plasma half-life of about four days, it also has some properties that erode its optimum therapeutic effectiveness. It is almost totally insoluble in water. At 30.9 ng/mL, Lumf is 10 000 times less soluble than Art (0.457 mg/mL). Its extreme hydrophobicity is demonstrated by a high LogP value that is greater than 8. A fatty-meal intake is recommended to assist in achieving significant plasma concentration of the drug. However, this dietary requirement poses a significant challenge for economically poor communities as obtaining a regular meal to accompany a treatment consisting of twenty-four tablets, taken over three days at 8 hour intervals is hard to achieve.<sup>25</sup>

The lipophilic nature of Lumf also prevents it from being administered parenterally for the treatment of complicated malaria.<sup>26,27</sup> The treatment option for complicated cases of malaria differs from that of uncomplicated malaria (Table 1.1). It is comprised of an initial intravenous (IV) or intramuscular (IM) administration of the water-soluble artemisinin derivative, artesunate, for a minimum of 24 hours which is followed by a full course of the recommended three-day oral ACT.<sup>12,21,28</sup>

The use of a monotherapy for the initial treatment phase of severe malaria raises concerns of drug resistance and disease recrudescence, which can threaten treatment outcomes and indeed the entire artemisinin armoury. Treatment failures associated with artemisinin monotherapy have been reported to be as high as 70%, with repeated dosing showing predictable patterns of disease recrudescence.<sup>29</sup> There is currently no suitable combination partner drug to artesunate for the intravenous treatment of severe malaria, as the oral partner drugs to the artemisinin, such as Lumf, are generally not soluble in water at therapeutically significant levels. It would therefore be a great boost to the treatment of severe malaria to

formulate a water-soluble partner drug to artesunate for a combination therapy to treat the disease.<sup>29</sup> There is therefore a need for a water-soluble partner drug for combination with the artemisinin-based drug.

### *Nanomedicine and its application to malaria chemotherapy*

Nanomedicine, defined as the application of nanotechnology for medicinal purposes, has been used to develop advanced delivery systems for the prevention, diagnosis, and treatment of diseases. Nanomedicines offer technological solutions to improve on the pharmacokinetics of drugs through incorporation into suitable delivery systems.<sup>26,30</sup> The application of the nanomedicine technology has been extensively researched in cancer treatment with attractive therapeutic outcomes.<sup>31,32</sup> Nanomedicines are reported to result in increased aqueous solubility, enhanced systemic circulation with apparent improvement in drug pharmacokinetics, reduced cytotoxicity, controlled drug release kinetics and even targeted drug delivery.<sup>33</sup> This is significant for highly toxic, lipophilic anticancer drugs like camptothecin and paclitaxel, which are among the most researched anticancer drugs to have shown improvement in their physicochemical and pharmacological properties when formulated into nanomedicines.<sup>34,35</sup>

Nanomedicinal drug delivery systems can be broadly classified, based on the way the drug is associated with the carrier, into two categories: encapsulation and polymer-drug conjugation (Figure 1.1). Encapsulation involves the physical entrapment of a drug in the core of a delivery vessel.<sup>36</sup> It has been used to formulate Lumf into nanoparticles. Du Plessis *et. al.* 2015 evaluated their “pheroid” technology on improving the pharmacological potential of Lumf in an *in vitro* and *in vivo* setting.<sup>27</sup> Their formulation showed a marked improvement of up to 3.5 times higher bioavailability compared to the reference drug formulation. The *in vitro* antimalarial efficacy of the pro-pheroid formulation was also shown to be improved by 46%.<sup>27</sup> This illustrated that the pro-pheroid technology effectively eliminated the required fatty-meal intake needed to enhance Lumf’s intestinal absorption. Similarly, Prabhu *et. al.* 2016 showed a significant reduction in the therapeutic dosage needed for therapeutic efficacy.<sup>37</sup> Their nanostructured lipid carriers (NLC) showed enhanced efficacy at only a fraction of the recommended dosage for administered Art/Lumf combination, protecting against disease recrudescence and having no toxic effects to the infected small animals.

Polymer-drug conjugation involves the chemical linkage of a drug to a polymeric carrier.<sup>38</sup> The polymers often have no pharmacological activity but have attractive properties like biocompatibility and water-solubility, and can be chemically modified to link a drug.<sup>39,40</sup> The



chemical conjugation of a drug to a carrier polymer was first proposed by Helmut Ringsdorf in 1975 when he published the concept of a pharmacologically active polymer.<sup>41</sup>

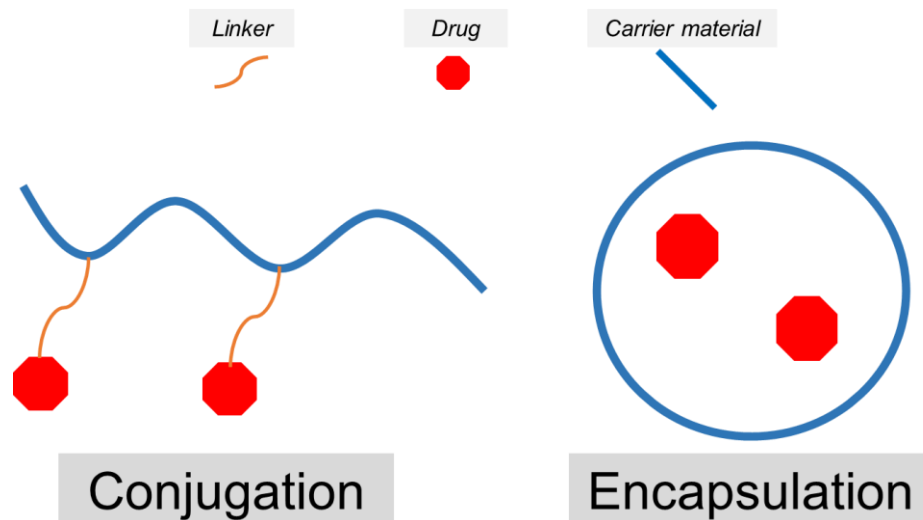


Figure 1.1: General categories of the nanomedicine platform.

Anticancer drugs like paclitaxel, camptothecin, and doxorubin have been conjugated to several water-soluble polymers to increase their aqueous solubilities and reduce the side effects experienced by patients. I and other co-authors published a review article in 2018 on the comparative merits of both nanomedicine technologies and their application to infectious diseases.<sup>42</sup> We argued that the advantages seen in cancer nanomedicines could be exploited for antimalarial drugs to improve malaria treatment in both endemic and non-endemic regions. Primaquine and dihydroartemisinin have been conjugated in combination to polymers by Kumar *et. al.* 2015 for the treatment of malaria.<sup>43</sup> This combination therapy showed promising protection against disease relapse for resistant or dormant stage *P. berghei* parasitaemia.

Recently, a polymer-Lumf conjugate was reported as a polymeric drug that self-aggregated to encapsulate artemether.<sup>44</sup> The Art-polymeric Lumf nanoaggregate however performed very poorly in antiplasmodial assays. Its  $IC_{50}$  was about a thousand times less than that of the free drug combination. There was no other evidence in the literature of other attempts to synthesize a water-soluble form of lumefantrine with antiplasmodial activity.

## Hypothesis

Chemical linkage of lumefantrine to a hydrophilic polymer can significantly increase its solubility without negatively affecting its antiplasmodial activity.

## **Aim**

To synthesize, characterize and investigate the antiplasmodial and cytotoxicity of a water-soluble polymer-lumefantrine conjugate.

## **Objectives**

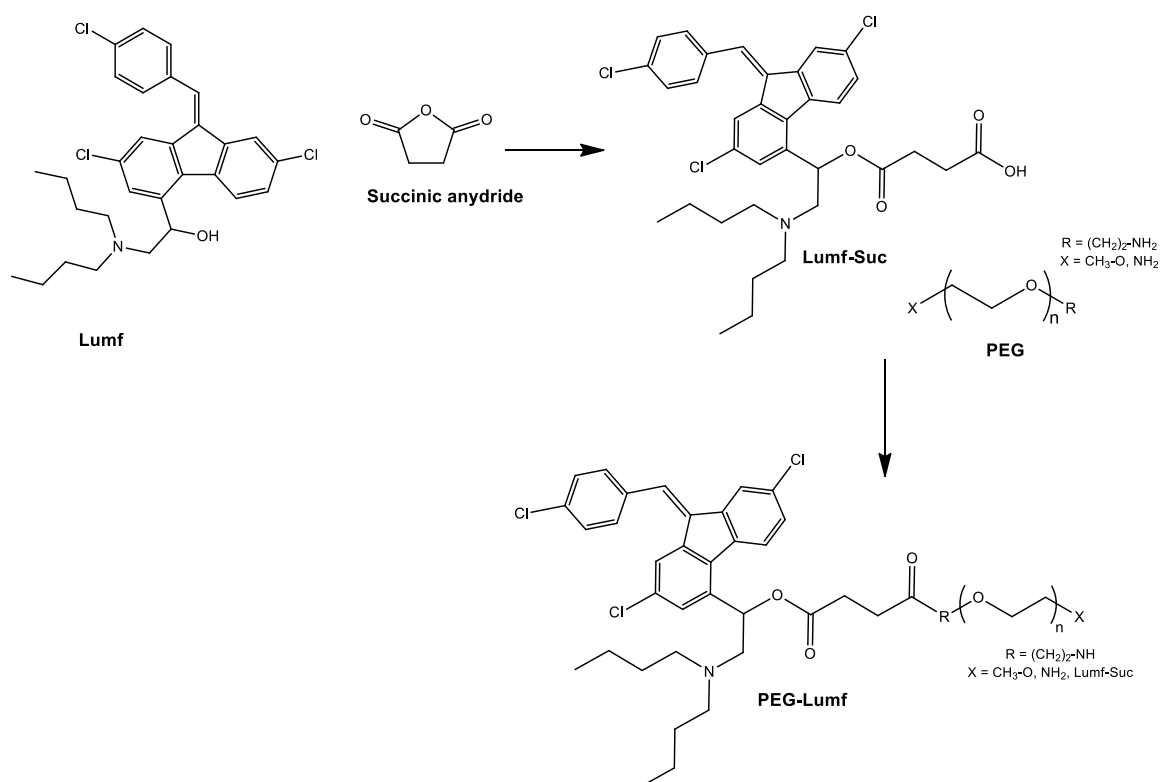
- a. To synthesize polymer-lumefantrine conjugates.
- b. To investigate the physicochemical properties of the polymer-lumefantrine conjugates.
- c. To assess the antiplasmodial and mammalian cytotoxicity of selected polymer-lumefantrine conjugates.

## 2. Chapter Two: Chemical synthesis of polymer-lumefantrine conjugates

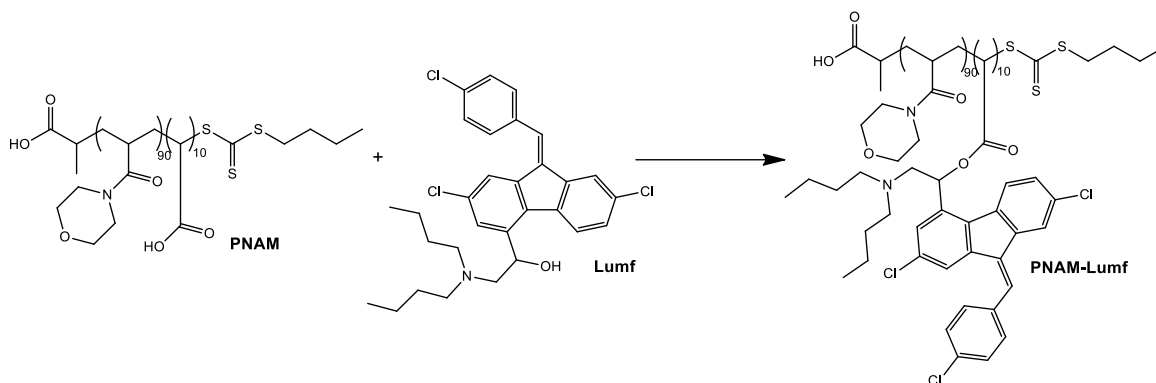
### Introduction

This chapter discusses the chemical conjugation of Lumf to two water-soluble polymers, and their characterization. Chemical modification strategies are mainly guided by the reactive functional groups between two or more chemical entities. Particular attention to these target functional groups and their reactivity are essential to conducting successful conjugation techniques.

The conjugation strategies used to link Lumf to the polymers polyethylene glycol (PEG) and a poly-acryloylmorpholine derivative (PNAM) are sketched out in Scheme 2.1 and Scheme 2.2 below. The following sections of this chapter provide a detailed description of the chemistry.



Scheme 2.1: Conjugation of Lumf to PEG.

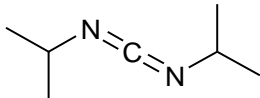
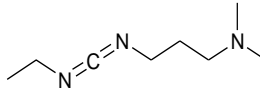
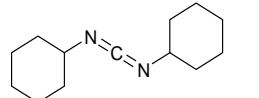
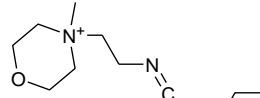
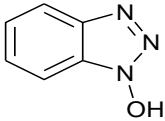
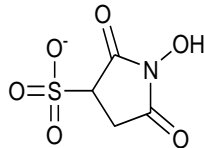
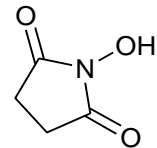
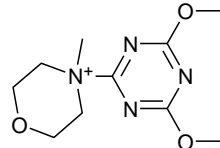


Scheme 2.2: Conjugation of Lumf to PNAM.

### *Chemical derivatization strategies*

The synthesis of antimalarial polymer-drug conjugates was mainly conducted using carbodiimide chemistry, which is commonly applied in peptide synthesis. The carbodiimide coupling reagents are efficient in producing small molecule conjugates of oligo- and macromolecules in both aqueous and organic solvent-based reaction conditions.<sup>45,46,47</sup> They are generally classified into two groups: water-soluble and water-insoluble coupling reagents. The carbodiimide family consists mainly of four coupling reagents: N-ethyl-N-(N-dimethylaminopropyl) carbodiimide hydrochloride (EDC), diisopropyl carbodiimide (DIC), dicyclohexyl carbodiimide (DCC) and 1-cyclohexyl-3-(2-morpholinoethyl) carbodiimide (CMC) (Table 2.1). EDC is the most used water-soluble coupling reagent with an optimal pH coupling efficiency of between 5-7. This, however, makes it highly susceptible to hydrolysis. The water-insoluble DIC reagent is presumed to be more advantageous across the carbodiimide family-members. A liquid at room temperature, unlike the water-insoluble wax-like appearance of DCC, makes for easier dispensing when conducting experiments. This makes it a better coupling reagent specifically for experiments which require anhydrous and inert reaction conditions. Other chemical linkage reagents used in conjugation experiments include hydroxybenzotriazole (HoBt), sulfo-hydroxysuccinimide (sulfo-NHS), N-hydroxysuccinimide (NHS) and (N,N-dimethoxy-triazinyl)methylmorpholinium (DMTMM). Although these reagents are less readily reactive, they are commonly used in combination with the more reactive carbodiimides to improve reaction efficiency and product yield.<sup>48</sup>

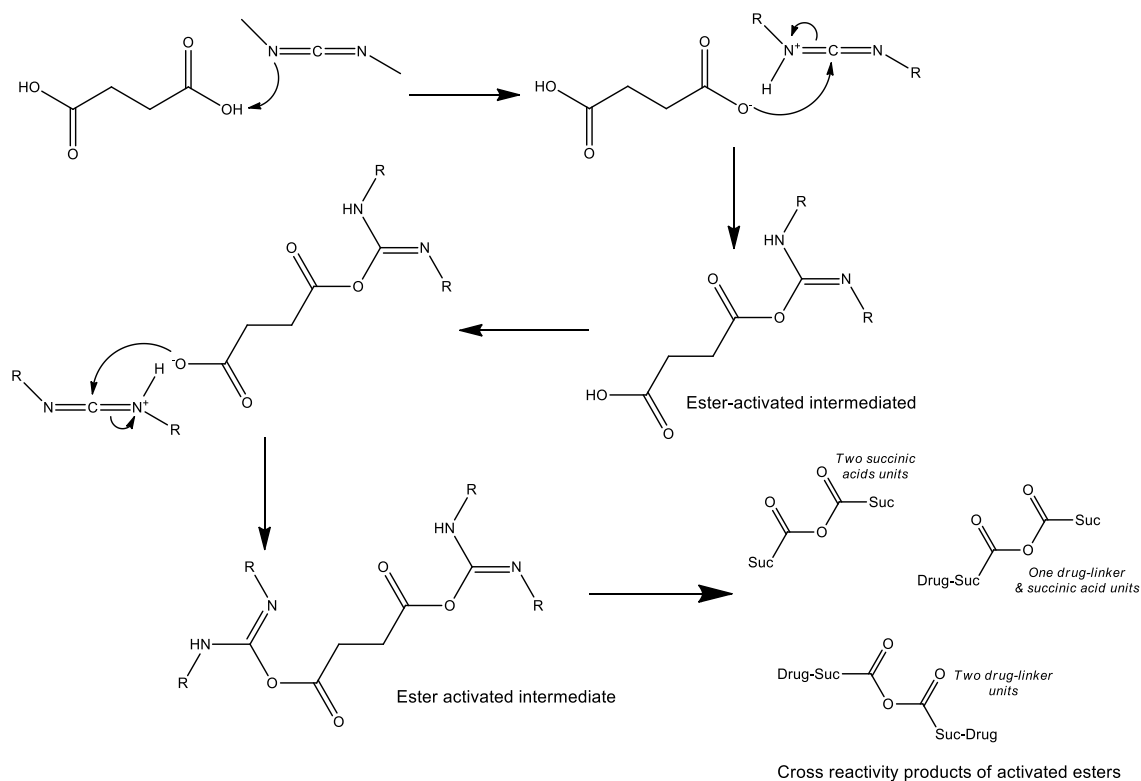
Table 2.1: Commonly used coupling reagents for chemical conjugation and modification.

<b>Carbodiimide coupling reagents</b>			
DIC 	EDC 	DCC 	CMC 
<b>Other coupling reagents</b>			
HoBt 	Sulfo-NHS 	NHS 	DMTMM 
<b>Properties</b>			
	<b>Solubility</b>	<b>By products: Solubility and reactivity</b>	<b>Advantages</b>
<b>DIC</b>	Organic solvent	Diisopropylurea: soluble in organic solvent and chemically non-reactive.	Quick ester-activating reagent
<b>EDC</b>	Aqueous	Isourea-derivative: aqueous soluble and chemically non-reactive.	Quick ester-activating reagent
<b>DCC</b>	Organic solvent	Dicyclohexylisourea: soluble in organic solvent and chemically non-reactive.	Quick ester-activating reagent
<b>CMC</b>	Aqueous	Isourea-derivative: soluble in organic solvent and chemically non-reactive.	Quick ester-activating reagent
<b>HoBt</b>	Organic solvent	Hobt (regenerated): soluble in organic solvent and chemically reactive.	Mainly used to reduce racemization of single-enantiomer chiral compounds. Also used to improve reaction efficiency.
<b>Sulfo-NHS</b>	Soluble in aqueous and organic solvent	Sulfo-NHS (regenerated): soluble in aqueous and organic solvent and chemically reactive.	Used to improve reaction efficiency.
<b>NHS</b>	Soluble in aqueous and organic solvent	NHS (regenerated): soluble in aqueous and organic solvent and chemically reactive.	Used to improve reaction efficiency.
<b>DMTMM</b>	Soluble in aqueous and organic solvent	Methylmorpholinium and hydroxy-dimethoxytriazine: aqueous soluble and chemically non-reactive.	Ester-activation in both aqueous and organic solvents.

### *Succinylation of lumefantrine*

To link Lumf to PEG, functional group complementarity between the polymer and the drug is essential for successful derivatization. Lumf is an aryl amino alcohol compound that has a single hydroxyl (-OH) group as the only functionality available for conjugation. The PEG used in this study present with either terminal -OH or primary amine (-NH<sub>2</sub>) functionalities. (Carboxylated PEG is not as readily available commercially as these two.) The linkage of Lumf-OH to either of these functional groups could result in the formation of an ether or imine linkage bond, which would require the use of complex linkage techniques.<sup>49,50,51</sup> Although possible, this can also lead to polymer-drug conjugates which could be less susceptible to hydrolysis and compromise the release of the drug from the polymer. Cleavage of stable chemical bonds such as ethers would require highly specialized reagents or conditions.<sup>52,53,54</sup> A probable solution to coupling such active chemical entities and ensuring conjugate release is the use of bi-functional linkers that have the following properties; (1) Bi-functional linkers allow for more than one chemical entity to be linked; (2) these chemical bonds can be cleaved under specific physiological conditions to release the original compounds involved, particularly for the release of the therapeutic compound; and (3) it is preferable that the linkers, like the polymers, do not elicit any pharmacological response.

In this work, the chemical derivatization of Lumf was conducted using a homo-bifunctional linker, succinic acid which is a relatively non-toxic molecule that can be readily metabolized by cells. Succinic acid is a natural metabolite present in all aerobic cells that carry out Krebs' cycle.<sup>55</sup> This molecule presents with two carboxylic acid (-COOH) groups which can form an ester or amide bond by linkage of the -OH of the drug. To achieve this would require the activation of one or both sets of -COOH groups which can result in the uncontrollable formation of activated esters leading to various linker and drug dimers (Scheme 2.3).



Scheme 2.3: Activation of succinic acid by carbodiimide chemistry.

The successful and efficient linkage of the acid linker could further be significantly affected by the stereo conformation of Lumf as illustrated in Figure 2.1a. The butyl and aromatic rings of the drug hinders the -OH group's nucleophilic action to the carbodiimide-activated ester of the linker. Succinic anhydride was used for the synthesis of a Lumf hemisuccinate (Lumf-Suc). The use of this chemical reagent offers a significantly simpler reaction route to the synthesis of the hemisuccinate. The chemistry involves the nucleophilic attack of the -OH group on a carbonyl carbon of the anhydride to open the ring into a Lumf-Suc ester (Figure 2.1b).

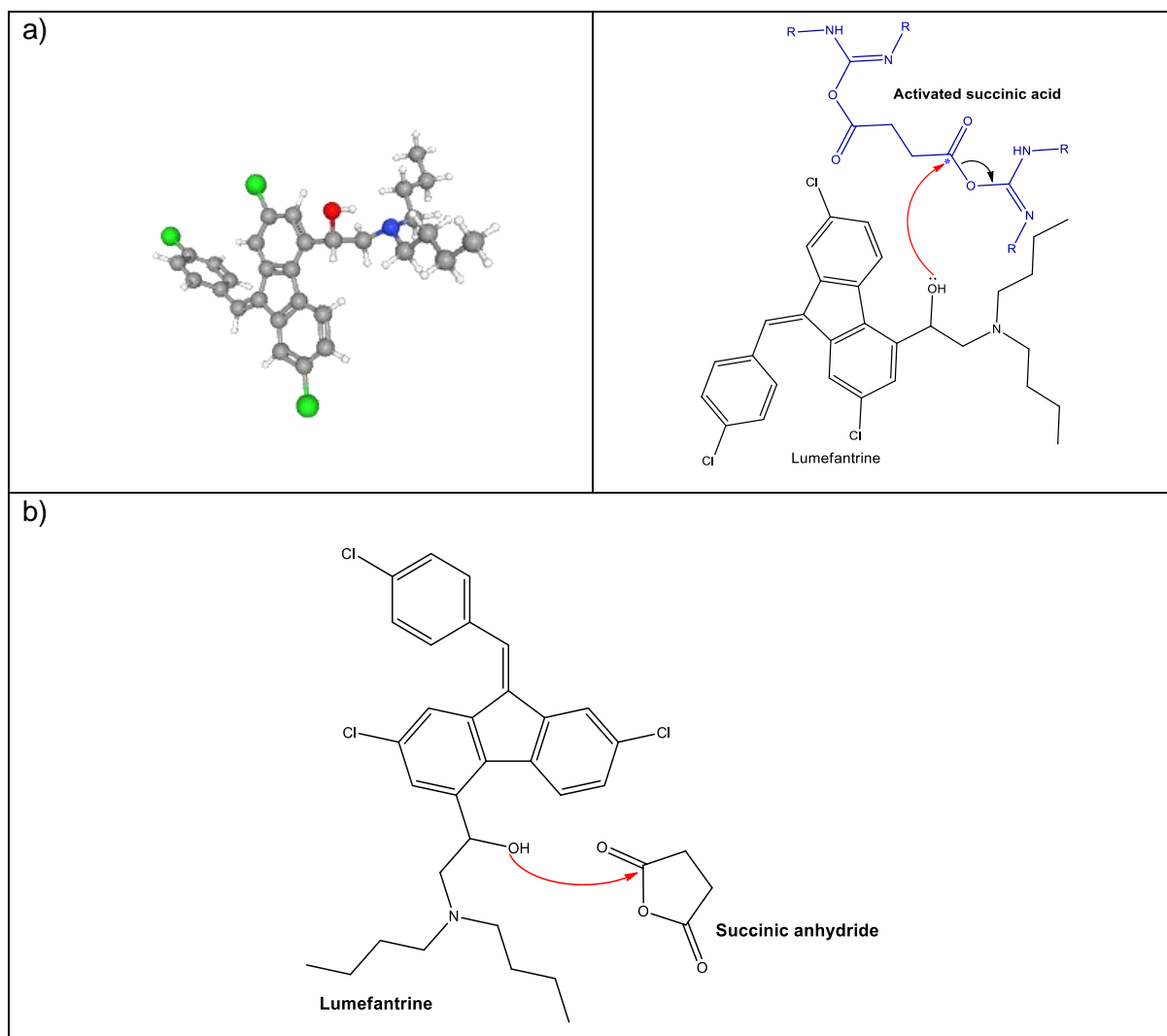


Figure 2.1: Schematic illustration of the stereochemical reactivity of ester-activated succinic acid vs succinic anhydride to the secondary alcohol of Lumf.

The synthesis was conducted in a slightly alkaline solution of Lumf in anhydrous DMF under nitrogen. Succinic anhydride was used in excess molar equivalence.

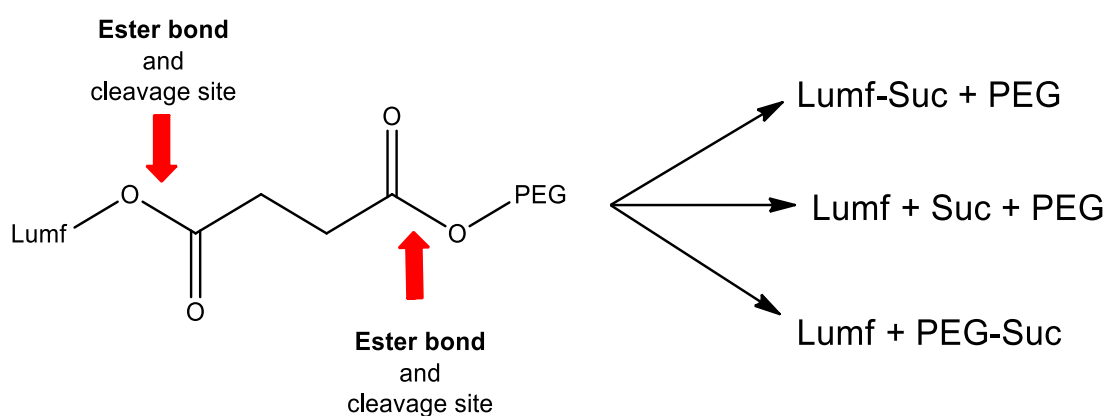
Chemical synthesis of polymer-Lumf conjugates.

#### *PEG-Lumf conjugate*

Water-soluble polymers, PEG and PNAM, were investigated as the carrier materials for succinylated and underived Lumf, respectively. These polymers present with functional groups which are readily susceptible to chemical derivatization. This section will firstly discuss the conjugation of the antimalarial drug Lumf to the ethylene glycol polymer. PEG has at least one

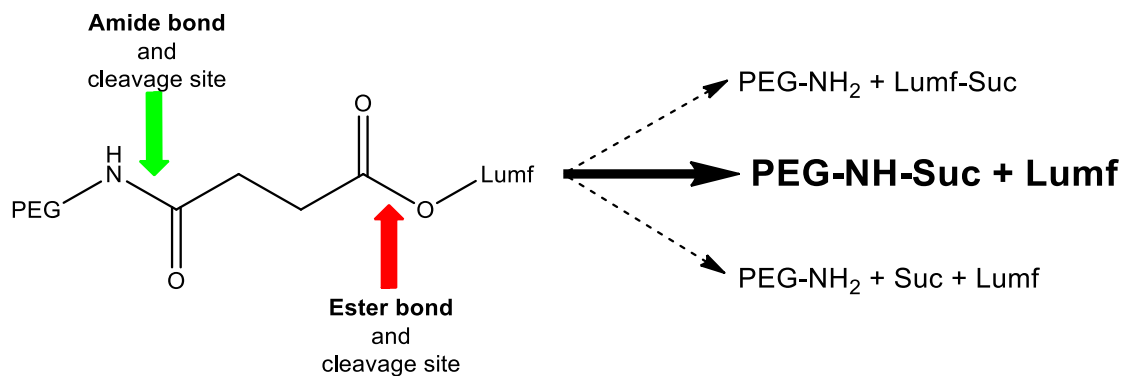


-OH group that can be linked to Lumf-Suc via an ester bond. The resultant PEG-Lumf conjugate would comprise of two ester linkages. This is an important consideration for the release of the drug in a biological system. Ester-bonds are known to be relatively susceptible to cleavage within moist or acid environments as well as cleaved by relevant enzymes *in vivo* compared to linkage bonds such as amides, carbonates and carbimates.<sup>56,57,58</sup> Although ester-bonds are ideal linkage functionalities, having two ester sites between the polymer and the drug via the linker can lead to non-selective cleavage within specific physiological and biological compartments. In the case of PEG-Lumf conjugate, this can give variable distributions of the 'degradation products' of PEG, succinylated PEG (PEG-Suc), Lumf-Suc and Lumf (Scheme 2.4).<sup>50</sup>



Scheme 2.4: Cleavage of PEG-Lumf conjugate linked by ester bonds and its probable degradation products.

The linkage of Lumf to PEG via ester linkages can have an unequal distribution of degradation products and may impact the therapeutic potential of the polymer-drug conjugate. This variable occurrence of products by cleavage of the ester bonds can be mitigated by introducing a less susceptible linkage which could favour the release of only the therapeutic agent (Scheme 2.5).



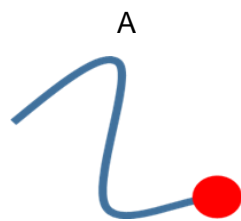
Scheme 2.5: Cleavage of PEG-Lumf conjugate linked by ester and amide bonds and its probable degradation products.

As such, chemical linkage of the Lumf was investigated with amine functionalized PEG (PEG-NH<sub>2</sub>) to enhance the probability of releasing the drug as illustrated in scenario B.

#### *PNAM-Lumf conjugate*

Chemical linkage of drugs to multivalent polymers can significantly enhance drug properties and subsequent therapeutic outcomes.<sup>59</sup> The advantage of using multivalent polymers is that several drug functional groups can be linked to a single polymer unit unlike monovalent polymers which would result in a 1:1 ratio of drug to polymer (Figure 2.2). This can lead to achieving higher drug loading which could in turn reduce the drug dosage required to be administered with comparable if not enhanced efficacies than standard treatment regimens. In this chapter, the chemical linkage of Lumf was conducted to a multivalent polymer, P-N-acryloylmorpholine-stat-p-acrylic acid (PNAM) (Figure 2.3). PNAM consists of an acryloylmorpholine, butyl carbonotrithioate and carboxylic acid functionalities to give a multifaceted polymer chain. The carboxylic acid group is the targeted site to which Lumf can be conjugated (Scheme 2.6). The acryloylmorpholine functionality offers the polymer aqueous solubility, while the butyl chain adds a hydrophobic property to the polymer. The PNAM polymer used in this work consists of on average ten carboxylic acid groups, with the majority of the polymer consisting of the acryloylmorpholine repeating units.

Drug linked to a monovalent carrier.



Multiple drugs linked to a multivalent carrier.

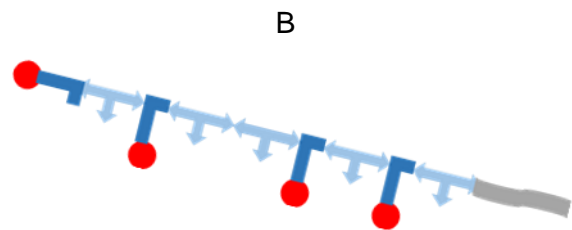


Figure 2.2: Schematic illustration of the linkage of drugs to (A) mono and (B) multivalent polymers.

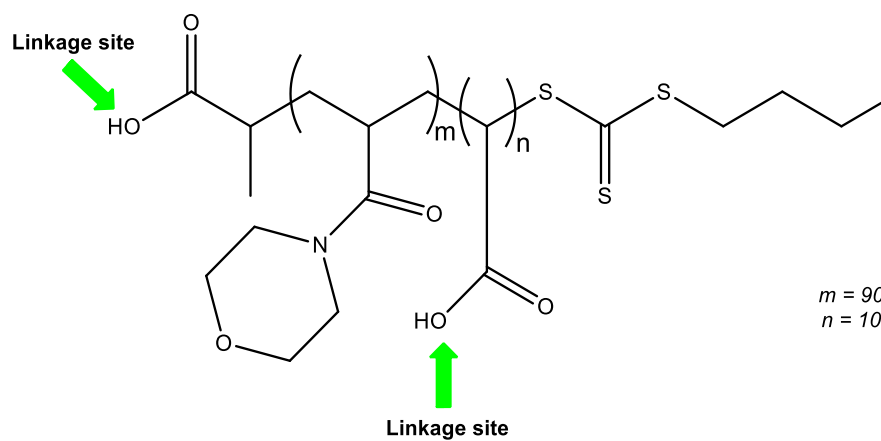
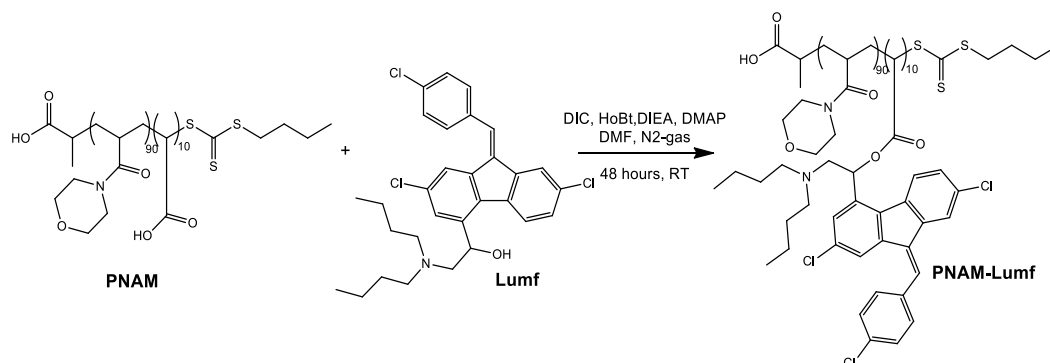


Figure 2.3: Chemical structure of P-N-acryloylmorpholine-stat-p-acrylic acid (PNAM) with the carboxylic acid functional groups shown by green arrow.



Scheme 2.6: Chemical synthesis of PNAM-Lumf conjugate.

## Materials and Methods

Lumefantrine (99%) and succinic anhydride (AR grade) were purchased from DB Fine Chemicals Pty Ltd (South Africa). Dimethylformamide (DMF, anhydrous 99.8%), dimethylaminopyridine (DMAP,  $\geq 99\%$ ), Diisopropylethylamine (DIEA,  $\geq 99\%$ ), diisopropylcarbodiimide (DIC,  $\geq 99\%$ ), hydroxybenzotriazole (HoBt,  $\geq 97\%$ ), polyethylene glycol diamine (PEG-NH<sub>2</sub>,  $\geq 99\%$ ), polyethylene glycol (PEG,  $\geq 99\%$ ), toluene sulfonyl chloride (ACS grade,  $\geq 99\%$ ), dichloromethane (DCM, ACS grade  $\geq 99\%$ ), ethylene diamine ( $\geq 99\%$ ), triethyl amine (TEA,  $\geq 99\%$ ), ethyl acetate (EA; ACS grade  $\geq 99\%$ ), were all purchased from either Sigma-Aldrich Ltd (RSA) or CRD Chemicals Pty Ltd (South Africa). P-N-acryloylmorpholine-stat-p-acrylic acid (PNAM, M<sub>n</sub>=17 kDa; D=1.13) was graciously gifted by collaborators from Monash University (Australia). Vivaspin® ultrapurification membranes (MWCO: 3 kDa) were purchased from Sigma-Aldrich Ltd (RSA). Agilent Captiva® EMR-Lipid 50 mg normal phase silica cartridges were obtained from Agilent Scientific Instruments *Inc.* (USA).

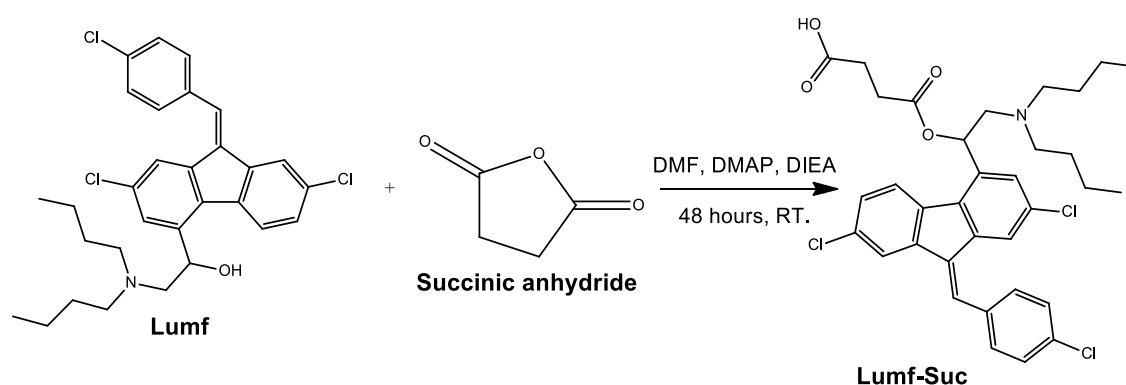
For moisture-sensitive experiments, glassware was dried in an air oven at 120°C for 24 hours before use. Anhydrous solvents were used, and the reactions conducted under N<sub>2</sub> gas where necessary. The <sup>1</sup>H-NMR spectra were acquired on a Bruker 400 MHz NMR instrument (Bruker, Germany) at 295.4 K, with dimethyl sulfoxide (DMSO-d<sub>6</sub>) or deuterium oxide (D<sub>2</sub>O) as solvents. Fourier-Transform Infrared spectroscopy (FTIR) spectra were obtained using Perkin Elmer Spectrum 100 (USA), dry powder anvil accessory conducted within a range of 650-4000 cm<sup>-1</sup> with 4 scans performed for each dry sample at a resolution of 4 cm<sup>-1</sup>, unless stated otherwise.

Flash chromatography was conducted using a Teledyne ISCO® CombiFlash Next Generation 300-Plus system (Teledyne TIC, USA). Separation was achieved using pre-packed 12 g normal phase gel cartridges. Thin layer chromatography (TLC) was conducted on Machery Nagel silica gel aluminium sheets purchased from Separations Pty Ltd. Where applicable, the TLC plates were visualised by spraying evenly with a 10% solution of phosphomolybdic acid (PMA) in ethanol and heating till the spots could be clearly seen using an electric heat gun.

## Results and Discussion

### *Succinylation Lumf*

Conjugation of Lumf to PEG is only possible through a linker with functional groups compatible with the –OH of the drug and the –NH<sub>2</sub> of the polymer. The dicarboxylic acid, succinic acid, is well suited for this. Lumf was reacted with an excess molar equivalence of succinic anhydride over a 24-hour period at room temperature in DMF (Scheme 2.7). In the initial experiments, 3 mol eqv of the anhydride was reacted with Lumf. After the 24-hour reaction period, TLC showed the appearance of a new UV-active spot ( $R_f = 0.76$ ) and disappearance of the Lumf spot ( $R_f = 0.82$ ) (Figure 2.4A). This indicated complete consumption of the Lumf in the reaction process.



Scheme 2.7: Synthesis of Lumf-Suc using succinic anhydride.

The purification of the reaction product was carried out, but with significant challenges to obtain a pure substance. Silica column chromatography was performed with an ethyl acetate: acetone (1:1) solvent system (Figure 2.4B). The maximum pure Lumf-Suc obtained by this method was 90% product yield. This route has a disadvantage of requiring large volumes of the mobile phase organic solvents and the product tended to elute off the silica column relatively slowly because of interactions between the –COOH of the Lumf-Suc and the –OH of the silica (Figure 2.5).

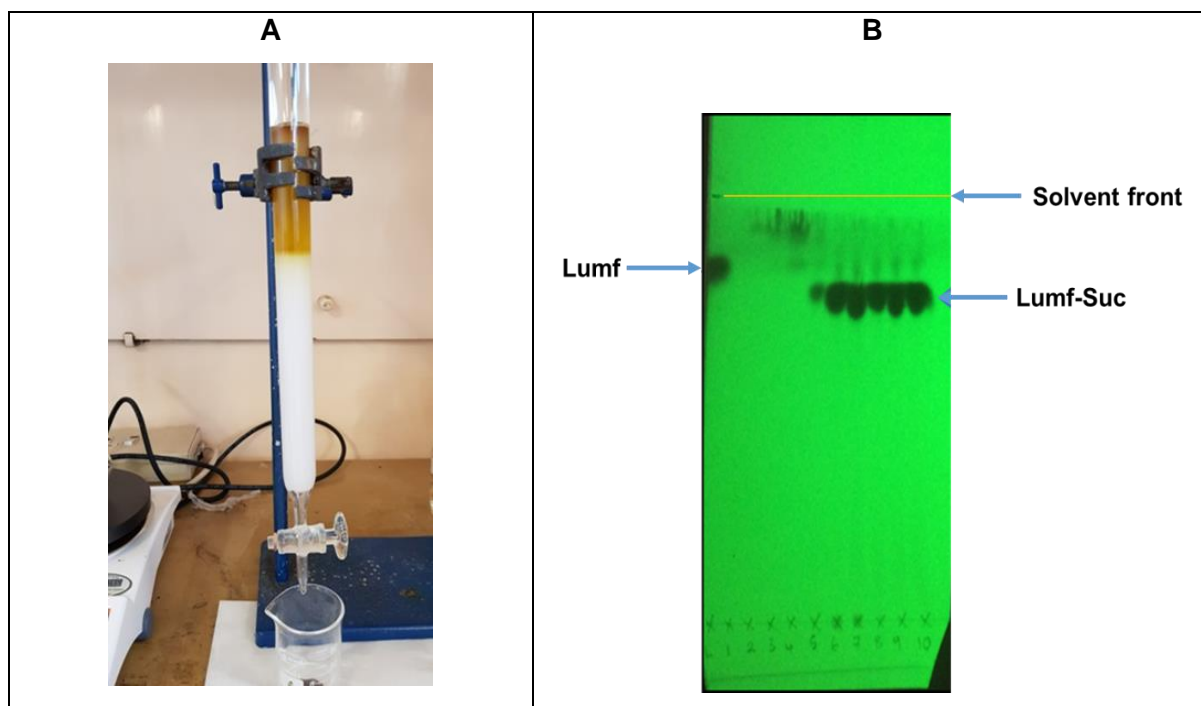


Figure 2.4: The product was purified by A) silica column chromatography. Collected fractions containing Lumf-Suc product were monitored by B) TLC was run using a solvent system of acetone: ethyl acetate at a ratio of 1:1.

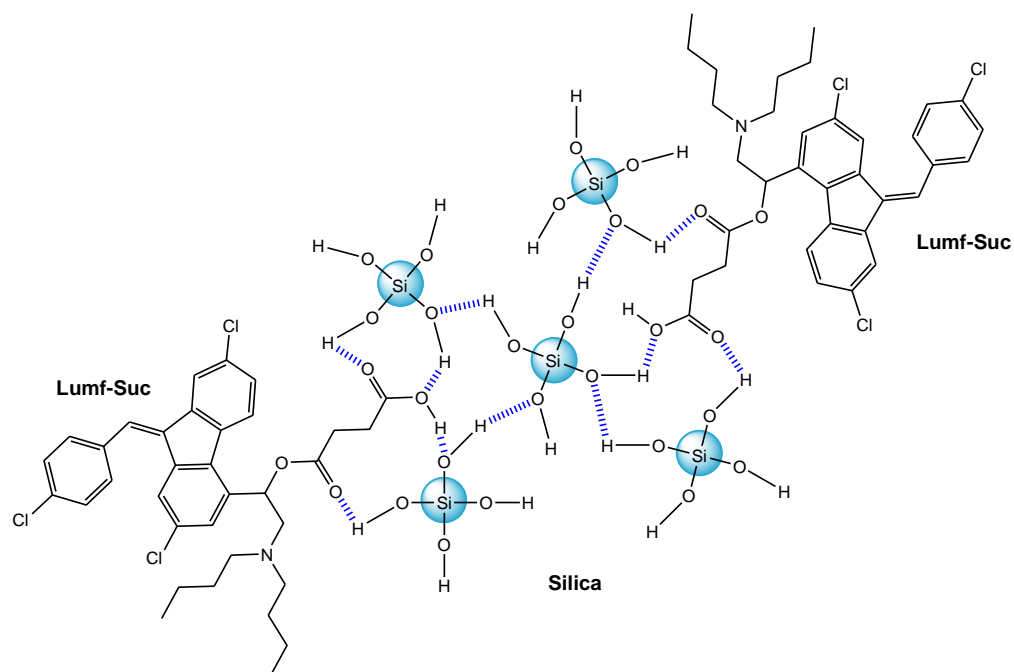


Figure 2.5: Schematic illustration of the interaction of the Lumf-Suc with a silica material.

Silica column chromatography is a traditional and simple route to obtaining pure organic compounds. A major disadvantage of this process is the use of large volumes of organic solvents as the mobile phase. It also generates significant amounts of solid silica waste. Apart from contributing to waste generation and environmental pollution, it also adds significant cost to the manufacturing process. It was observed that at an increased scale of the Lum-Suc synthesis (approximately 10 g), elution of the product off the column took as long as several days and co-elution of contaminants remained a problem.

It is with these considerations that an alternative, greener route of sample clean-up that involved the use of water was investigated for the purification of the Lum-Suc.

A PBS (pH 7.4) solution was added to a slurry of the crude Lum-Suc product after concentration under vacuum. An aqueous suspension of the Lum-Suc was obtained, which was centrifuged in order to pellet the solid. The solid Lum-Suc pellet was freeze-dried to obtain a dry free-flowing yellow powder (Figure 2.6).



Figure 2.6: Free flowing powder of Lumf-Suc.

The Lum-Suc products obtained by silica column chromatography and aqueous washing were characterized by FTIR (Figure 2.7). The Lumf-Suc purified by silica column chromatography showed a characteristic absorption at  $1726\text{ cm}^{-1}$ , which was assigned to the carbonyl C=O stretching of the ester and carboxylic acid functional groups. No IR peaks for the -OH stretching were observed at  $3390\text{-}3400\text{ cm}^{-1}$ , an indication of the absence of unreacted Lum. However, both -OH ( $3396\text{ cm}^{-1}$ ) and C=O ( $1736\text{ cm}^{-1}$ ) stretching signals were observed for the Lumf-Suc purified by aqueous precipitation. The presence of both -OH and C=O peaks were indicative of the presence of Lumf-Suc and the unreacted drug even though the latter was not seen on TLC analysis of the product. It was assumed that unreacted Lumf was present in very

low concentration at the end of the chemical reaction. In spite of this contamination of unreacted Lumf, the purification by aqueous precipitation was still deemed as the preferential purification route. It would circumvent the unnecessary wastage of copious volumes of organic solvents to remove a relatively low quantity of Lumf, which would have negligible reactivity in the next reaction step to conjugate the Lumf-Suc to the amine group of maPEG. The activating reagents can only activate the carboxylic group of Lumf-Suc, not the hydroxyl of Lumf. Furthermore, the  $-OH$  is a less potent nucleophile than the  $-NH_2$  of the PEG (Scheme 2.8). The conjugation reaction to link the Lumf-Suc to PEG in the next reaction step would have therefore not be interfered with by the presence of the  $-OH$  functional group of unreacted Lumf and it can be more readily removed from the final PEG-Lumf conjugate.



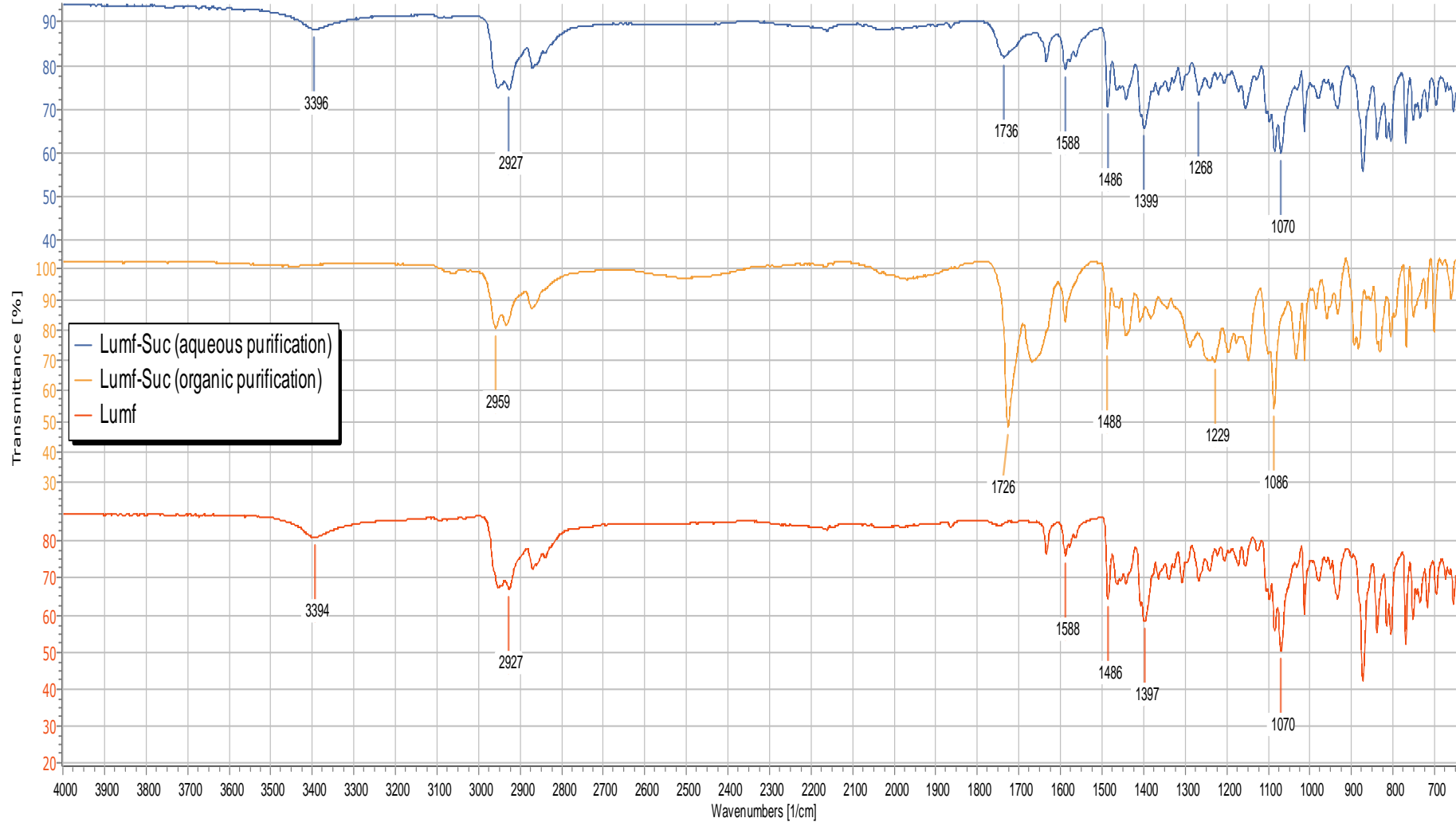


Figure 2.7: IR spectra of unmodified Lumf and Lumf-Suc purified by precipitation and silica flash chromatography.

Lumf-Suc product was further characterized by  $^1\text{H-NMR}$  (Figure 2.8). The  $^1\text{H}$  spectra showed a peak shift from 5.32 ppm to 6.62 ppm which was assigned to the hydrogen (H) of the chiral carbon of Lumf. This chemical shift was the most significant indicator for the successful derivatization of particularly the -OH group of Lumf to an ester functionality for Lumf-Suc.

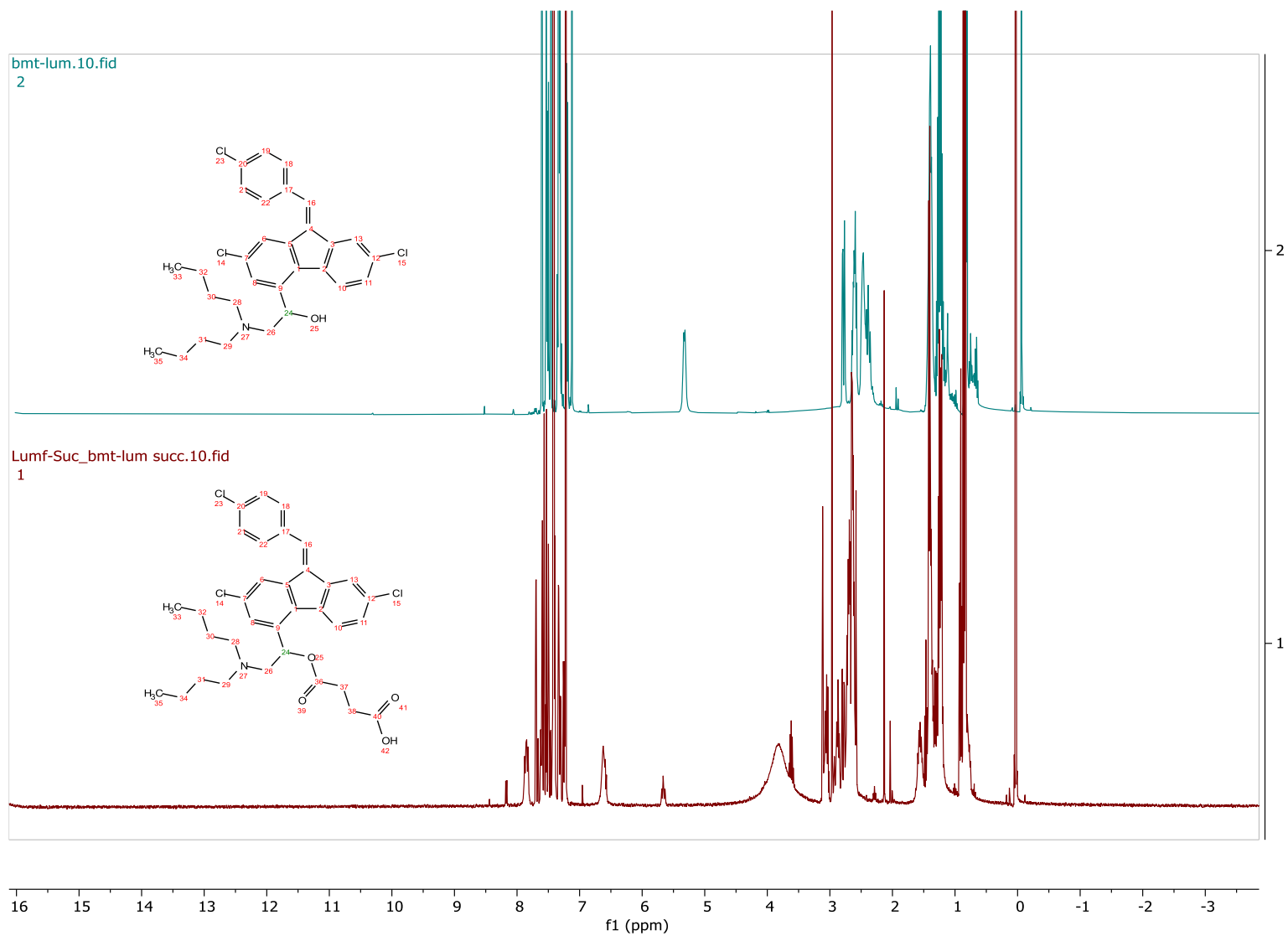
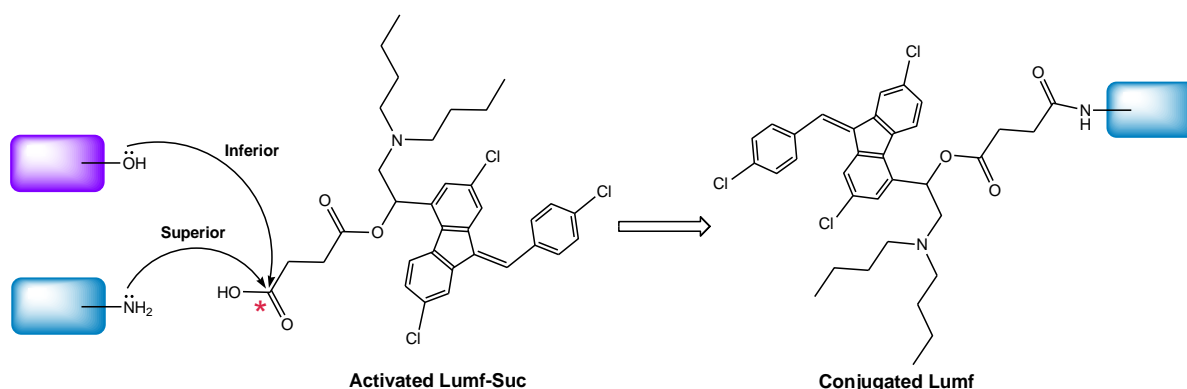


Figure 2.8:  $^1\text{H-NMR}$  spectra of Lumf and Lumf-Suc both prepared in  $\text{CDCl}_3$ .



Scheme 2.8: Chemical reactivity of -OH and -NH<sub>2</sub> functional groups as nucleophiles to an activated carboxylic acid.

In another effort to improve the efficiency of the reaction to succinylated Lumf, the molar equivalence of the succinate anhydride used was investigated. In the first reactions to succinylate Lumf, 3.0 mol eqv of succinic anhydride was used. This was to ensure maximum yield. Subsequently, a parallel synthesis experiment was set-up with three reaction vessels containing Lumf and 3.0 mol eqv, 2.0 mol eqv and 1.5 mol eqv of succinic anhydride, respectively (Figure 2.9). All reaction conditions were identical on the Carousel parallel synthesis station. At the end of the reaction period, TLC showed identical product formation for all three vessels. Again, there was no indication of any unreacted Lumf in any of the three experiments (Figure 2.10). The ability to obtain the Lumf-Suc in high yields but with only 50% excess succinic anhydride is a great improvement in cost saving.

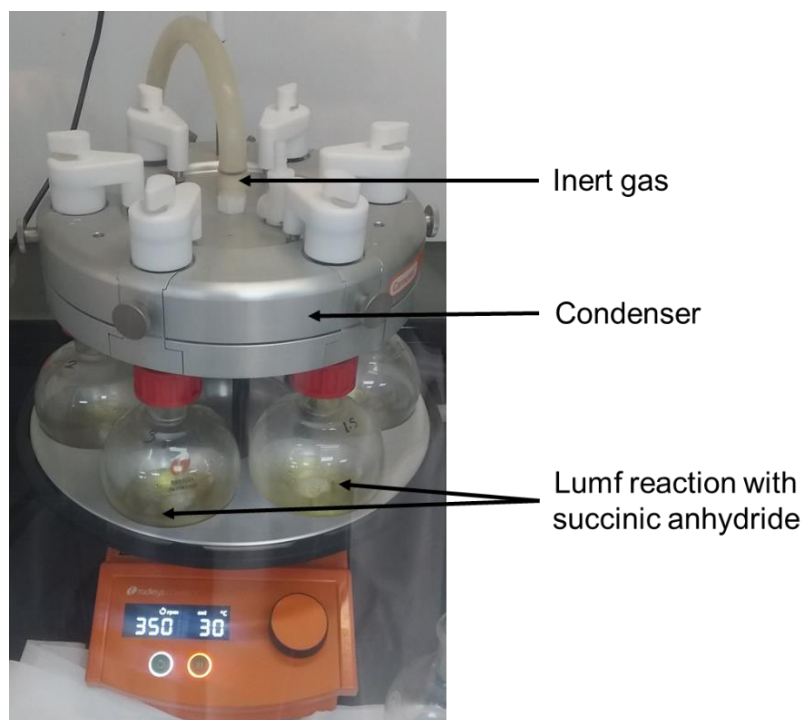


Figure 2.9: Radley's ® Carousel 6+ Parallel synthesis unit.

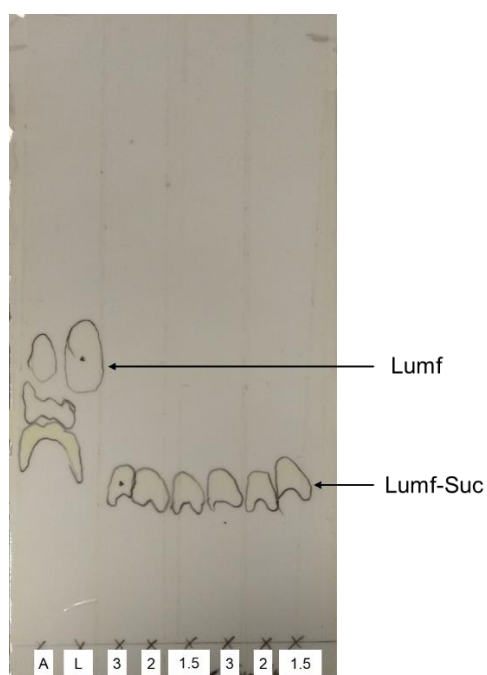


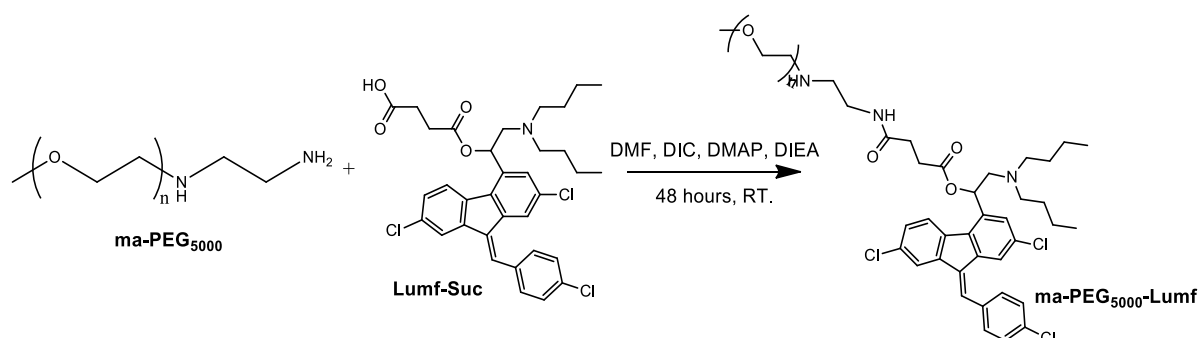
Figure 2.10: TLC for the chemical synthesis of Lumf-Suc using 3, 2 and 1.5 mol eqv of succinic anhydride. A – All materials spotted; L- lumefantrine. TLC was run using solvent system of ethyl acetate: hexane at a 4:1 ratio.

## Chemical synthesis of polymer-Lumf conjugates.

### PEG-Lumf conjugate

Conjugation of Lumf-Suc to PEG-NH<sub>2</sub> was conducted by carbodiimide coupling chemistry. The chemical linkage of Lumf-Suc was first conducted to a monoamine PEG of molecular weight 5 kDa (ma-PEG<sub>5000</sub>) (Scheme 2.9). The chemical linkage to this polymer was used to investigate enhancing the aqueous solubility of Lumf.

The use of this relatively low molecular weight PEG was based mainly on the cytotoxic effects associated with the molecular weight of the polymer. PEGs of molecular weight higher than 10.0 kDa are reported to cause toxic vacuolization due to accumulation in tissues.<sup>60</sup> Cytotoxic effects are also similarly echoed for PEGs of molecular weight between 0.2 kDa and 1 kDa albeit by an unknown mechanism.<sup>61</sup> As PEG is non-biodegradable, renal clearance is the only route of removal from the body. Molecular weight sizes of approximately 1.5 kDa to 6.0 kDa are considerably less cytotoxic as they can undergo renal clearance more effectively.



Scheme 2.9: Chemical conjugation of Lumf-Suc to ma-PEG<sub>5000</sub>.

The free carboxylic acid of the Lumf-Suc (3 mmol) was activated using DIC (6 mmol) in DMF and the reaction catalysed by DMAP (0.01 mmol). A solution of ma-PEG<sub>5000</sub> (5.0 g, 1 mmol) dissolved in DMF was added to the activated Lumf-Suc and left to react for 48 hours at room temperature. After the 48-hour reaction period, TLC showed a noticeably reduced UV-spot for Lumf-Suc relative to the other UV-active spot of the polymer conjugate (Figure 2.11). The polymer, which does not move with the mobile phase, is non-UV active and would not be visible under UV light on the TLC. However, if chemically conjugated with the drug, it would show UV activity and would be visible at the sample application point of the chromatography plate. As such, the UV active spot seen at the bottom of the TLC plate can be largely attributed

to the PEG linked to the Lumf compound. To further give confidence of a PEG-Lumf conjugate, the reaction solvent was removed *in vacuo* and buffer added to the crude product. The mixture was stirred at room temperature and subsequently centrifuged. This step was conducted to precipitate the water-insoluble substances like the unreacted drug and the by-products of the coupling reagents, leaving principally the water-soluble PEG-Lumf conjugate in the supernatant (Figure 2.12). The yellowish aqueous solution was then further purified by centrifugation using semipermeable membrane of MWCO 3 kDa. This would allow smaller water-soluble reagents like DMAP through and retain the larger much larger PEG-Lumf conjugate. The conjugate was then frozen and freeze dried to obtain a pure free flowing powder of 49% product yield.

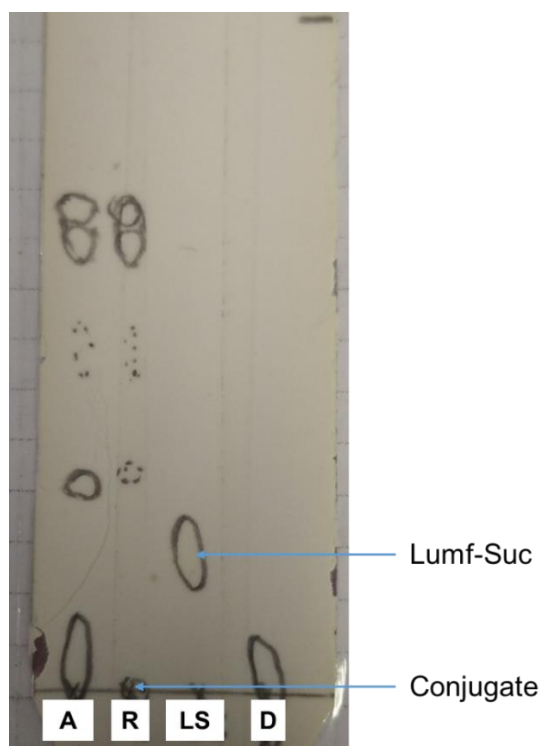


Figure 2.11: TLC for the chemical synthesis of a ma-PEG<sub>5000</sub>-Lumf conjugate. A – All materials; R – chemical reaction of ma-PEG<sub>5000</sub>-Lumf synthesis; LS – Lumefantrine-succinic acid (Lumf-Suc); D – dimethylaminopyridine (DMAP). TLC was run using solvent system of ethyl acetate: hexane at 4:1 ratio.

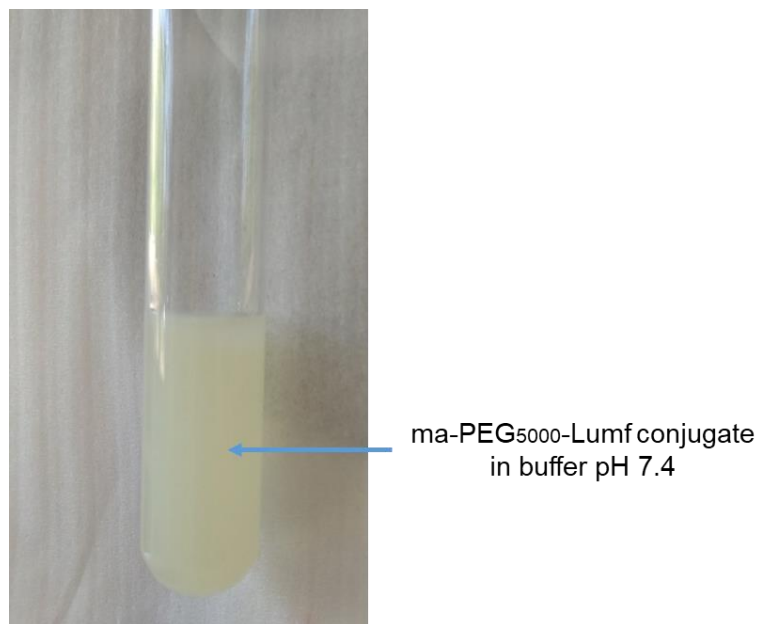


Figure 2.12: ma-PEG<sub>5000</sub>-Lumf conjugate in phosphate buffer (1.0 M, pH 7.4).

The pure dry material of ma-PEG<sub>5000</sub>-Lumf product was characterized by FTIR (

Figure 2.13). The IR spectra for ma-PEG<sub>5000</sub>-Lumf conjugate showed a transmission peak at 1671 cm<sup>-1</sup> of which was attributed to the C=O stretching of the amide group on the conjugate. This new peak seen for the polymer-drug conjugate was a significant shift from the C=O (1737 cm<sup>-1</sup>) stretching assigned to the free carboxylic end of Lumf-Suc. Peaks at 2883 cm<sup>-1</sup> and 1467 cm<sup>-1</sup> for the ma-PEG<sub>5000</sub>-Lumf were mainly attributed to the hydrocarbon (C-H) stretching of the polymer backbone.



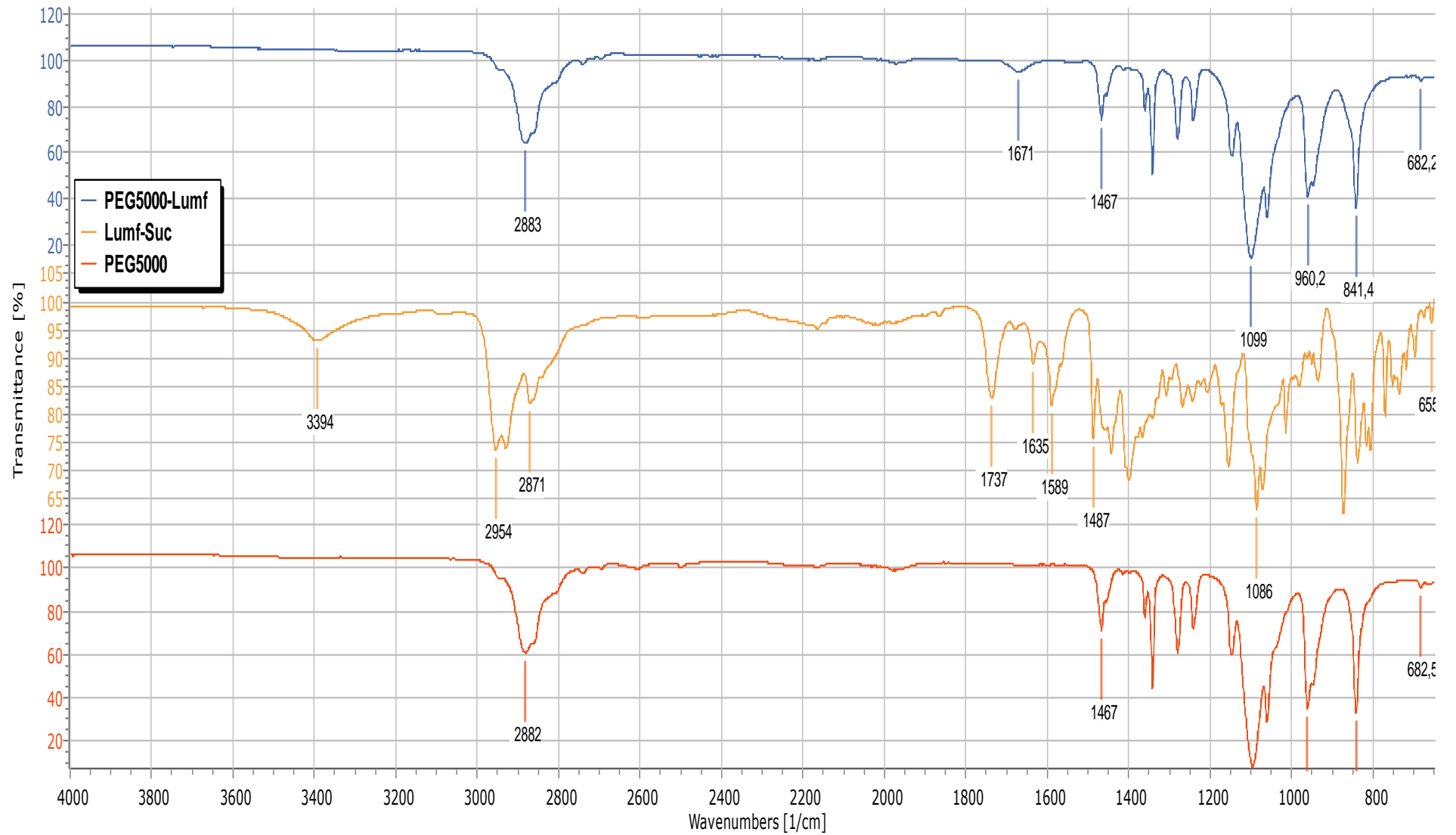


Figure 2.13: IR spectra for ma-PEG<sub>5000</sub>-Lumf, Lumf-Suc and ma-PEG<sub>5000</sub>.

The successful linkage of Lumf to ma-PEG<sub>5000</sub> was further substantiated by NMR characterization (Figure 2.14). The most telling signal peaks from the NMR spectra were seen at between 7.00 ppm and 8.00 ppm, which were assigned to the aromatic rings of the Lumf compound. The occurrence of these signals were seen for the ma-PEG<sub>5000</sub>-Lumf when overlaid with the free drug. Having conducted an extensive purification method, highspeed centrifugation followed by dialysis (MWCO: 1 kDa), to obtaining a pure conjugate material and the occurrence of the aromatic signals for Lumf was further supportive of a drug covalently linked to the water-soluble ma-PEG<sub>5000</sub>.

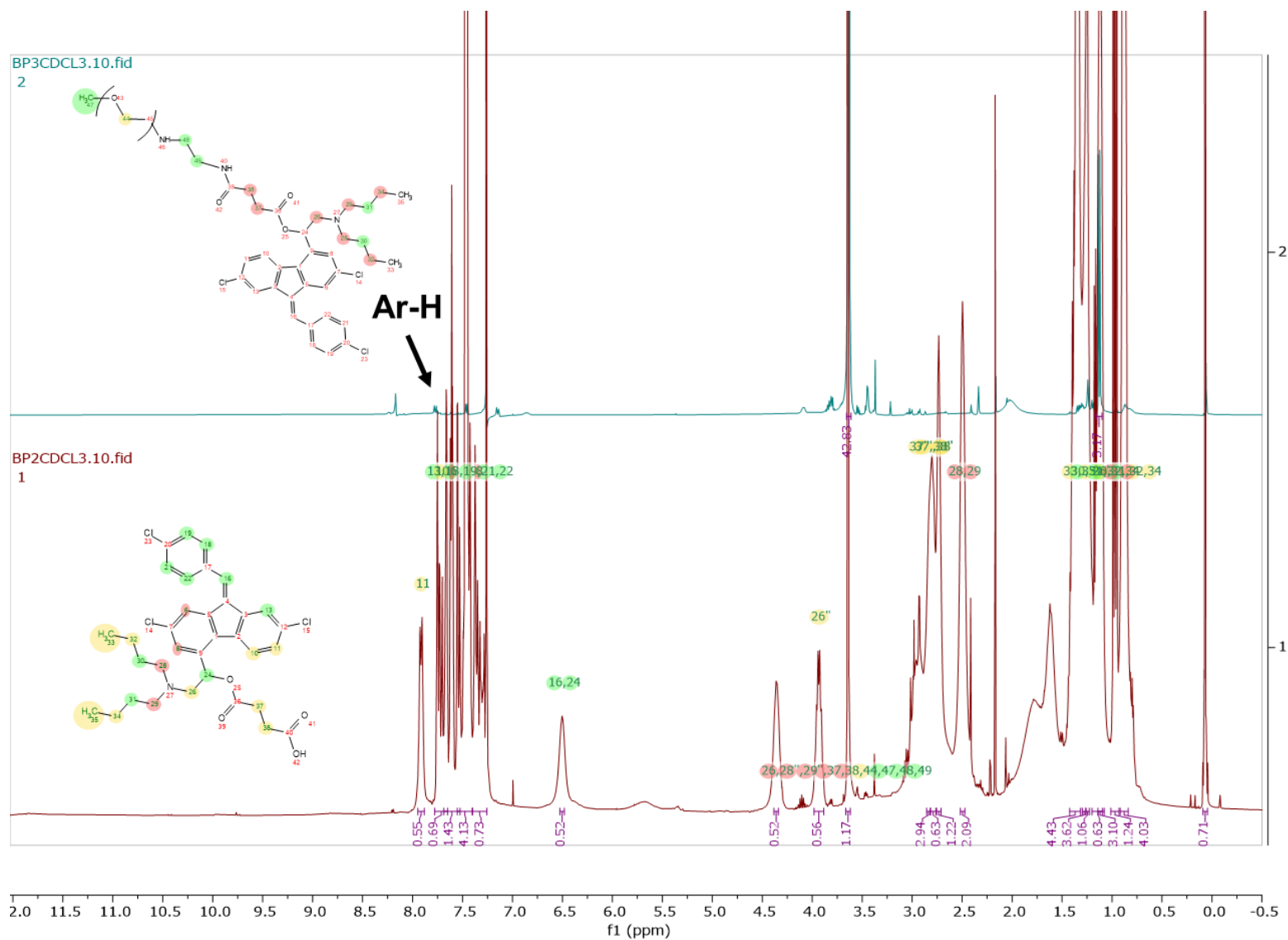


Figure 2.14: <sup>1</sup>H NMR spectra of ma-PEG<sub>5000</sub>-Lumf and Lumf-Suc prepared in CDCl<sub>3</sub>. Ar-H: proton signals of the aromatic rings of the Lumf drug.

Drug loading for any given polymeric carrier is in part limited by the number of linkage sites present for the polymer. ma-PEG<sub>5000</sub> in this instance can only accommodate one drug unit per polymer chain. Considering the Mw of the polymer, this too would have a noticeable impact on the drug content for the polymer-drug conjugate. The maximum theoretical drug loading that can be achieved for this monovalent polymer would be at the midway point of between 9% and 10% (Figure 2.15). However, the actual drug loading achieved for ma-PEG<sub>5000</sub>-Lumf, determined by UV/Vis analysis, was 8.68 µg of drug per mg of conjugate. This was determined to be less than 1% drug loading, below a 10<sup>th</sup> of the theoretical drug content.

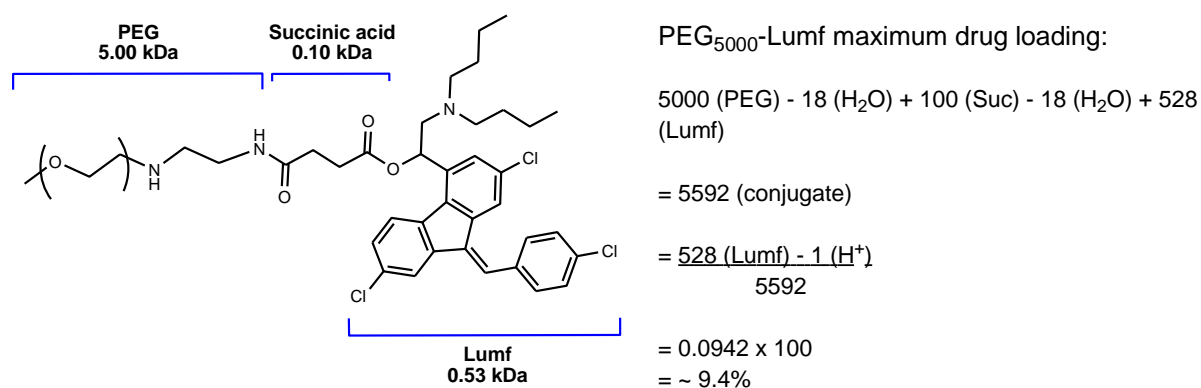


Figure 2.15: Theoretical calculation of determining the maximum drug loading for ma-PEG<sub>5000</sub>.

To increase the drug to polymer mass ratio, the conjugation reaction was repeated with a lower molecular weight, divalent PEG. Commercially available dihydroxy PEG (1.0 g, 0.67 mmol, dh-PEG) of molecular weight 1.5 kDa was reacted with ethylene diamine to obtain a diamine PEG (da-PEG<sub>1500</sub>) (Figure 2.16). Again, an amine functionalized PEG is preferred for conjugation as the amino group (-NH<sub>2</sub>), among other reasons (described in Chapter 02, Scheme 2.7) is more nucleophilic than the hydroxyl functional group. A two-step process was undertaken to synthesize da-PEG<sub>1500</sub> which involved firstly tosylating (3.33 mmol) the hydroxyl groups for 3 hours in cold DCM in an inert atmosphere condition (Figure 2.16: step 01). After the 3-hour cold reaction, the solvent was removed and a binary solvent system of DCM and DMF at a ratio of 1:3 was added to the tosylated crude product (0.67 mmol). Ethylene diamine (2.00 mmol) was added and allowed to react for 48 hours (Figure 2.16: step 02). The da-PEG<sub>1500</sub> product was purified by washing with diethyl ether to obtain a dry off-white material.

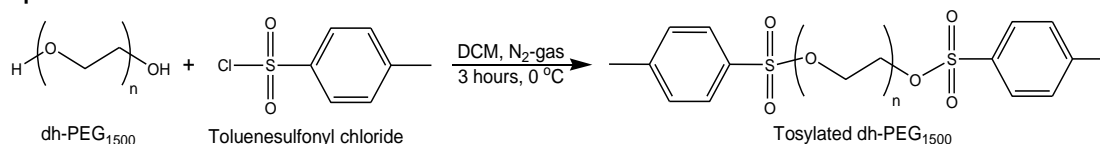
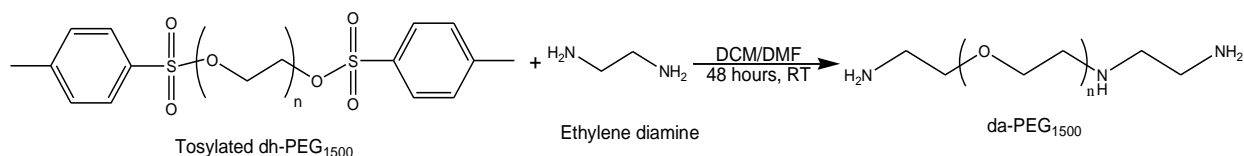
**Step 01:**

**Step 02:**


Figure 2.16: A two-step chemical derivation process of dh-PEG<sub>1500</sub> to da-PEG<sub>1500</sub>.

The da-PEG<sub>1500</sub> product was characterized by FTIR (Figure 2.17) and <sup>1</sup>H-NMR (Figure 2.18). The successful derivatization of dh-PEG<sub>1500</sub> to da-PEG<sub>1500</sub> was shown to be inconclusive by elemental analysis. IR analysis of the da-PEG<sub>1500</sub> product showed peak at 1662 cm<sup>-1</sup> which was assigned to the –NH<sub>2</sub> stretching. The occurrence of peaks at 1742 cm<sup>-1</sup>, 1822 cm<sup>-1</sup> and 2051 cm<sup>-1</sup> were suggestive of intermediary products likely as a result of the tosyl-group present in the final material. NMR analysis of the final product supported the notion of a crude product mixture. Signal peaks seen at 7.00-8.00 ppm for the final product could only be as a result of the aromatic protons of the tosyl-group. The signal peaks indicative of a –OH to –NH<sub>2</sub> derivatization could also not be determined in the final product. A chemical shift was expected at approximately 2.70 ppm (PEG-OH) to around 3.00-3.50 ppm (PEG-NH<sub>2</sub>) as evidence for an amine PEG. These signals peaks however also overlap substantially with proton signals of the polymer backbone, adding to the complexity of determining a modified material.

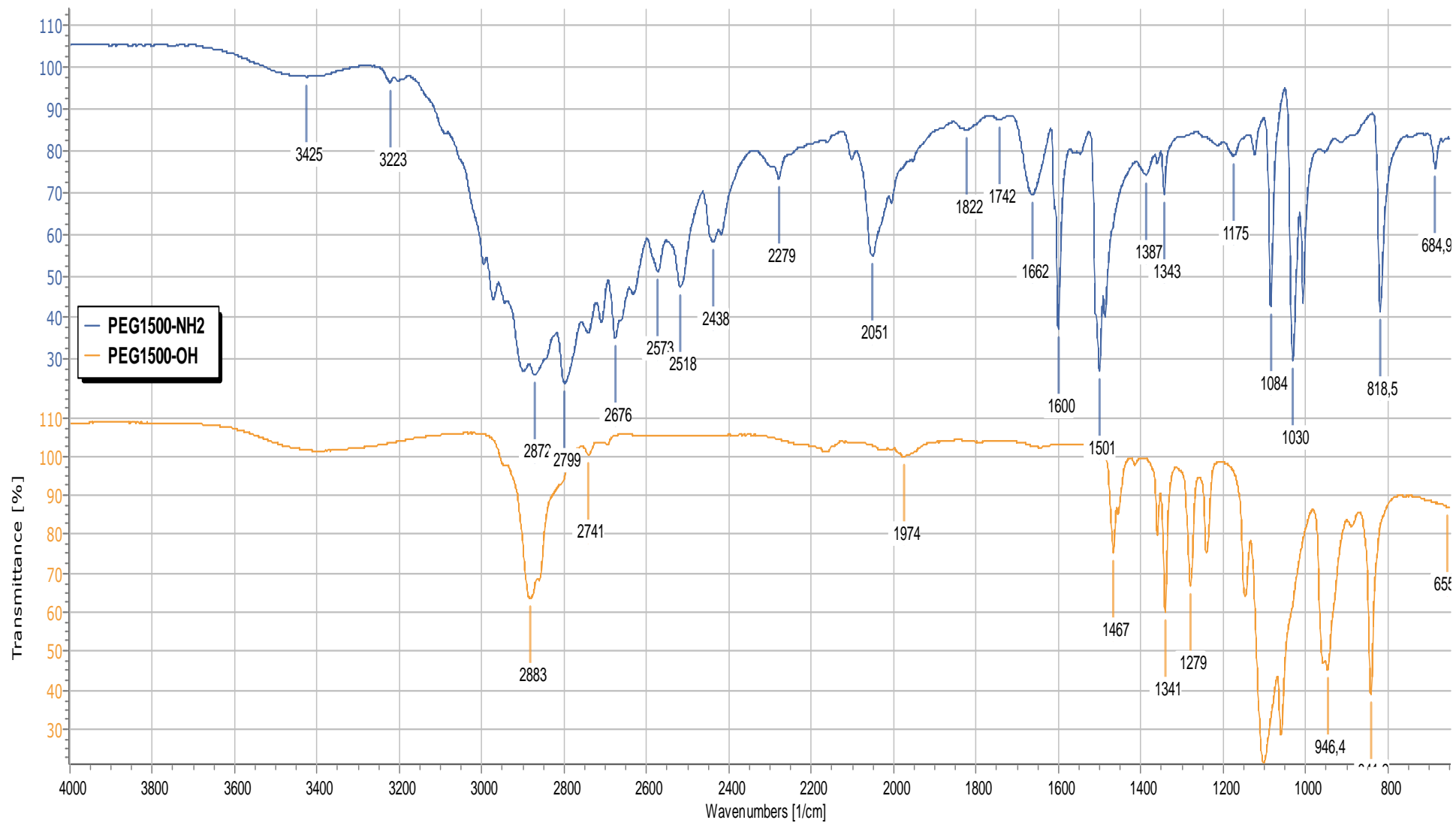


Figure 2.17: IR analysis of chemically derivatized da-PEG<sub>1500</sub>.

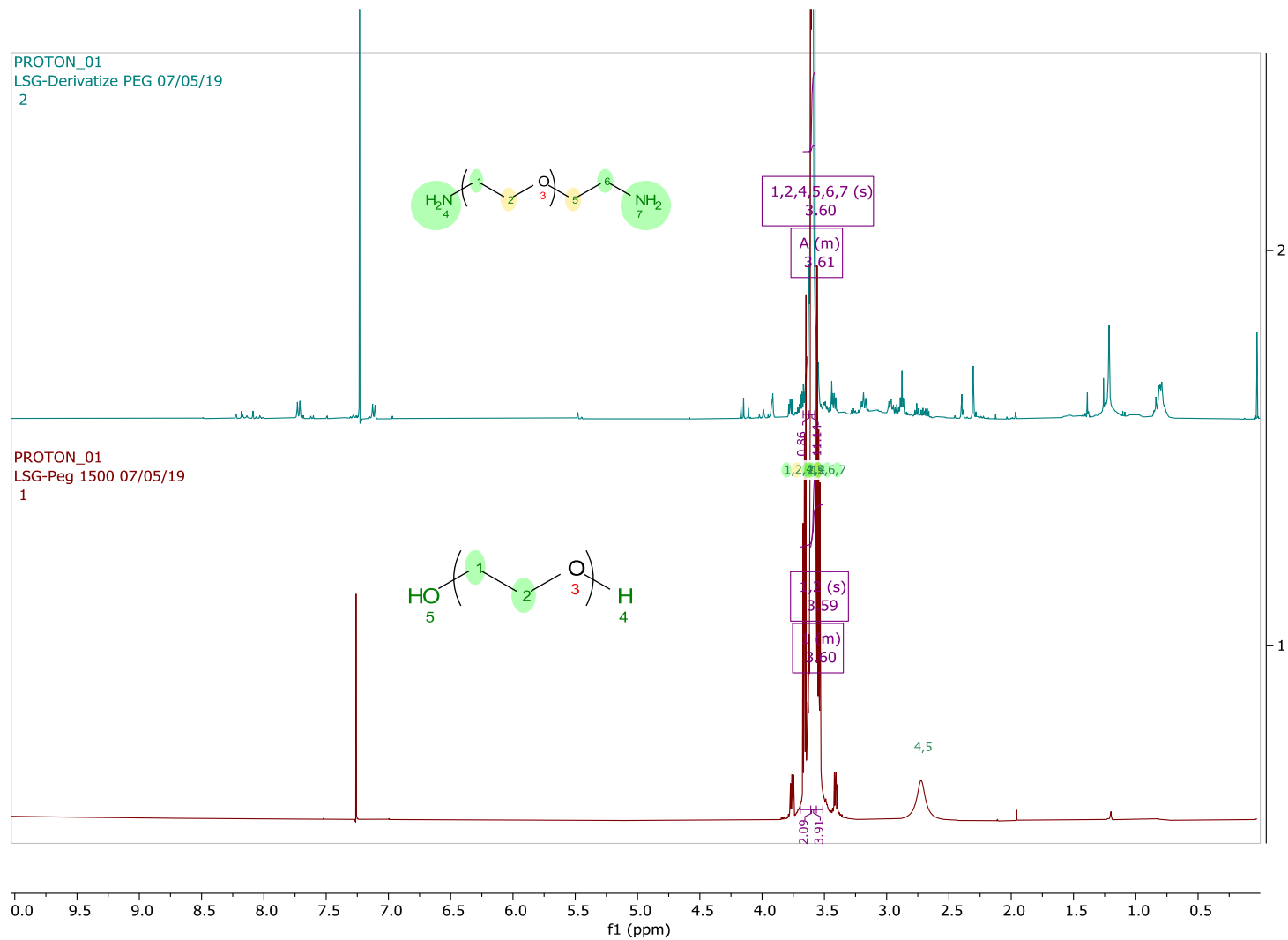
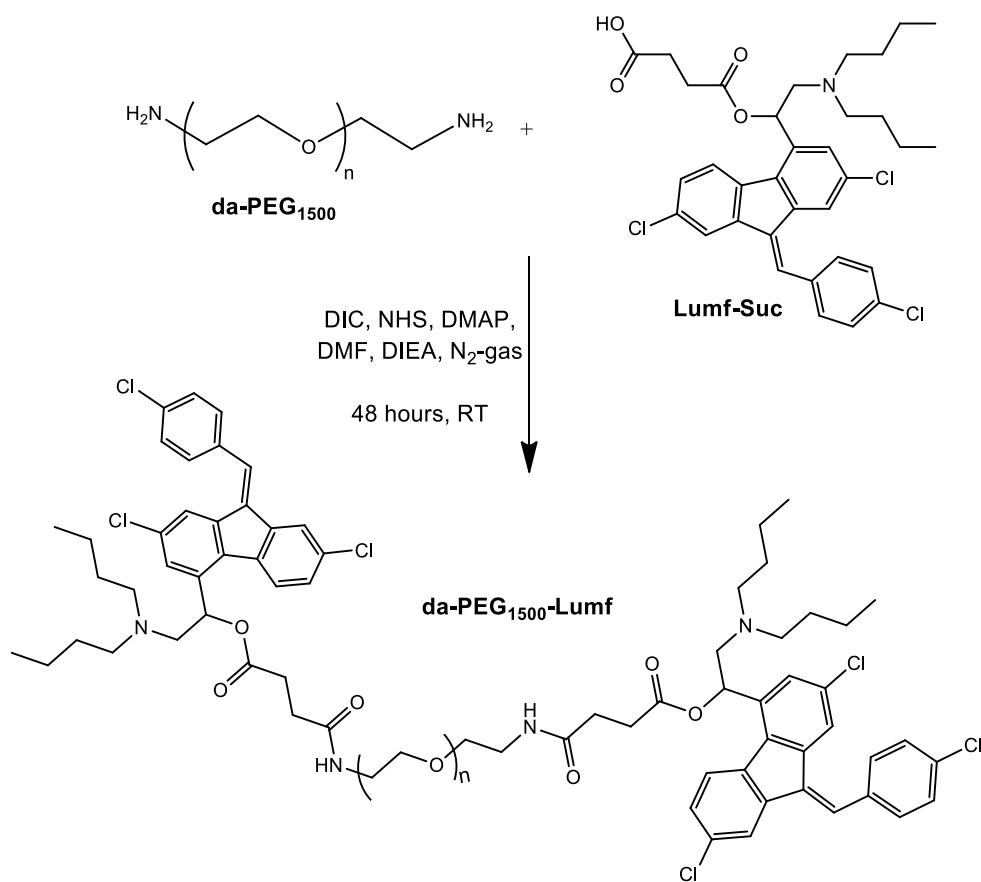


Figure 2.18: <sup>1</sup>H-NMR spectra of da-PEG<sub>1500</sub> and dh-PEG<sub>1500</sub>. Polymers were dissolved in CDCl<sub>3</sub>.

The difficulty with obtaining a pure da-PEG<sub>1500</sub> was circumvented by the purchase of a commercially available da-PEG<sub>1500</sub> to save time spent on the chemical synthesis aspect of this project. The commercial da-PEG<sub>1500</sub> was used in all the subsequent chemical conjugation reactions.

Chemical linkage of Lumf to da-PEG<sub>1500</sub> was investigated for 10 mol eqv's of the drug (Scheme 2.10). Lumf-Suc was firstly activated using DIC coupling reagent. The activated solution of Lumf-Suc was then added dropwise to a stirring solution of da-PEG<sub>1500</sub> and left to react for 48 hours at room temperature. Much like the synthesis procedure for ma-PEG<sub>5000</sub>-Lumf, TLC showed a noticeable reduction of the UV-active spot for Lumf-Suc and an increased intensity of the UV-active spot at the sample application point of the chromatography plate. The UV-active spot for the conjugate appeared to smudge from the application spot of the TLC plate. This "smudging" could be because of having Lumf linked to both ends of the polymer's amine groups, which could result in a reduced hydrophilic interaction between PEG and the silica. The combination of the dispersity of the polymer's molecular mass and conjugation of one or two drug units could explain the observed UV-absorption pattern of the reaction product starting at the application point of the TLC plate.





Scheme 2.10: Complete conjugation reaction of Lumf-Suc to da-PEG<sub>1500</sub>.

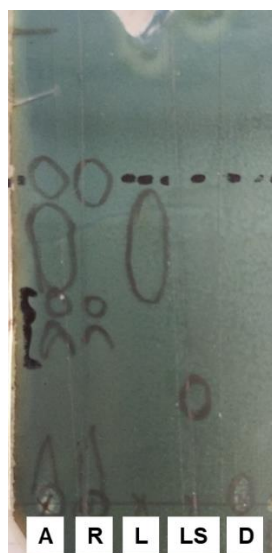


Figure 2.19: TLC for the chemical synthesis of da-PEG<sub>1500</sub>-Lumf conjugate. A – All materials; R – chemical reaction of Lumf conjugation to da-PEG<sub>1500</sub>; L – lumefantrine; LS – lumefantrine-succinate; D – dimethylaminopyridine (DMAP). TLC was run using a solvent system of ethyl acetate: hexane at a ratio of 4:1.

After the 48-hour reaction period, the crude reaction mixture was concentrated by removing the solvent under vacuum. Phosphate buffer solution was added to the crude product and the insoluble material were removed by centrifugation to obtain a yellowish supernatant (Figure 2.20). The occurrence of this yellow solution showed that PEG of molecular weight as low 1.5 kDa can be a sufficient carrier to the solubilization of Lumf. Conducting further purification steps such as dialysis was limited by the availability of membranes with MWCO's lower than 1 kDa which can significantly reduce the loss of product. Nonetheless, the solution was then frozen and subsequently freeze dried to obtain a pure da-PEG<sub>1500</sub>-Lumf material.

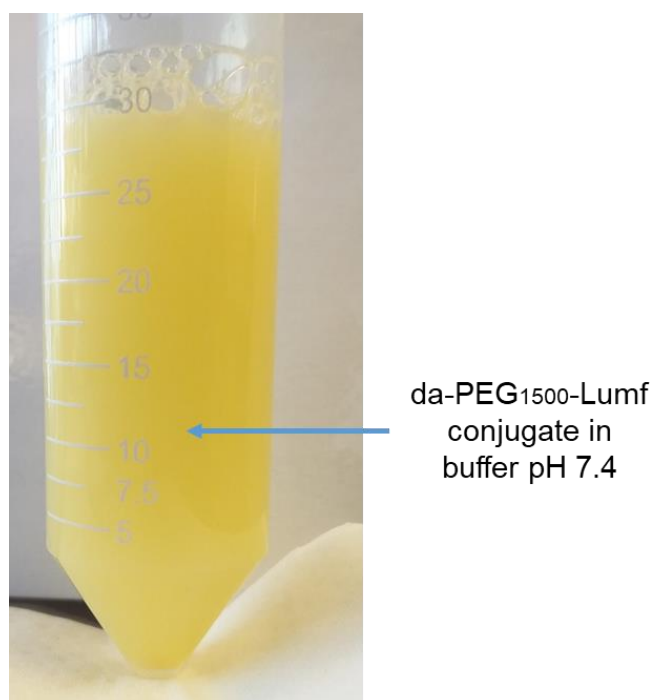


Figure 2.20: da-PEG<sub>1500</sub>-Lumf conjugate in buffer (pH 7.4).

The da-PEG<sub>1500</sub>-Lumf product was characterized by FTIR (Figure 2.21) and NMR (Figure 2.22). IR analysis of the conjugate showed the occurrence of a peak at 1662 cm<sup>-1</sup> which was assigned to the C=O stretching of the amide group for the da-PEG<sub>1500</sub>-Lumf. This was the more noticeable shift in IR absorption peak from the C=O stretching of Lumf-Suc (1736 cm<sup>-1</sup>), which was suggestive of a Lumf-Suc linked to da-PEG<sub>1500</sub> by an amide bond. NMR analysis of da-PEG<sub>1500</sub>-Lumf showed the occurrence of signal peaks at 7.50-8.00 ppm which are assigned to the aromatic ring signals of the Lumf drug. These signal peaks were not seen when overlaid with the free unmodified da-PEG<sub>1500</sub> which mainly comprised of signal peaks

at 3.50-3.70 ppm and 4.80 ppm assigned to the ethylene oxide repeating units. This spectral analysis further supported da-PEG<sub>1500</sub>-Lumf conjugate as the major final product.

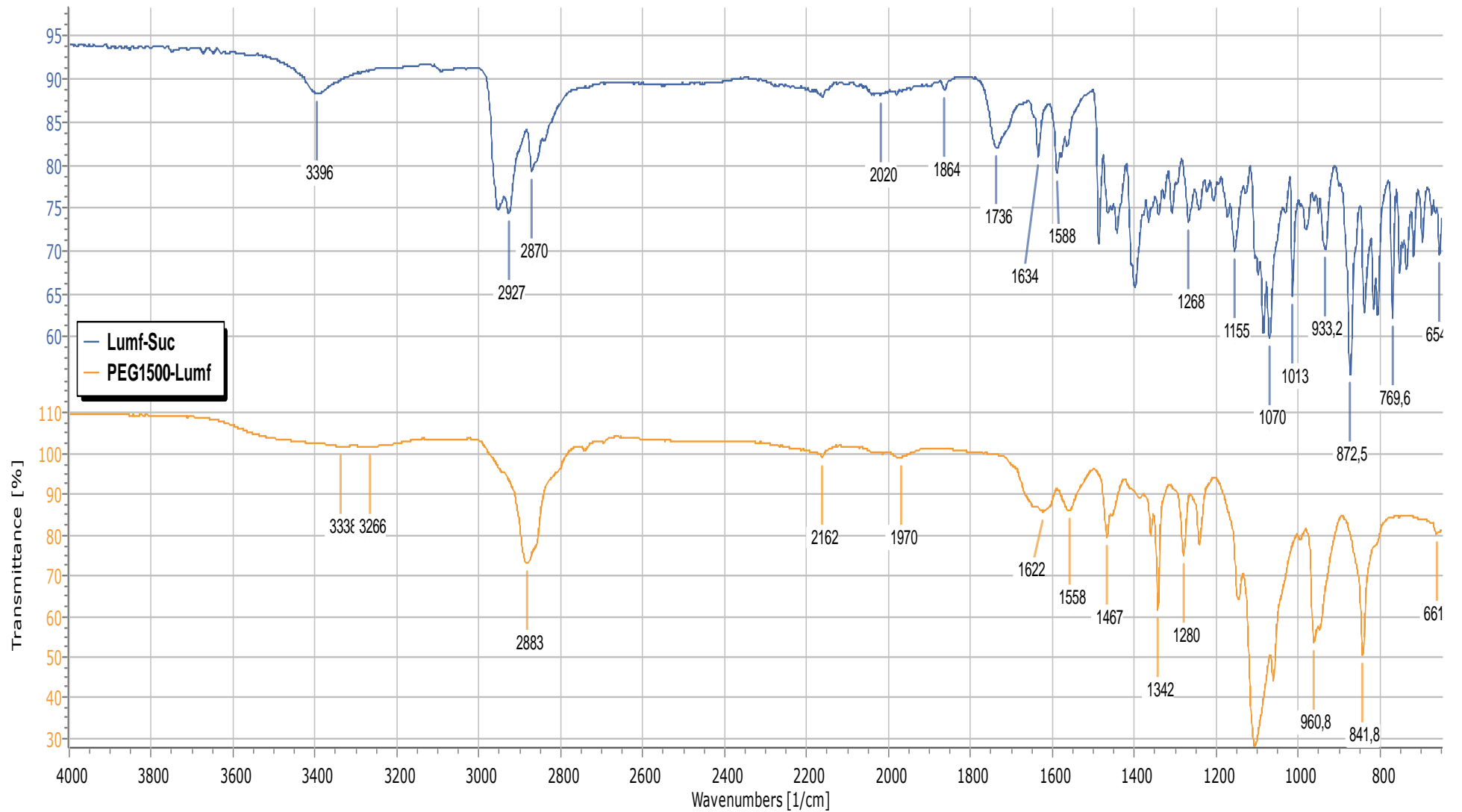


Figure 2.21: IR spectra of Lumf-Suc and da-PEG<sub>1500</sub>-Lumf conjugate.

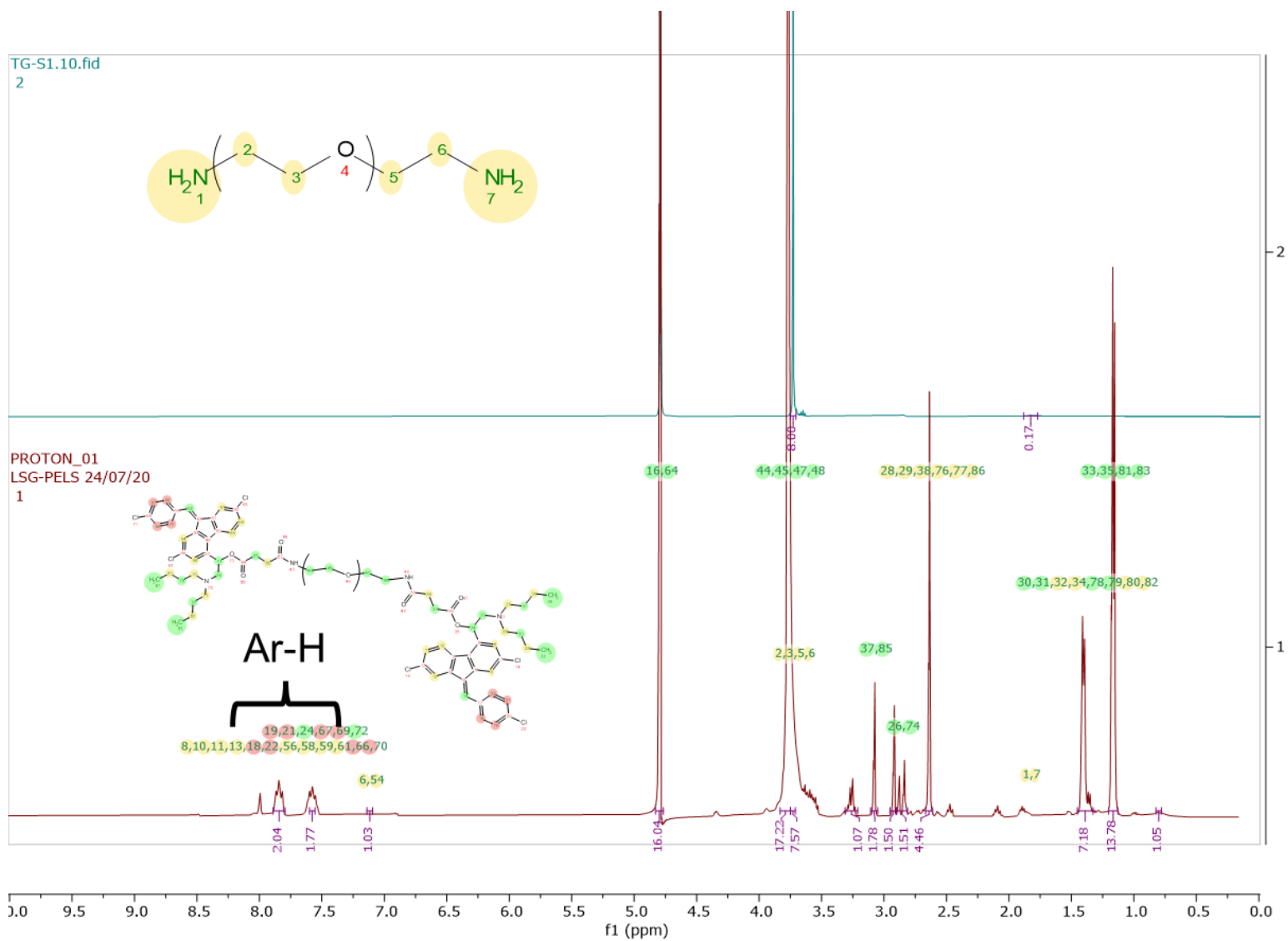


Figure 2.22: <sup>1</sup>H-NMR spectra of da-PEG<sub>1500</sub>-Lumf and da-PEG<sub>1500</sub> both prepared in D<sub>2</sub>O.

### *PNAM-Lumf conjugate*

Polymers which offer two or more derivatization sites can be particularly advantageous as to enhancing the drug payload per unit of polymer. PNAM in this instance, offers on average 10 attachment sites to which Lumf can be linked. Although in theory each carboxylic acid functional group present on a PNAM chain can conjugate a Lumf-Suc molecule, only a fraction of very lipophilic drugs such as Lumf, can be linked before significantly altering the aqueous solubility of the polymer-Lumf conjugate, as reported by Singer *et al* in 2006 while developing a polyglutamic acid-camptothecin therapeutic.<sup>59</sup> It is on this premise that the chemical conjugation of Lumf to PNAM was investigated at 2 and 24 mol eqv's of Lumf. The first linkage step involved activation of the carboxylic acid moieties of PNAM (200 mg, 0.015 mmol) using DIC (58.228 mg,  $p = 0.815$  g/mL, 30 mol eqv) and HoBt (62.64 mg, 30 mol eqv) as the coupling reagents, stirring in anhydrous DMF (5 ml) before the addition of DMAP (0.01 mol eqv) and then Lumf. The solution was alkalinized using DIEA and left to react for 48 hours at room temperature. TLC analysis showed a relative decrease in the UV-active spot for Lumf (Figure 2.23). After the 48-hour reaction, the crude mixture was concentrated by removing the solvent *in vacuo* at 5 mBar (40 °C). Buffer (10 ml) was added to the crude mixture and stirred at room temperature for 1 hour before being centrifuged at 10 000  $\times g$  for 30 min (5 °C). A control reaction comprised of Lumf and PNAM but with no coupling reagents added as a comparative study. The PNAM investigated here is an amphiphilic polymer, that is consists of both hydrophobic and hydrophilic moieties. The lipophilic Lumf can interact with the hydrophobic moiety of the polymer, resulting in the formation of a hydrophobic core much like encapsulation technology. Comparing this to a reaction mixture inclusive of coupling reagents, would distinguish the Lumf chemically linked to the polymer from the drug which has a "physical" interaction with the relevant moieties, especially after conducting highspeed centrifugation. UV/Vis absorption profile of the polymer, discussed in the preceding Chapter 3, was shown to overlapped with that of Lumf drug. The control experiment in which no coupling reagent was included in the reaction, was conducted so to provide insight into the extent at which the polymer's UV/Vis absorption would overlap with that of the drug. This was particularly important to determining the conjugate's drug loading by UV/Vis analysis.



Figure 2.23: TLC of Lumf conjugation reaction to PNAM. A – All materials; R – chemical reaction of Lumf conjugation to PNAM; L – lumefantrine; D – dimethylaminopyridine (DMAP); H – hydroxybenzotriazole (HoBT). TLC was run using a solvent system of ethyl acetate: hexane at a ratio of 4:1.

After centrifuging the buffer extracts, the supernatants of each reaction were withdrawn (Figure 2.24). The aqueous solution of the control reaction appeared slightly discoloured (Figure 2.24a). This was attributed to the PNAM polymer dissolved in the water. The supernatant for the reaction of PNAM with 24 mol eqv of the drug appeared clear (Figure 2.24b). The reaction solution of PNAM reacted with 2 mol eqv of the drug appeared significantly more yellow compared to the control reaction solution with no coupling reagent and with the reaction of higher drug equivalent reaction (Figure 2.24c). This could be the result of high lipophilic drug loading of the polymer that would have a significant effect on its aqueous-solubility. The reaction in the presence of high drug eqv could result in most of the carboxylic units of the polymer being conjugated to a drug molecule resulting in a conjugate product with a limited number of charged sites that would normally enhance aqueous solubility. Heavily conjugated polymer could promote aggregation of the conjugated particulates in solution that would decrease the aqueous solubility further. Under significant gravitational force, these aggregated particles would sediment out of suspension and result in a colour-less supernatant. However, limiting the loading ratio by reacting the polymer with lower quantities of the drug, can greatly enhance the probability of obtaining a water-soluble PNAM-Lumf conjugate. By having a reduced number of drug molecules linked to a polymer unit a significant

number of free carboxylic acid moieties would be available to enhance water solubility. This would promote PNAM-Lumf solubility.

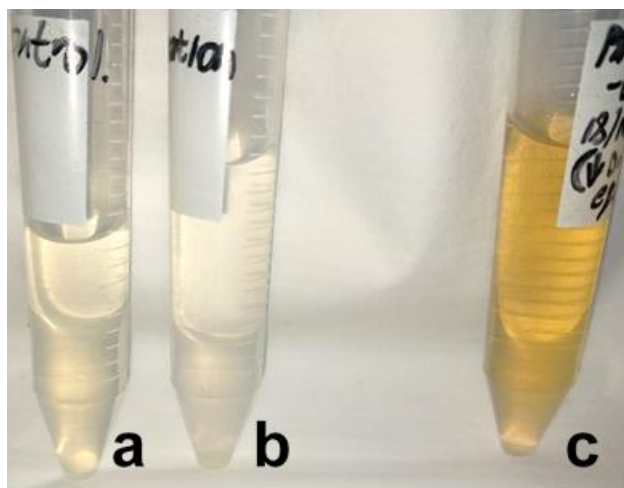


Figure 2.24: Chemical reaction of PNAM and Lumf with the addition of a) No coupling reagents, b) coupling reaction with 24 mol eqv's and c) 2 mol eqv's of Lumf conducted under anhydrous conditions.

The PNAM-Lumf conjugate of the lower drug mol eqv's was subsequently frozen and freeze dried to obtain a pure dry material. This product was then characterized by FTIR (Figure 2.25) and NMR (Figure 2.26). IR analysis of the PNAM-Lumf conjugate showed a shift in transmission peak from  $1723\text{ cm}^{-1}$  for the unmodified polymer to  $1699\text{ cm}^{-1}$  for the conjugate. This shift can be assigned to the change in transmission for the C=O stretching of the free polymer carboxylic acid group, to the C=O ester of the polymer-drug conjugate. The successful synthesis of PNAM-Lumf was further substantiated by the appearance of NMR signals peaks at 7.50-7.90 ppm which were assigned to the aromatic rings of the Lumf drug. The occurrence of these signals and shifts proved to be the most distinguishable features indicative of a successful chemical derivation.



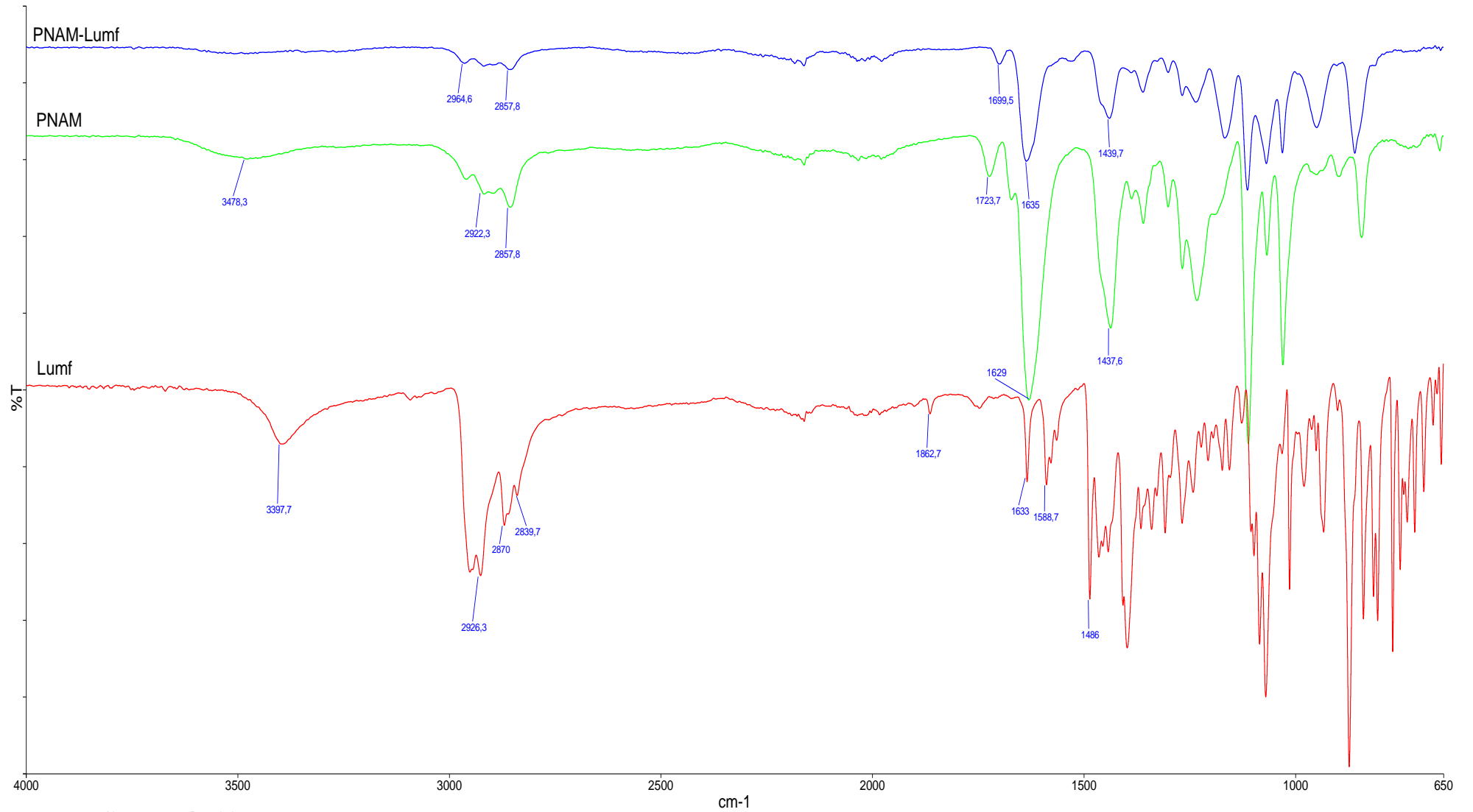


Figure 2.25: IR analysis of PNAM-Lumf, PNAM and Lumf.

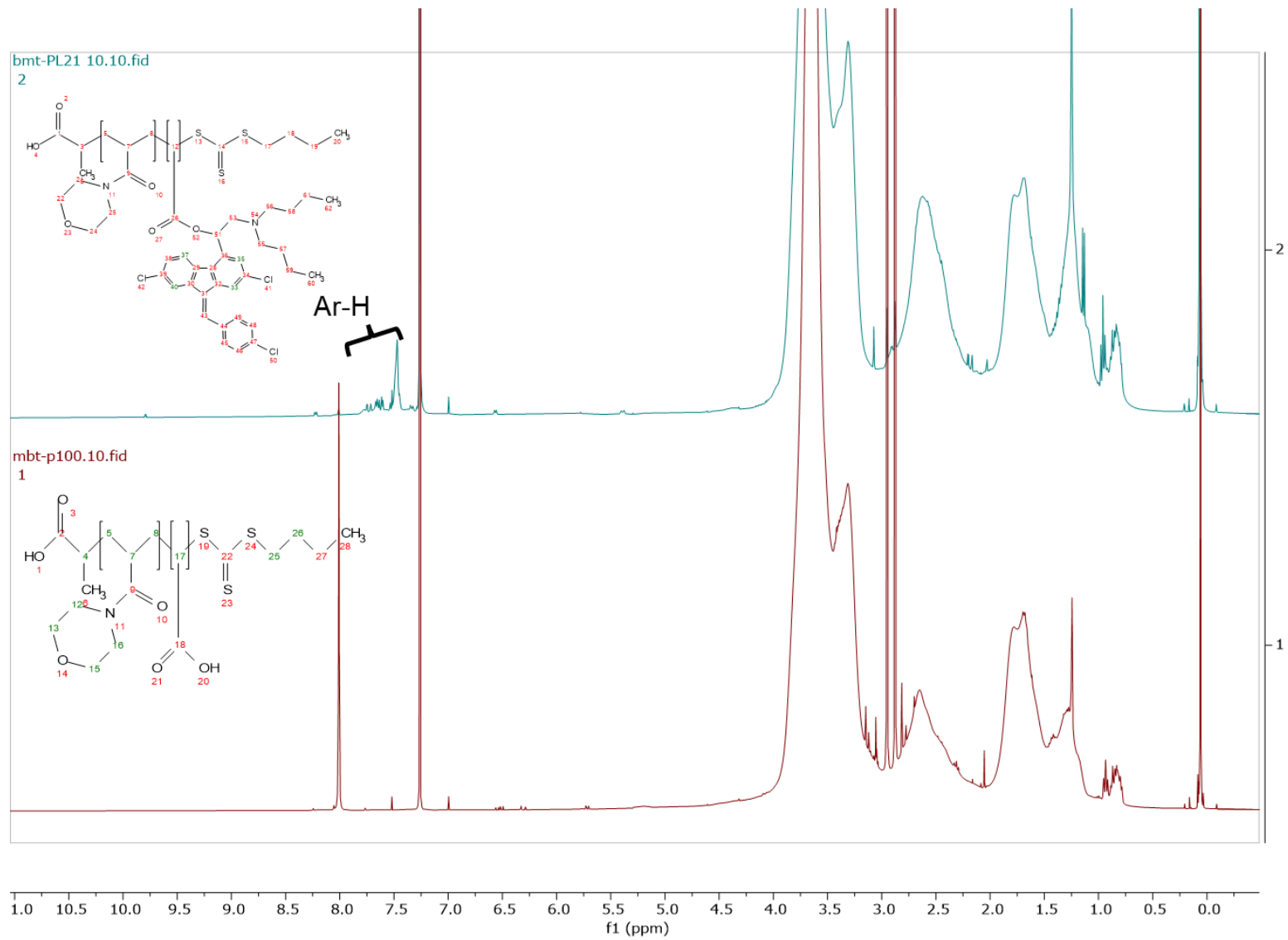


Figure 2.26: <sup>1</sup>H-NMR analysis of PNAM and PNAM-Lumf conjugate prepared in CDCl<sub>3</sub>.

## Conclusion

The successful conjugation of Lumf to the water-soluble polymers PEG and PNAM was supported by <sup>1</sup>H-NMR and FTIR analyses. Derivatization of the polymers with Lumf were shown by changes and shifts in spectral signals which were indicative of new chemical functional groups. For all the polymer-drug conjugates, signal peaks of the aromatic rings of Lumf for purified polymer conjugates further supported successful synthesis thereof. The synthesis of PNAM-Lumf, using a 2.0 mol equivalence of Lumf, showed to have a higher drug content in aqueous solution, as compared to the reaction of 24.0 mol equivalence of the drug. This can be attributed to having the multivalent polymer overloaded with Lumf and thus an inability to solubilize the drug.

### 3. Chapter Three: Characterization of polymer-lumefantrine conjugates

#### Introduction

Several characterization techniques and methodologies can be used to investigate the physicochemical properties of relevance to the final clinical purpose of the polymer therapeutic.<sup>62</sup> They include the drug content or loading of the conjugate and its hydrodynamic size and charge. This chapter reports on the investigation of these properties of the polymer-Lumf conjugates synthesized in Chapter Two.

#### Materials and Methods

Lumefantrine (99%) was purchased from DB Fine Chemicals Pty Ltd (South Africa). Ethyl acetate (EA; ACS grade  $\geq 99\%$ ), acetone ( $\geq 90\%$ ), acetonitrile (ACS grade,  $\geq 99\%$ ), formic acid (FA, HPLC grade  $\geq 98\%$ ), polyethylene glycol diamine (da-PEG,  $\geq 99\%$ ), were all purchased from either Sigma-Aldrich Ltd (RSA) or CRD Chemicals Pty Ltd (South Africa). Disodium hydrogen phosphate (ACS reagent grade,  $\geq 99\%$ ), sodium chloride (ACS reagent grade,  $\geq 99\%$ ), potassium chloride (ACS reagent grade,  $\geq 99\%$ ), potassium dihydrogen phosphate (Emprove® Essential) – used to make the buffer solution were also purchased from Sigma-Aldrich Ltd (RSA).

The Ultraviolet/visible light (UV/Vis) spectra were measured using a Mettler Toledo UltraViolet5Bio (UV5Bio) instrument. A Malvern Zetasizer Nano-ZS90 (Malvern Instruments, United Kingdom) was used to determine the hydrodynamic properties of the polymer-Lumf conjugates.

#### *UV/Vis analysis*

A 1.0 mg/mL stock solution of lumefantrine prepared in ethyl acetate, was diluted to 2  $\mu\text{g/mL}$ , 5  $\mu\text{g/mL}$ , 10  $\mu\text{g/mL}$ , 15  $\mu\text{g/mL}$ , 20  $\mu\text{g/mL}$ , and 25  $\mu\text{g/mL}$  in ethyl acetate. The polymer-Lumf conjugates were prepared in aqueous phosphate buffer (pH 7.4) or dH<sub>2</sub>O unless mentioned otherwise. The absorbance of the samples were measured at wavelength 335 nm on a Mettler Toledo UV5Bio instrument to obtain a standard curve. The data for absorbance vs concentration were processed using Microsoft Office Excel. A linear regression equation of  $y = 40.237x + 0.0032$  ( $R^2 = 0.99$ ) was obtained.

### *Hydrodynamic properties*

The particle size (d.nm) and zeta potential (mV) of the polymer-Lumf conjugates were measured by dynamic light scattering (DLS) on a Malvern Zetasizer instrument (United Kingdom). ma-PEG<sub>5000</sub>-Lumf, da-PEG<sub>1500</sub>-Lumf and PNAM-Lumf conjugates were prepared in 1.0 M phosphate buffer (pH 7.4) at room temperature. The samples were injected into a disposable capillary cell prior to insertion into the DLS instrument. Three measurements comprised of ten repeats each were conducted at the highest resolution and the average calculated by the Malvern Zetasizer software. Refractive indexes used for the DLS measurements were 1.460 and 1.508 for the PEG and PNAM polymers, respectively. A standard absorption value of 0.001 was applied to all the measurements.

## **Results and Discussion**

### *UV/Vis analysis*

The drug loadings of PEG and PNAM drug conjugates were determined by UV/Vis spectroscopy at wavelength 335 nm. This wavelength was used by Huang *et. al.* 2010 in the analysis of Lumf as it showed to be highly specific and selective for the drug.<sup>63</sup> Lumf stock solutions was prepared at a 1.0 mg/mL concentration in ethyl acetate and serial dilutions were made down to 2.0 µg/mL. Only the 2.0 µg/mL to 25.0 µg/mL range was within the linear absorbance range and these were used to construct a linear regression curve of absorbance vs drug concentration.

The polymer-Lumf conjugates which were soluble in aqueous media, were prepared in 1.0 M phosphate buffer (pH 7.4) and analysed by UV/Vis spectroscopy. ma-PEG<sub>5000</sub>-Lumf was determined to have a Lumf loading of 8.69 µg/mg conjugate. The drug loading was however not enhanced for da-PEG<sub>1500</sub> despite its lower molecular weight and two available binding sites, where a Lumf loading of 8.82 µg/mg conjugate was determined (Table 3.1).

Table 3.1: Drug content of polymer-Lumf conjugates determined by UV/Vis analysis at 335 nm.

Sample	Absorbance 335 nm	Drug loading ( $\mu\text{g}$ )
ma-PEG <sub>5000</sub> -Lumf (1 mg/mL)	0.35	8.69
da-PEG <sub>1500</sub> -Lumf (10 eqv mol reaction)	0.69	923.14
PNAM (no coupling reagent)	0.35	N/A
PNAM-Lumf 24 eqv reaction	0.70	34.63
PNAM-Lumf 2 eqv reaction	0.90	605.81

The drug loading of PNAM-Lumf conjugate was similarly determined by UV/Vis spectroscopy. The UV/Vis analysis of the PNAM-Lumf conjugate was complicated by the low absorption of the unmodified PNAM at the wavelength of 335 nm deemed to be specific to Lumf (Figure 3.1, Figure 3.2 and Figure 3.3). To mitigate this challenge, the free PNAM and the PNAM-Lumf conjugate were prepared separately in buffer (pH 7.4) at 1.00 mg/mL each. The absorbance value for the unmodified PNAM at 335 nm was subtracted from that of the PNAM-Lumf at the same wavelength and the resultant drug loading was determined to be 27.81  $\mu\text{g}/\text{mg}$  of conjugate (Table 3.1).

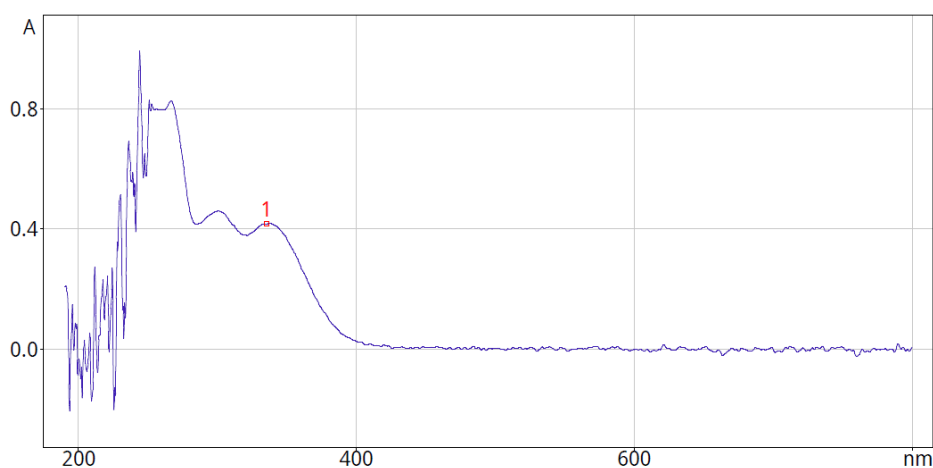


Figure 3.1: Absorbance spectra of Lumf dissolved in ethyl acetate (25  $\mu\text{g}/\text{mL}$ ) and measured in a glass cuvette. (1) Absorbance value measured at 335 nm.

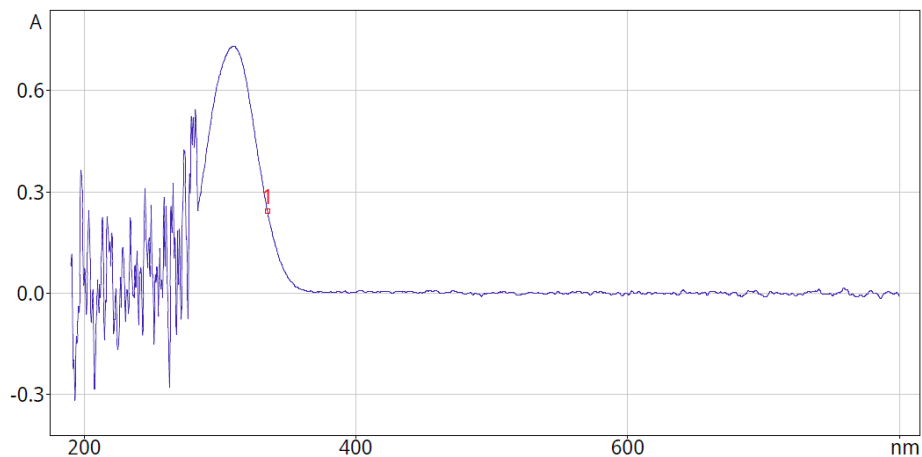


Figure 3.2: Absorbance spectrum of PNAM dissolved in 1.0 M phosphate buffer (1 mg/mL).  
(1) Absorbance measured at 335 nm.

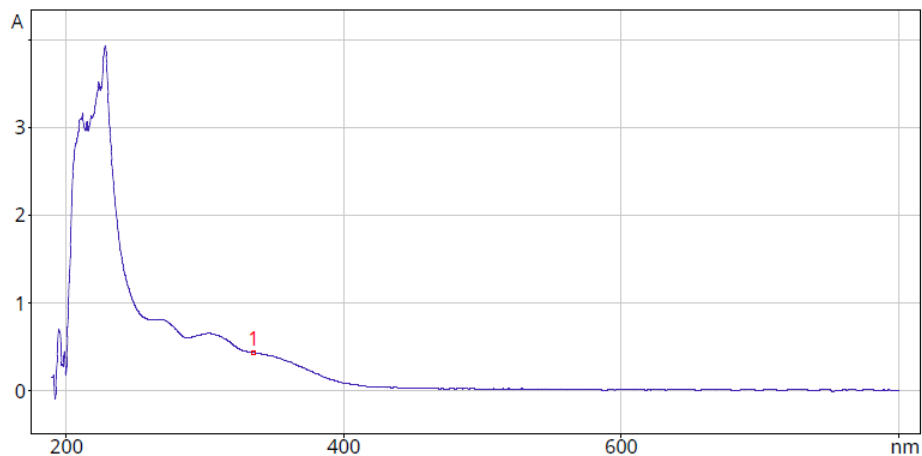


Figure 3.3: Absorbance spectra of PNAM-Lumf conjugate dissolved in 1.0 M phosphate buffer.  
(1) absorbance measured at 335 nm.

This drug loading of 27.81  $\mu\text{g}$  was determined on equivalent mass w/v concentration for the conjugate and the free polymer. To compensate for the UV absorption of PNAM when determining the drug loading of the conjugate, a stock solution of PNAM was prepared in  $\text{dH}_2\text{O}$  and diluted to 0.10 mg/mL, 0.25 mg/mL, 0.50 mg/mL and 1.00 mg/mL before being analysed by UV/Vis (Figure 3.4). The increase in absorbance seen for the conjugate in Figure 3.3 can be attributed to the Lumf chemically linked to the PNAM polymer.

### UV/Vis analysis of PNAM

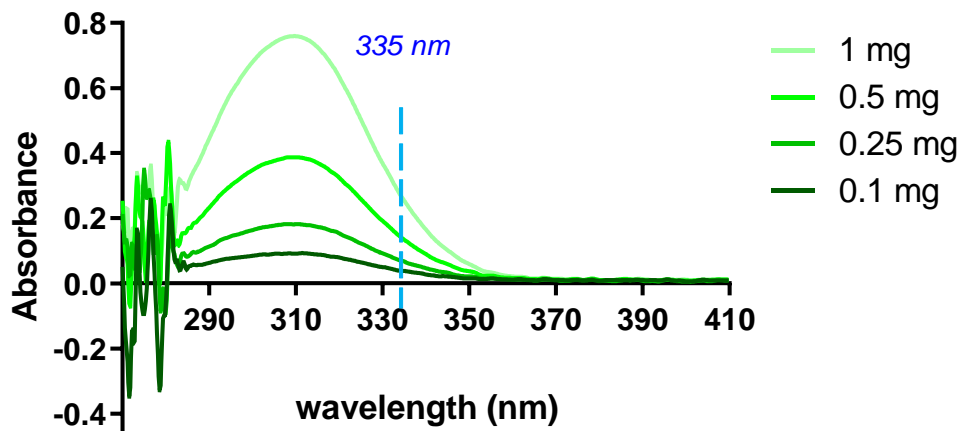


Figure 3.4: UV/Vis analysis of free PNAM.

Two reactions were conducted in which an eqv mass of PNAM was reacted with equal mol eqv of Lumf (2.0 mol eqv), in the presence (PNAM-Lumf-Y) and absence (PNAM-Lumf-O) of a coupling reagent. The experiments were conducted in anhydrous DMF for 48 hours in the dark. After the 48-hour period, the DMF reaction mixtures were diluted with water, frozen and subsequently freeze dried. To the dry materials, an equal volume of water was added and stirred to obtain yellow-coloured solutions. These solutions were then centrifuged at 10 000  $\times$   $g$  and the supernatants withdrawn for UV/Vis analysis at wavelength 335 nm (Table 3.2). After conducting a background scan of just water, the UV/Vis absorbance reading taken at wavelength 335 nm for PNAM-Lumf-O was 3.69. The UV absorbance reading for PNAM-Lumf-Y was 3.85. These solutions were then diluted by a factor of 10 to obtain absorbance readings of 0.39 for PNAM-Lumf-O and 2.84 for PNAM-Lumf-Y. Lumf was also stirred in DMF for a period of 48 hours, however dry material by lyophilization could not be obtained. To mitigate this experimental shortfall, Lumf (16.30 mg) was added to 10 mL dH<sub>2</sub>O and stirred for a period of 2 hours at 35 °C. The suspension of Lumf was centrifuged at 10 000  $\times$   $g$  for 30 min (5 °C) and the supernatant withdrawn for UV/Vis analysis. An absorbance reading of 0.01 was obtained at 335 nm for the Lumf supernatant.



Table 3.2: UV/Vis absorbance results for PNAM and Lumf.

Sample	Dilution factor	Absorbance 335 nm
Lumf	N/A	0.010
PNAM-Lumf-O	10x	0.39
PNAM-Lumf-Y	10x	2.84

#### *Drug aqueous solubility*

Conjugation of a lipophilic pendant molecule to a hydrophilic polymer increases its aqueous solubility due to the higher solubility and molecular weight of the polymer. The increase in solubility of Lumf resulting from conjugation to PEG and PNAM was determined by UV analysis of the supernatant of a centrifuged sample of the polymer-Lumf conjugate.

The difference in the absorbance readings between PNAM-Lumf-Y and PNAM-Lumf-O could in this instance be solely attributed to the chemically linked Lumf onto the PNAM polymer in aqueous solution. This meant that the solubility of Lumf was enhanced by 2450 times, compared to Lumf in water at the concentrations tested.

Similarly, a saturated solution of ma-PEG<sub>5000</sub>-Lumf (100 mg/ml of PBS pH 7.4) was centrifuged at 10 000 x g and the supernatant withdrawn for UV/Vis analysis. The solubility was shown to be enhanced by 4000 times compared to the maximum solubility of 3.09 ng/mL reported for Lumf. This was shown to be further improved to 6500 times for the da-PEG<sub>1500</sub>-Lumf conjugate.

#### *Drug release*

The polymer-Lumf conjugates were all designed to have an acid-labile ester bond between the polymer and the conjugated Lumf. The Lumf release profile was investigated in a buffered aqueous solution at pH 5.5 which mimics the pH of the intracellular endolysosomal vesicle where degradation of the conjugate is expected to occur after uptake.<sup>64</sup> The pH of the *Plasmodium* parasite food vacuoles are also reported to be in this range.<sup>65</sup>

The drug release profile of the ma-PEG<sub>5000</sub>-Lumf was evaluated. The conjugate prepared in buffer (pH 5.5) was incubated at 37 °C and the samples collected at different time points in triplicate for individual periods up to five days and subsequently stored at -80 °C. The frozen samples were then freeze dried to obtain dry powder materials. These materials were then

reconstituted with ethyl acetate and passed through normal phase silica SPE columns to obtain fine, yellow-coloured crystals after evaporating the solvent. The crystals were then resolubilised using acetonitrile (0.1% formic acid) and analysed by HPLC for drug quantification. The drug release profile was erratic particularly for samples collected within the first 24 hours (Figure 3.5). This Lumf release profile was observed up to Day 5. The Lumf appeared to elute at three different retention times of 3.8 min, 21.5 min and 23.8 min. The same batch of samples were re-analysed and yielded an identical erratic release profile.

### Lumf release from ma-PEG<sub>5000</sub>-Lumf

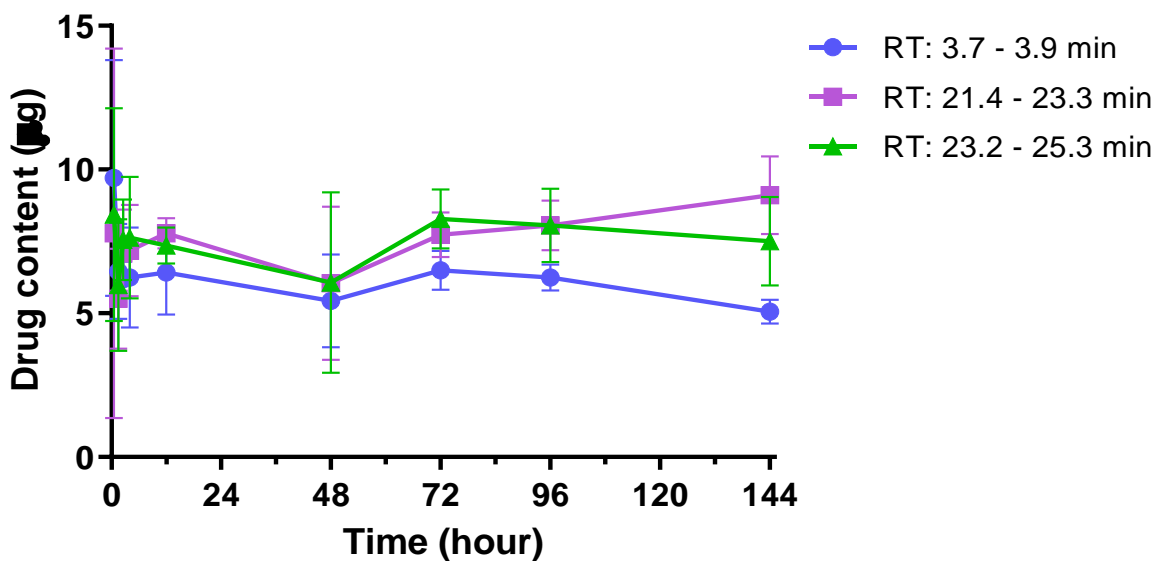


Figure 3.5: Total Lumf release from ma-PEG<sub>5000</sub>-Lumf at pH 5.5 (37 °C) conducted at different incubation times extending over a five-day period.

After obtaining an erratic drug release kinetics, an experiment was conducted to investigate the percent recovery of Lumf from a silica column. A stock solution of Lumf (1 mg/mL in ethyl acetate) was freshly prepared and diluted to 5 µg/mL, 10 µg/mL, 15 µg/mL, 20 µg/mL, and 25 µg/mL. The standard samples were eluted through 1 cm length normal phase silica columns and analysed by UV/Vis at 335 nm. Less than 50% of drug was recovered from 10 µg/mL to 25 µg/mL samples and the 5 µg/mL sample had a significantly large standard deviation for its recovery (Figure 3.6).

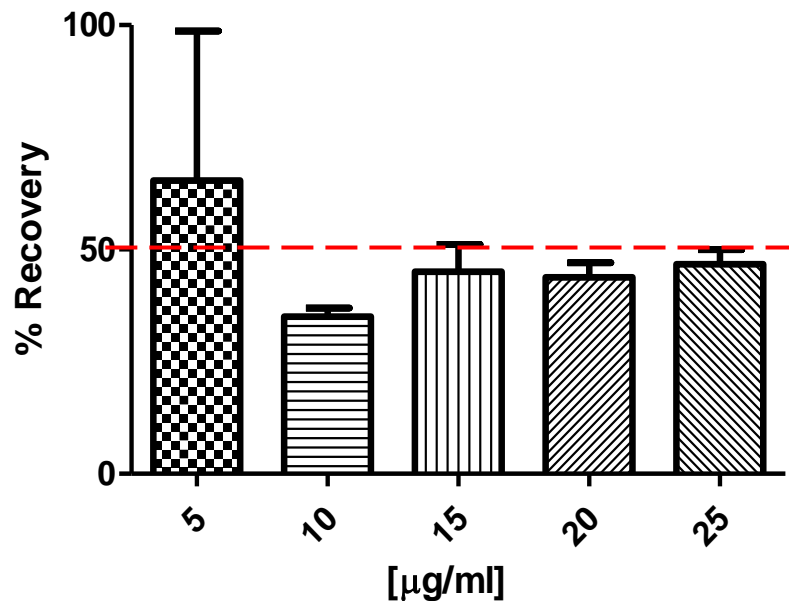


Figure 3.6: Lumf drug recovered from a small silica column when concentrations of 5 µg/mL to 25 µg/mL Lumf (1.0 mL volume) dissolved in ethyl acetate were passed through the column. n = 3.

#### *Hydrodynamic properties of polymer-Lumf conjugates*

The polymer-Lumf conjugates were prepared in aqueous solutions (pH 7.4) and measured for their particle size and surface charge (Figure 3.7). Analyses for the PEG and PNAM conjugates were conducted using refractive index of 1.46 and 1.51, respectively.<sup>65,66</sup> The particle size of ma-PEG<sub>5000</sub>-Lumf was recorded as  $161.9 \pm 1.45$  d.nm with a surface charge of  $0.719 \pm 1.62$  mV (PDI:  $0.046 \pm 0.02$ ). This particle size was over double the size compared to da-PEG<sub>1500</sub>-Lumf with average diameter of  $63.63 \pm 0.54$  d.nm with a surface charge of  $-8.83 \pm 1.42$  mV (PDI:  $0.092 \pm 0.004$ ). The particle size of the PNAM-Lumf conjugate was shown to be spread into two populations which were both larger than the da-PEG-Lumf conjugate with an average diameter of  $191.0 \pm 8.42$  nm with a surface charge of  $-8.98 \pm 0.047$  mV (PDI:  $0.286 \pm 0.03$ ).

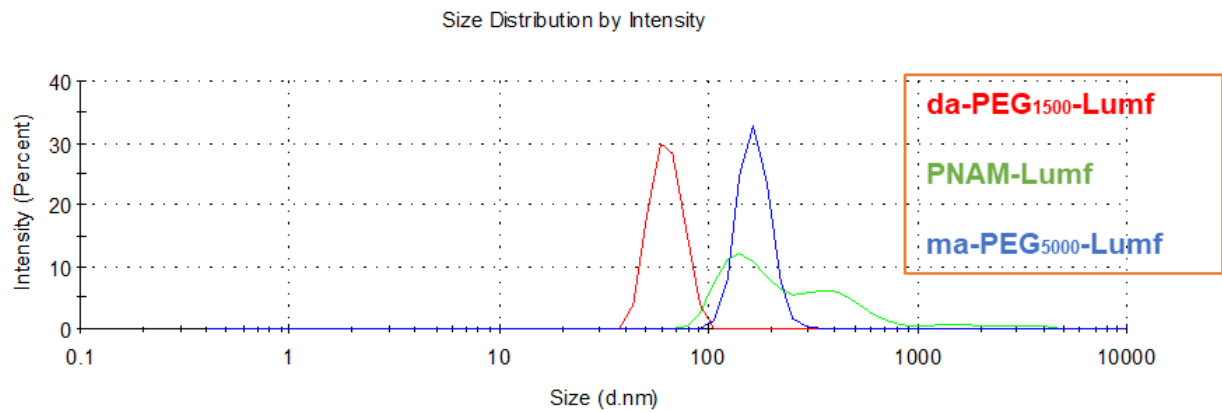


Figure 3.7: Hydrodynamic properties of polymer-Lumf conjugates.

## Conclusion

The conjugation of Lumf to PEG and PNAM showed to enhance the drug's aqueous solubility by more than 4 orders of magnitude. The percent drug loading achieved was comparable across all the polymers used. The PEG polymers of molecular weight 5.00 kDa and 1.5 kDa were less than 1%, approximately a third of the drug loading achieved for PNAM (2.78%). PNAM, however, is over three-times the molecular weight of PEG and is a multivalent polymer. The particle size distribution for PEG-Lumf conjugates were narrower compared to that the PNAM-Lumf. This can be attributed to the sizes of the polymers. PEG, unlike the PNAM used in this study, is amongst the widely used carrier materials in nanomedicine, appreciated so for its biocompatibility and being readily available commercially. The ma-PEG<sub>5000</sub>-Lumf was thus selected to be investigated further for its *in vitro* biological properties discussed in the proceeding Chapter 04.

## 4. Chapter Four: *In vitro* biological analyses of polymer-lumefantrine conjugates

### Introduction

*In vitro* biological assessment of compounds is another important screening step in the process of developing any therapeutic. Compounds which provide significant activity against model pathogens with little to no cytotoxic effect to mammalian cells, can be taken forward for further development. This chapter will discuss the cultivation of *Plasmodium* parasites and their subsequent use in determining the *in vitro* antiplasmodial activity of the ma-PEG<sub>5000</sub>-Lumf. This will be followed by the investigation of the RBC toxicity of ma-PEG<sub>5000</sub>-Lumf conjugate, which is an important marker of a potential acute toxicity risk of an IV therapeutic. A challenge encountered during this stage of the research was the limited availability of culture media reagents due to a global supply shortage as well as difficulty in obtaining whole blood from the SANBS due to the COVID-19 pandemic. This meant that not all conjugates could be tested.

#### *Cultivation of Plasmodium parasites and antiplasmodial testing*

Chloroquine-sensitive *P. falciparum* strains 3D7 and NF54 are commonly used in cultivating the asexual stage of the and can be relatively easily differentiated to form the sexual stage of the parasite.<sup>67,68</sup> The intra-erythrocytic trophozoite stage of the parasite life cycle is the most susceptible developmental stage where Lumf can exert its antiplasmodial activity. Trophozoites are the most active stage of the parasite life cycle by virtue of the endocytoses of large quantities of haemoglobin that is digested within the parasite vacuole.<sup>64,69</sup> The parasitaemia level within the culture is determined by counting the number of trophozoite infected RBCs against the total number of infected and uninfected RBCs observed by microscopy (Table 4.1, Figure 4.1). Counts from several areas of a smear of the cultures are averaged to obtain a percent (%) parasitaemia level within culture using the Equation 1.<sup>70</sup>

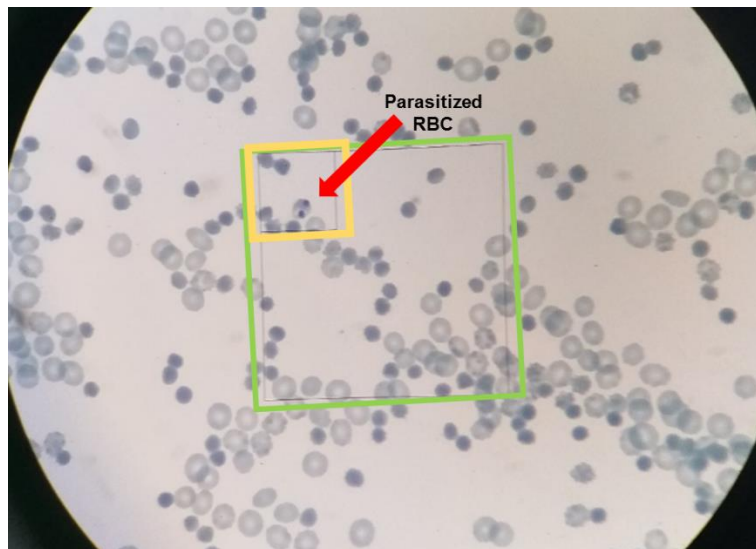


Figure 4.1: Bright field microscopy image of Giemsa-stained pRBCs. Infected and uninfected RBCs are observed in the yellow and green square grid. The yellow and green grids are used to determine the parasitaemia level. Infected RBCs are counted only within the green grid.

Table 4.1: Calculation of the percentage parasitaemia during the cultivation process.

<b>Parasitaemia count:</b>											
Count	1	2	3	4	5	6	7	8	9	10	Total
RBC	10	10	7	8	9	7	6	8	9	7	81
Parasite	3	2	1	1	2	2	2	1	2	1	17

$$\text{Equation 1 - \%Parasitaemia} = \frac{\text{Infected RBCs in large square}}{9 \times \text{Total RBC in small square}} \times 100\%$$

### *Haemolysis activity*

RBCs are amongst the simplest structured cells of the mammalian species. These small cells have no nucleus or DNA with a simple biconcave discoid structure filled mainly of haemoglobin enclosed by a lipid-bilayer membrane decorated with integral and surface proteins which are essential to maintaining the cell's morphology and cellular functions.<sup>71,72</sup> The cell membrane is relatively fragile despite being highly flexible, and alters cell shape and form due to many physiological conditions like osmolarity, pH, electrostatic effects and changed surface interactions with ions, lipids or drugs. The membrane fragility can result in disruption of the RBC, referred to as haemolysis, which leads to structural changes and irreversible loss of the cell's viability and critical cellular functions such as O<sub>2</sub>/CO<sub>2</sub> transport. Although haemolysis affects the RBCs ability to "host" the *Plasmodium* parasite during parasite differentiation and

maturation, this is a condition that compromises the general health of the host. For this reason, testing the potential haemolytic activity of the synthetic water-soluble polymer-Lumf conjugates can provide valuable insight into the Lumf conjugate's consideration for parenteral administration.

### *Cytotoxicity assessment of polymer-Lumf conjugates*

The African green monkey kidney *Chlorocebus sp.* (Vero) cells and human colon (Caco-2) cells served as model mammalian cells to which the cytotoxic effects of the polymer-Lumf conjugates were investigated. The Vero cells are immortal non-human kidney epithelial cells which are used widely for toxicity screening of a variety of compounds. Caco-2 cells are immortalized human colorectal adenocarcinoma cells used typically in the toxicity screening of a myriad of different compounds. Caco-2 cells are attractive for their cultivation properties as it spontaneously differentiates into a monolayer of cells with properties typical of that of normal enterocytes. Half maximal cytotoxicity (LC<sub>50</sub>, mg/mL) studies completed at the Onderstepoort Veterinary Institute of the University of Pretoria, were conducted using the 3-(4,5-dimethylthiazol-2-yl)-2,5-diphenyl-2 H-tetrazolium bromide (MTT) assay with minor volume adaptations.<sup>73,74</sup>

## **Materials and Methods**

Glucose ( $\geq 99.5\%$ ), hypoxanthine ( $\geq 99\%$ ), gentamycin solution (50 mg/ml in deionized water, BioReagent), sodium chloride (NaCl,  $\geq 99\%$ ), sodium hydroxide (NaOH,  $\geq 98\%$ ), triton x-100 (laboratory grade), L-lactate ( $\geq 98\%$ ), Trizma base ( $\geq 99.9\%$ ), acetylpyridine adenine dinucleotide (APAD,  $\geq 85\%$ ), nitrotetrazolium blue chloride (NBT,  $\geq 90\%$ ), phenazine ethosulphate (PES,  $\geq 95\%$ ) and Giemsa stain solution were all purchased from either Sigma-Aldrich Ltd (RSA) or CRD Chemicals Pty Ltd (South Africa). Special gas mixture (5% CO<sub>2</sub>, 5% O<sub>2</sub>, 90% N<sub>2</sub>) were purchased from African Oxygen Ltd (South Africa). 3D7 and NF54 *Plasmodium* parasite strains were purchased from the American Type Culture Collection organization (ATCC®, United States of America). The Lonza RPMI culture media was purchased from Whitehead Scientific Pty Ltd (South Africa). Serum and whole blood were purchased from the Interstate Blood Bank Inc. (United States of America) and the South African National Blood Services (South Africa) respectively. Biological studies were conducted in biosafety level (BSL) two cabinets which were sterilized using 70% ethanol and UV-light before and after experimental procedures. Where applicable, laboratory consumables used within the biosafety cabinet were sterilized at 120 °C for 21 min and by spraying with 70%

ethanol. The minimum essential medium (MEM) and Dulbecco's Modified Eagle's Medium (DMEM) were obtained from Highveld Biological (South Africa). Foetal calf serum was obtained from Adcock-Ingram (South Africa). Gentamycin was purchased from Virbac (South Africa). Non-essential amino acids were purchased from BioWhittaker (USA). The African green monkey (Vero) cells and Human colon (Caco-2, ATCC HTB 37) cells were both obtained from the American Type Culture Collection organization (ATCC, USA). Dimethyl sulfoxide (DMSO,  $\geq 99.9\%$ ), penicillin ( $\geq 99.9\%$ ), streptomycin ( $\geq 99.9\%$ ), 3-(4,5-dimethylthiazol)-2,5-diphenyl tetrazolium bromide (MTT,  $\geq 99.0\%$ ) and phosphate buffered saline (PBS, 1.0 M) were purchased from Sigma-Aldrich (RSA).

Absorbance readings of the multiwell plate were measured at 620 nm using a Tecan Infinite F500 spectrophotometer plate reader (Tecan, Switzerland). Absorbance readings for the cytotoxicity assessments were measured at 570 nm using a BioTek Synergy microplate reader (USA).

#### *Plasmodium parasite cultivation*

The standard operating procedures (SOPs) for the cultivation of two laboratory strains of the *P. falciparum* parasites and the pLDH assay were obtained with permission from the CSIR's Next Generation Health (NextGenHealth) Pharmacology group. All the experimental procedures were conducted aseptically, adhering to the use of standard personal protective equipment (PPE) and adopting standard sterile cell culture laboratory practices. This includes conducting all biological preparations and experiments within a biosafety laminar flow cabinet where applicable, and the disinfection of the cabinet interior and relevant laboratory consumables and equipment with 70% ethanol solution.

#### *Preparation of culture media and red blood cells*

Hypoxanthine (44 mg) dissolved in sodium hydroxide (1 N NaOH, 1 mL) and Gentamycin (0.450 mL, 50 mg/mL) were added under continuous stirring to 20 mL of sterile RPMI 1640 media aliquoted from a 500 mL stock and transferred into a sterile 50 mL centrifuge tube. Whole blood was centrifuged at 500 x g for 5 min to obtain pelleted RBC and plasma. The plasma was withdrawn, filter sterilized and added aseptically to the remaining RPMI 1640 media. This was mixed thoroughly to obtain a homogenous mixture of complete media, which was stored at 4 °C until used.



Whole blood obtained from the South African National Blood Services (SANBS) was gently mixed and aliquoted into sterile 50 mL centrifuge tubes. The whole blood was centrifuged at 500 x g for 5 min and the plasma withdrawn and dispensed into a clean sterile 50 mL tube. The pelleted RBCs were then washed three times using RPMI 1640 media by centrifugation at 500 x g for 5 min with the supernatant removed with each wash. The pelleted RBCs were resuspended in RPMI media at a ratio of 1:1 and stored at 4 °C for period of up to 4 weeks.

#### *Thawing of cryopreserved infected RBCs*

Thawing solutions were prepared as follows: A stock solution of NaCl (12% w/v) was prepared in a 50 mL centrifuged tube (Solution A). Solution A was then diluted to obtain a 1.8% w/v NaCl (10 mL) labelled Solution B. A volume of 750 µL of Solution A was spiked with 2 mg glucose and diluted to 0.9% NaCl w/v by diluting to 10 mL using dH<sub>2</sub>O which was mixed thoroughly and labelled Solution C.

Cryopreserved tubes containing RBCs infected with *P. falciparum* (NF54, chloroquine sensitive) parasites were obtain from the Next Generation Health Research Group (CSIR). A cryotube (2 mL) containing frozen parasite infected RBCs (pRBCs) was thawed using a warm water bath of 37 °C and transferred into a sterile 50 mL conical tube. Solution A (0.4 mL) was added dropwise to the pRBCs under constant swirling and allowed to stand for 5 min. Thereafter, Solution B (10 mL) was added dropwise under constant swirling and was subsequently centrifuged at 500 x g for 5 min. The supernatant was removed and the pelleted pRBCs were treated with Solution C (10 mL) under constant swirling. This suspension was allowed to stand for 5 min before centrifugation at 500 x g for 5 min. The supernatant was once again removed and complete media (20 mL) was added to the pelleted pRBCs under constant swirling before been centrifuged at 500 x g for 5 min. Thereafter, supernatant was removed and 100 µL fresh uninfected RBCs (uRBCs) added (prepared as described in the previous section) followed by 20 mL complete media prewarmed to 37 °C. This suspension of pRBCs was transferred to a T75 culture flask, gassed using a special gas mixture of 5% CO<sub>2</sub>, 5% O<sub>2</sub> 90% N<sub>2</sub> blown through an autoclaved glass Pasteur Pipette with cotton wool plug. The culture was sealed quickly and mixed gently then incubated at 37 °C for 48 hours.

#### *Cultivation and routine maintenance of parasitaemia*

Proceeding from the incubation of pRBCs, cultures were maintained every 48 hours as per standard procedure as follows: The culture media was carefully removed from the layer of pRBCs using sterile glass Pasteur pipette connected to a vacuum pump. This was conducted

with care to not agitate the flask or aspirate the layer of pRBCs. A few drops of the pRBCs were then deposited onto two microscope slides and a thick and thin smear made using another glass slide. The smears were air dried for 10 min and the cells fixed onto the glass slide with methanol for a period of 30 seconds. Thereafter, the methanol was left to air dry and residual solvent droplets carefully blotted off using blotting paper. Giemsa stain purchased from Sigma-Aldrich as a concentrated solution, was diluted 10x using water before it were deposited onto the layer of pRBC cells and left to stain for 5 min at room temperature. The excess stain was then washed off using water, the residual water blotted off and then dried using a heat-gun. The slide was then viewed under bright-field microscopy using a 100x oil-immersed objective lens to assess stage of parasite development and percentage parasitaemia. After investigating the level of parasitaemia, fresh complete media (30 mL) was added to the T75 culture flask, mixed gently, before being gassed with the special gas mixture and be kept at 37 °C for a 48-hour incubation period.

#### *In vitro antiplasmodial screening*

Parasitaemia levels were determined from a Giemsa-stained microscope slide where the total cells were viewed and counted within the vision grid of the microscope lens. The parasites and RBCs (both infected and uninfected) were counted from 10 random grids across the slide. The percent (%) parasitaemia was determined using the following formula:

$$\% \text{ Parasitaemia} = \frac{\text{Infected RBC in large square}}{9 \times \text{RBCs in small square}} \times 100\%$$

A parasitaemia level of 4.9% was often achieved. This was diluted to a 2% parasitaemia level prepared in complete media as follows: Volume pRBC = 2/%P x 200 µL; Volume of uRBC = 200 µL – Volume of pRBC. A fresh solution of 2% uninfected RBCs was prepared separately. A volume of 100 µl of pRBCs suspension was dispensed into wells of a 96-well microtiter plate. Stock solutions (1 mg/mL) of ma-PEG<sub>5000</sub>-Lumf, ma-PEG<sub>5000</sub>, chloroquine (CQ) and primaquine (PQ) were all prepared in dH<sub>2</sub>O. A stock solution (20 mg/mL) of lumefantrine (Lumf) was prepared in DMSO. The stock solutions were diluted to 2 µg/mL, 10 µg/mL and 20 µg/mL test sample concentrations using complete culture media. The test samples were then added to the pRBCs in the 96-well plate in triplicates to obtain a final in-well concentration of 1 µg/mL, 5 µg/mL and 10 µg/mL. The plate was then placed into a sealable plastic container, gassed using the special gas mixture for 2 min and incubated at 37 °C for 48 hours.

### *Plate development and spectrophotometric analysis*

Malstat and nitroblue tetrazolium salt/ phenazine ethosulphate (NBT/PES) solutions used for the development of the microtiter plate were prepared as follows: Triton X-100 (400  $\mu$ L), L-lactate (4 g), trizma base (1.32 g, Tris buffer) and acetylpyridine adenine dinucleotide (APAD, 22 mg) were added to 200 mL of water and stirred to obtain a homogenous mixture labelled as Malstat solution. Nitroblue tetrazolium salt (160 mg) and phenazine ethosulphate (8 mg) were added to 100 mL of water and stirred to obtain a homogenous mixture labelled as NBT/PES solution. The flask containing NBT/PES solution was covered with foil paper as the reagent mixture is sensitive to light. This was stored at 4 °C.

Following the 48-hour incubation period of the microtiter plate, the cells within the wells on the plate were re-suspended by pipetting action using a multichannel pipette. Malstat solution (100  $\mu$ l) was added to the wells of a new microtiter plate. The cultured RBCs were resuspended using a pipette and 20  $\mu$ L then added to the corresponding Malstat solution wells and mixed gently by pipetting action. Addition of 25  $\mu$ L NBT/PES solution to the wells containing pRBCs and Malstat solution was conducted in the dark. Air bubbles were removed gently using a hot-air gun. Thereafter, colour development of the plate was conducted in the dark for 35 min. The absorbance readings of the plate were measured at 620 nm using a Tecan Infinite F500 plate reader spectrophotometer.

### *Haemolytic activity*

Whole blood obtain from the South African National Blood Services (SANBS) was centrifuged at 300 x g for 10 min to pellet the red blood cells (RBCs) from the plasma solution. The plasma was withdrawn and dispensed into a separate conical tube. The pelleted RBCs were washed three times with PBS (pH 7.4), using six times the volume of pelleted RBCs, by centrifugation at 300 x g for 10 min. A 2% RBC suspension was prepared in the phosphate buffer (pH 7.4) solution and stored at 4 °C. Stock solutions of ma-PEG<sub>5000</sub>-Lumf (4.00 mg/mL drug eqv), chloroquine (CQ, 4.0 mg/mL) and primaquine (PQ, 4.0 mg/mL) prepared in PBS (pH 7.4), were all diluted to obtain 0.10 mg/mL, 0.25 mg/mL, 0.50 mg/mL and 1.00 mg/mL sample concentrations for each test compound. Each test sample was added in triplicate to 2% RBC suspension in glass vials at a volume ratio of 4:1 (compound: RBC suspension) and incubated at 37 °C for 4 hours. After the incubation period, the samples were centrifuged at 300 x g at room temperature and an aliquot of the supernatants withdrawn (1 mL) for haemoglobin content analysis by UV/Vis spectrophotometry at wavelength 570 nm. Triton X-100 (1% v/v) was used as the positive control causing 100% haemolysis and PBS (pH 7.4) as the negative control. The percent (%) haemolytic activity was determined as follows:

$$\% \text{ Haemolytic activity} = \frac{\Delta \text{ Absorbance [Test compound]}}{\Delta \text{ Absorbance [100\% haemolytic agent]}} \times 100\%$$

### *Cytotoxicity assessment of polymer-Lumf conjugates*

The Vero cells were maintained in minimal essential medium (MEM) supplemented with 5% foetal calf serum and 0.1% gentamicin maintained in a 5% CO<sub>2</sub> incubator. The Caco-2 cells were grown in Dulbecco's Modified Eagle's Medium (DMEM) supplemented with 10% foetal calf plasma, 1% non-essential amino acids and 1% penicillin-streptomycin at 10,000 U/mL and 10 mg/mL streptomycin, respectively, maintained in a 5% CO<sub>2</sub> incubator.

Cell suspensions were prepared from 70-80% confluent monolayer cultures and plated at a density of  $5 \times 10^4$  cells into each well of sterile flat-bottomed 96-well microtiter cell culture plates. The plates were incubated for 24 hours at 37 °C in a 5% CO<sub>2</sub> incubator before exposure to the polymer-Lumf conjugates, the polymer and drug controls. The Lumf and doxorubicin were prepared in DMSO. The free polymer and polymer-Lumf conjugates were prepared in water. The stock solutions for each compound were diluted to obtain 5.0 µg/mL, 10.0 µg/mL, 12.5 µg/mL, 25.0 µg/mL, 50.0 µg/mL, 100.0 µg/mL and 200.0 µg/mL sample concentrations for each compound and added to the cells in quadruplicates to incubate for 48 hours. The assay was repeated twice (n = 8). Doxorubicin and DMSO served as positive and negative controls, respectively. After 48-hour incubation period, the wells were rinsed twice with 200 µL of PBS and 200 µL of fresh medium was dispensed into the wells. A volume of 30 µL of MTT (5.00 mg/mL) solution dissolved in PBS was added to each well and the plates were incubated for a further 4-hour at 37 °C. Thereafter, the medium from within the wells were discarded before adding 50 µL of 100% DMSO into the wells and shaking for 1 hour to dissolve the formazan crystals which were formed. The absorbance was measured using a BioTek Synergy microplate reader at a wavelength of 570 nm. The resulting equation from the log concentration versus absorbance was used to calculate the LD<sub>50</sub> concentrations (concentration causing 50% lethality of the model mammalian cells).

## Results and discussion

### *Cultivation of P. falciparum parasites*

To cultivate the parasite cells, a standard operating procedure was followed to maintain asexual stage of the *P. falciparum* parasite. This stage of the parasite life cycle is where Lumf exerts its antimalarial activity by disrupting the conversion of haem to hemozoin, during the digestion of the haemoglobin by the parasite within the RBC.

The parasite cultivation experiments were initiated by thawing two cryopreserved vials containing 3D7 and NF54 *P. falciparum* strain infected and were cultivated and monitored as per SOP. The 3D7 cell line culture produced no viable levels of parasitaemia after several cycles of cultivation and was subsequently discarded.

### *Cultivation of NF54 P. falciparum for antiplasmodial testing*

The cultivation of the NF54 *P. falciparum* strain showed noticeably better parasite proliferation. The first cultivation procedure saw a parasitaemia level of 2.3%, which was sufficient to explore the antiplasmodial activity of the polymer-Lumf conjugate (Table 4.2).

Table 4.2: Calculation of parasitaemia levels – first cultivation.

<b>Parasitaemia count:</b>											
Count	1	2	3	4	5	6	7	8	9	10	Total
RBC	10	10	7	8	9	7	6	8	9	7	81
Parasite	3	2	1	1	2	2	2	1	2	1	17

$$\begin{aligned}
 \%Parasitaemia &= \frac{\text{Infected RBCs in large square}}{9 \times \text{Total RBC in small square}} \times 100\% \\
 &= \frac{17}{9 \times 81} \times 100\% \\
 &= \mathbf{2.3\%}
 \end{aligned}$$

The cultivation procedure was conducted once more by seeding another cryopreserved vial of the NF54 *P. falciparum* cell line and monitored as per standard protocol. After conducting sequential routine cultivation steps, a parasitaemia level of 4.9% was achieved without synchronization and was subsequently used for antiplasmodial activity testing of the ma-PEG<sub>5000</sub>-Lumf conjugate (Table 4.3).

Table 4.3: Calculation of parasitaemia levels – second cultivation.

<b>Parasitaemia count:</b>											
Count	1	2	3	4	5	6	7	8	9	10	Total
RBC	6	7	9	8	5	7	6	5	6	4	63
Parasite	3	2	5	5	2	5	2	4	2	3	28

$$\begin{aligned}
 \%Parasitaemia &= \frac{\text{Infected RBCs}}{9 \times \text{Total RBC}} \times 100\% \\
 &= \frac{28}{9 \times 63} \times 100\% \\
 &= \mathbf{4.9\%}
 \end{aligned}$$

#### *Antiplasmodium activity of ma-PEG<sub>5000</sub>-Lumf conjugate*

An activity screening experiment was conducted to assess the antiplasmodial activity of ma-PEG<sub>5000</sub>-Lumf conjugate compared to free Lumf. Stock solutions of 1 mg/mL drug eqv for ma-PEG<sub>5000</sub>-Lumf and chloroquine were prepared in dH<sub>2</sub>O, and Lumf dissolved in DMSO. The unmodified polymer was also prepared at a concentration of 1 mg/mL in dH<sub>2</sub>O. Each of the stock solutions were diluted in triplicate to 2.0 µg/mL, 10 µg/mL and 20.0 µg/mL using complete culture media. The parasite culture containing a parasitaemia level of 4.9% was then diluted to 2% parasitaemia level as per standard protocol. The diluted parasite culture was then aliquoted into a 96-well plate. Each sample of test compound was then added to the parasite culture to a 1:1 ratio of parasitaemia culture to obtain a final in-well drug concentration of 1.0 µg/mL, 5.0 µg/mL, and 10.0 µg/mL (Figure 4.2). The plate was placed in a sealable container, thereafter, gassed with the special gas mixture, sealed, and incubated for a period of 48 hours at 37 °C.

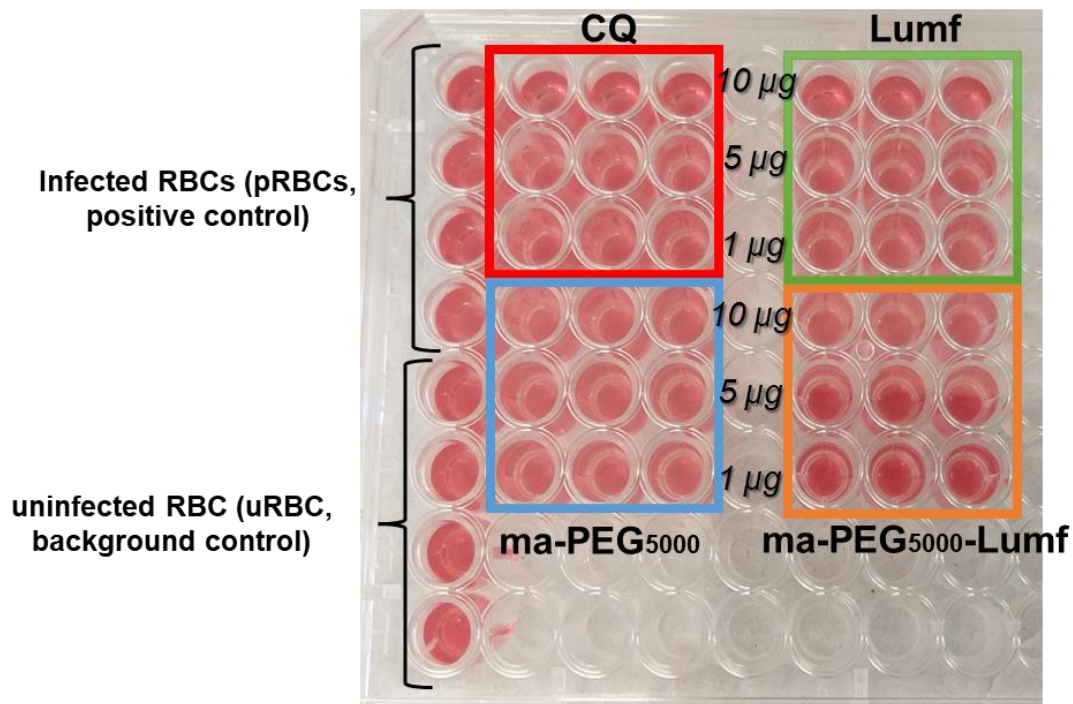


Figure 4.2: Plate layout for the antiplasmodial activity screening of ma-PEG<sub>5000</sub>-Lumf compared to lumefantrine (Lumf), chloroquine (CQ, positive control) and ma-PEG<sub>5000</sub>. Infected RBCs (pRBCs) and uninfected RBCs (uRBCs) served as controls. n = 3, ±SD.

After the 48-hour incubation period, the plate was removed and prepared for colour development by re-suspending the cultures gently to obtain a homogeneous mixture. Malstat solution was dispensed into a separate clean 96 well microtitre plate, aliquots of the incubated cultures were added to the equivalent wells followed by the addition of NBT/PES solution. The process of adding NBT/PES to the culture mixture was conducted in the dark as the NBT/PES solution is light sensitive. The absorbance was measured at time points 5 min, 10 min, 15 min and 25 min using a Tecan Infinite F500 spectrophotometer at wavelength 620 nm. No significant differences in the absorbance were seen at these time points for the uRBCs, pRBCs and the treated pRBCs samples. Adequate differences in the absorbance readings were only achieved after 35 min of the plate development in the dark. The results were analysed using Graphpad Prism 5 software for Windows (Graphpad Software, USA, [www.graphpad.com](http://www.graphpad.com)) to obtain the percent (%) parasite viability as measured by the parasite's lactate dehydrogenase activity (pLDH) (Figure 4.3).

## Antiplasmodial activity of polymer-lumefantrine conjugate

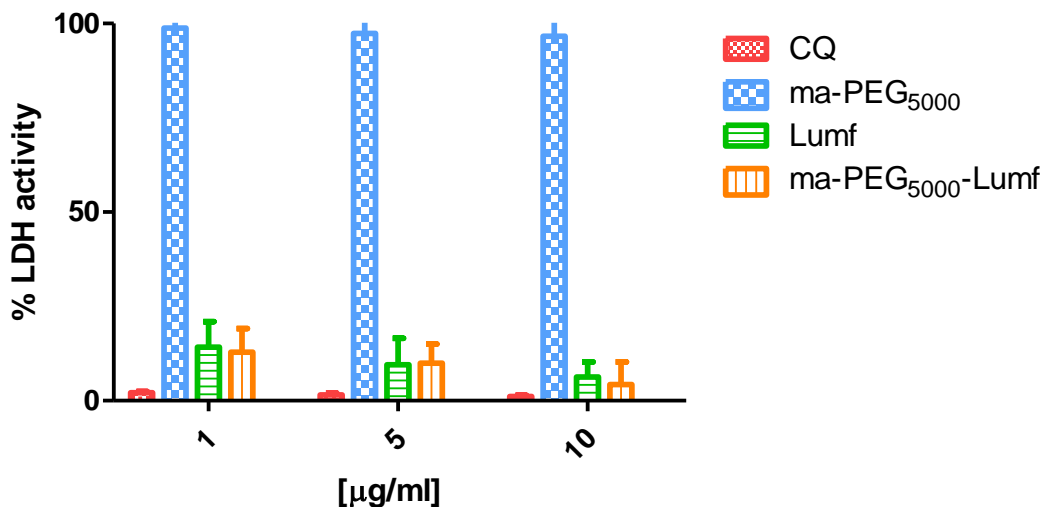


Figure 4.3: Antiplasmodial activity of ma-PEG<sub>5000</sub>-Lumf at concentrations of 1 µg/mL, 5 µg/mL and 10 µg/mL of the Lumf drug from the conjugate. n = 3, ±SD.

The antiplasmodial pLDH activity of ma-PEG<sub>5000</sub>-Lumf was shown to be  $12.8 \pm 6.3\%$ ,  $10.0 \pm 5.1\%$  and  $4.3 \pm 6.0\%$  of the untreated control activity at 1 µg/mL, 5 µg/mL and 10 µg/mL drug concentrations. This level of activity was comparable to that of unconjugated Lumf;  $14.2 \pm 6.8\%$ ,  $9.5 \pm 7.0\%$  and  $6.3 \pm 4.0\%$  at the same drug concentrations. The activity levels seen for CQ that was used as the positive control was expected as this was tested against a CQ-sensitive *P. falciparum* strain. The polymer carrier material, ma-PEG<sub>5000</sub> showed no antiplasmodial activity across any of the concentrations tested as the percentage pLDH activity was maintained at 100% relative to the untreated control. The testing of hydrophobic drugs such as Lumf, require preparation of the compounds in organic solvents as DMSO or ethanol at solvent concentrations that needed to be diluted to below 1% v/v to maintain cell viability of the RBCs used as host for the parasites. This process is significantly altered by having a water-soluble polymer-Lumf conjugate which would be easily prepared in aqueous medium to the desired concentrations for *in vitro* biological testing.

Although comparable antiplasmodial activity is seen for ma-PEG<sub>5000</sub>-Lumf, the mechanism in which the conjugate exerts its activity is still unknown, i.e whether the drug is released within the microenvironment of the parasite, or the conjugate behaves as the active drug. Infected RBCs undergo morphological changes to their membrane which is essential to the survival of the *Plasmodium* parasite.<sup>75,76</sup> These changes occur as microscopic channels, referred to as “new permeability pathways” (NPPs), of approximately 50-80 nm in diameter which allows the



'free' exchange of low-molecular-weight solutes required by the parasite to mature.<sup>77,78</sup> Although these channels present a feasible route through which the water-soluble polymer-Lumf conjugates can diffuse at particle sizes of below 80 d.nm, further investigation would be required to substantiate this hypothesis.

### *Haemolytic activity*

The enhanced solubility seen for the ma-PEG<sub>5000</sub>-Lumf conjugate could potentially allow the conjugated drug to be considered for IV administration. The clinical presentation of the disease is mainly associated with the erythrocytic stage of the parasite life cycle where it matures within RBCs in circulation. The polymer-Lumf conjugate may cause RBC lysis when introduced into the circulatory system through IV administration and was investigated for potential haemolytic activity towards healthy uninfected RBCs. A 4.00 mg/mL polymer-Lumf concentration was prepared in phosphate buffer saline (1.0 M, pH 7.4) then further diluted to 100.0 µg/mL, 250.0 µg/mL, 500.0 µg/mL and 1000 µg/mL (Figure 4.4). The samples were added to a 2% RBC suspension at a ratio of 4:1 for the test compounds to the RBC suspension and then incubated for 4 hours at 37 °C. After the 4-hour incubation period, the cell suspensions were centrifuged, and the supernatants withdrawn for haemoglobin concentration analysis. PQ, for its known haemolytic activity although generally used for assays with parasite infected cells, served as a positive control. The haemolysis results were expressed as % haemoglobin release (Figure 4.5).

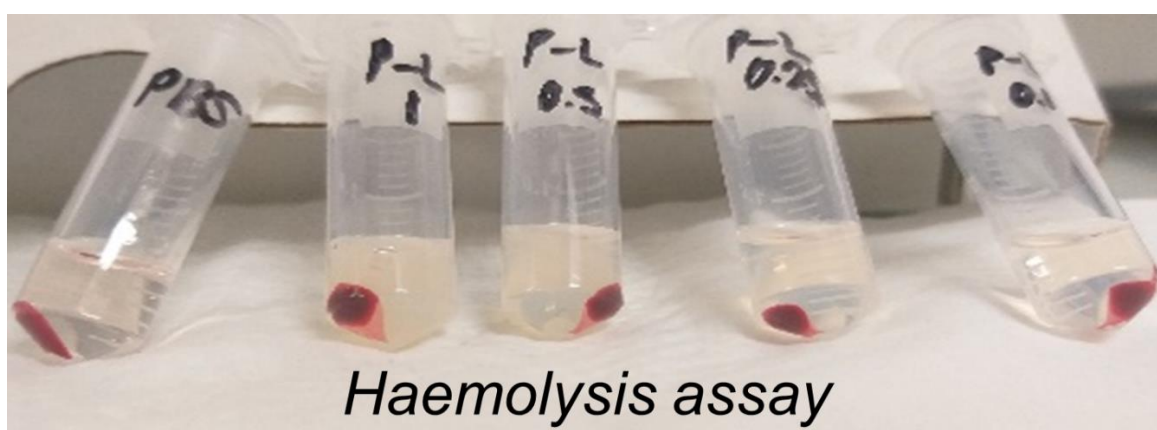


Figure 4.4: Actual haemolysis samples for ma-PEG<sub>5000</sub>-Lumf conjugate after centrifugation step for subsequent haemoglobin analysis.

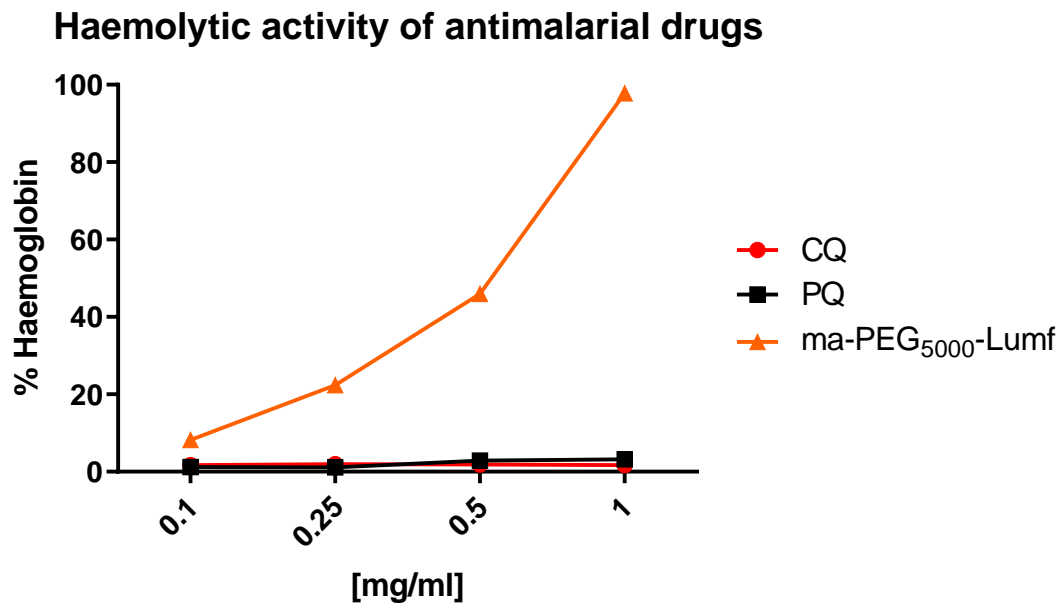


Figure 4.5: Haemolytic activity of ma-PEG<sub>5000</sub>-Lumf.

ma-PEG<sub>5000</sub>-Lumf's haemolytic activity was shown to be less than 10% at a drug concentration of 100 µg/mL. This was substantially higher compared to PQ, which served as the positive control, with haemolytic activity of less than 4% at a drug equivalent concentration. This relatively high haemolytic activity of the conjugate may be as a result of the low drug loading achieved for ma-PEG<sub>5000</sub>-Lumf (1% drug loading). The drug concentrations needed to conduct the haemolytic testing would require a considerable amount of conjugate to be dissolved in the aqueous medium. This can be seen as a relatively cloudy appearance in Figure 4.4 particularly for the higher concentrations of the test samples. Although PEGs of this molecular weight size are generally considered to be non-cytotoxic, concentration-dependant cellular toxicities have been shown, despite the very low drug loading achieved for ma-PEG<sub>5000</sub>-Lumf.<sup>61,79</sup>

#### *Cytotoxicity assessment of polymer-Lumf conjugates*

LC<sub>50</sub> studies were conducted for ma-PEG<sub>5000</sub>-Lumf against Vero and Caco-2 cells (Table 4.4). Doxorubicin which served as the positive cytotoxic drug control, was 50% lethal to Vero cells at a concentration of 12.0 ± 4.0 µg/mL and 30.0 ± 6.0 µg/mL to Caco-2 cells. Greater than 50% cell viability was observed for ma-PEG<sub>5000</sub>-Lumf conjugate, the free polymer, and the free drug, up to a concentration of 200 µg/mL. The chemical modification of Lumf with succinic acid greatly influenced the toxic profile of Lumf-Suc derivative. The LC<sub>50</sub> of Lumf-Suc to Vero cells

was observed at a concentration of  $20.0 \pm 0.5 \mu\text{g/mL}$  and  $50.0 \pm 0.5 \mu\text{g/mL}$  to Caco-2 cells. This toxicity profile for Lumf-Suc can be linked to the acid functionality introduced onto the aminoquinolone-drug, as conversion to the salt form of the drug could have significantly reduced the cytotoxicity. However, Lumf-Suc is an intermediary product from the synthetic process and is less likely to be released from the polymer as a drug-linker unit, due to the less cleavable amide bond between the linker and the polymer, describe in Scheme 2.5.

Table 4.4: Half maximal cytotoxicity ( $LC_{50}$ , mg/mL) of ma-PEG<sub>5000</sub>-Lumf and control tested against Vero and Caco-2 cells.

Compound	VERO		Caco-2	
	MEAN (mg/mL)	SD	MEAN	SD
<b>Doxorubicin</b>	0.012	0.004	0.03	0.006
<b>Lumf</b>	>0.2	NA	>0.2	NA
<b>Lumf-Suc</b>	0.02	0.0005	0.05	0.0005
<b>PEG<sub>5000</sub></b>	>0.2	N/A	>0.2	N/A
<b>ma-PEG<sub>5000</sub>-Lumf</b>	>0.2	N/A	>0.2	N/A

## Conclusion

The cultivation of the *Plasmodium* parasites to acceptable parasitaemia levels requires routine management of the culture's environment which include its haematocrit and nutrient composition. This is to maintain the cellular integrity of both the host cell and the environment for ideal proliferation of the parasite. A parasitaemia culture to conduct antiplasmodial testing was obtained with NF54 *Plasmodium* parasite strain. The ma-PEG<sub>5000</sub>-Lumf showed to have similar antiplasmodial activity compared to the free Lumf at equivalent drug concentrations. The mechanism by which this antiplasmodial activity is afforded by the conjugate is currently unknown. However, the proposed accessibility of the conjugate to the parasite through the NPP's of the infected RBCs presents a plausible entry point which warrants further investigation. At low pH, the Lumf drug is expected to be released from the polymer-linker unit to exert its antiplasmodial activity. The observed antimalarial activity coupled with the relatively non-toxic profile of the conjugate to RBCs and mammalian cells, provide a promising antimalarial polymer-Lumf conjugate which can improve current treatment strategies.

## 5. Chapter Five: Final Conclusion

Malaria remains a public health threat despite the interventions that have been deployed to help curb its infectiousness. Like many WHO-listed neglected diseases, malaria prevalence has been largely attributed to the lack of major technological advancements which can contribute to major breakthroughs in treatment strategies. Although the latest data shows that the worse-case scenario projected by the WHO – a doubling in malaria deaths for sub-Saharan African – was avoided, a significant increase in both incidences and deaths were reported for the 2020-2021 period compared to the previous year.<sup>80</sup>

The treatment of malaria spans at least 300 years since the prescription of the bark of the “*cinchona*” tree used to treat patients suffering from “*intermittent fever*”, now known to be malaria, before the synthetic production of anti-malarial drugs from the 1920s.<sup>81</sup> The current gold standard treatment for uncomplicated malaria recommended by WHO, comprises of at least two drugs for a comprehensive treatment strategy. The standard treatment however needs large doses of the chemotherapy to be administered coupled with the requirement of a fatty-meal intake to achieve adequate drug absorption to reach therapeutic blood-plasma concentrations.

The disease can progress further to severe or complicated malaria, mainly affecting child-bearing women and children aged  $\leq 5$  years. The treatment option in such cases requires an initial IV administration of water-soluble artesunate, followed by a standard 3-day oral ACT course. This two-part treatment regimen goes against WHO’s firm principle of a combination therapy and can influence patient-adherence to the full course, and further increase the likelihood of drug resistance and disease recrudescence to occur. Currently, the need to develop a suitable water-soluble partner drug to the already commercially available artesunate as an IV-administered combination therapy, is yet to be seen clinically.

This project proposed to synthesize, characterize, and investigate the antiparasmodial and cytotoxicity of a water-soluble polymer-lumefantrine conjugate. The first objective to achieve this was to conjugate lumefantrine to a water-soluble polymeric carrier. PEG and a synthetic polymer, PNAM, were investigated as probable carriers for Lumf. Physicochemical characterization of these PEG-Lumf and PNAM-Lumf conjugates supported the successful synthesis of a water-soluble polymer-lumefantrine conjugate, of which the conjugate’s water-solubility by improved by up to 6500x. Further investigation of polymer-Lumf conjugate’s antiparasmodial activity, tested against a CQ-sensitive *P. falciparum* parasite strain, showed to be active, comparably so to the free Lumf. This suggests the chemical linkage of Lumf to a

water-soluble polymer had little to no effect on the antimalarial activity of the drug. The polymer-Lumf conjugate(s) also showed no overt cytotoxicity tested against Vero and Caco-2 cell lines.

The enhanced aqueous solubility of Lumf conjugated to water-soluble polymer, could be considered as a candidate for IV-administration, especially as the clinical presentation of the disease are linked to the erythrocytic stage of the parasite life cycle. The enhanced properties of the polymer-Lumf conjugate presents as a promising chemotherapeutic to partner the already commercially available water-soluble antimalarial drug, artesunate. This probable water-soluble combination therapy would adhere to WHO's firm principle to treating malaria to achieve enhanced efficacy while combatting drug resistance, and the ultimate goal of reducing disease prevalence.

## References

1. World Health Organization. World malaria report 2020: 20 years of global progress and challenges. 2020.
2. Caulfield LE, Richard SA, Black RE. Undernutrition as an underlying cause of malaria morbidity and mortality in children less than five years old. *The American Journal of Tropical Medicine and Hygiene*. 2004;71(2\_suppl):55-63.
3. Rogerson SJ, Hviid L, Duffy PE, Leke RF, Taylor DW. Malaria in pregnancy: Pathogenesis and immunity. *The Lancet Infectious Diseases*. 2007;7(2):105-17.
4. Antinori S, Galimberti L, Milazzo L, Corbellino M. Biology of human malaria plasmodia including plasmodium knowlesi. *Mediterranean Journal of Hematology and Infectious Diseases*. 2012;4(1).
5. Crawley J, Chu C, Mtove G, Nosten F. Malaria in children. *The Lancet*. 2010;375(9724):1468-81.
6. Wassmer SC, Taylor TE, Rathod PK, Mishra SK, Mohanty S, Arevalo-Herrera M, et al. Investigating the pathogenesis of severe malaria: A multidisciplinary and cross-geographical approach. *The American journal of tropical medicine and hygiene*. 2015;93(3\_Suppl):42-56.
7. Cowman AF, Healer J, Marapana D, Marsh K. Malaria: Biology and disease. *Cell*. 2016;167(3):610-24.
8. Grobusch M, Kremsner P. Uncomplicated malaria. *Malaria: Drugs, Disease and Post-genomic Biology*. 2005:81-104.
9. Trampuz A, Jereb M, Muzlovic I, Prabhu RM. Clinical review: Severe malaria. *Critical Care*. 2003;7(4):1-9.
10. Peter G, Manuel AL, Shetty A. Study comparing the clinical profile of complicated cases of plasmodium falciparum malaria among adults and children. *Asian Pacific Journal of Tropical Disease*. 2011;1(1):35-7.
11. Mishra S, Mohanty S, Mohanty A, Das B. Management of severe and complicated malaria. *Journal of Postgraduate Medicine*. 2006;52(4):281.
12. World Health Organization. Guidelines for the treatment of malaria: World Health Organization; 2015.
13. White NJ. Antimalarial drug resistance. *The Journal of Clinical Investigation*. 2004;113(8):1084-92.
14. Bosman A, Mendis KN. A major transition in malaria treatment: The adoption and deployment of artemisinin-based combination therapies. *The American Journal of Tropical Medicine and Hygiene*. 2007;77(6\_Suppl):193-7.
15. Okombo J, Chibale K. Recent updates in the discovery and development of novel antimalarial drug candidates. *Medicinal Chemistry Communications*. 2018;9(3):437-53.

16. Bloland PB, Ettlign M, Meek S. Combination therapy for malaria in africa: Hype or hope? *Bulletin of the World Health Organization*. 2000;78:1378-88.
17. Haldar K, Bhattacharjee S, Safeukui I. Drug resistance in plasmodium. *Nature Reviews Microbiology*. 2018;16(3):156-70.
18. White NJ, van Vugt M, Ezzet FD. Clinical pharmacokinetics and pharmacodynamics of artemether-lumefantrine. *Clinical Pharmacokinetics*. 1999;37(2):105-25.
19. Simpson JA, Agbenyega T, Barnes KI, Di Perri G, Folb P, Gomes M, et al. Population pharmacokinetics of artesunate and dihydroartemisinin following intra-rectal dosing of artesunate in malaria patients. *PLoS Medicine*. 2006;3(11):e444.
20. Hencken CP, Jones-Brando L, Bordón C, Stohler R, Mott BT, Yolken R, et al. Thiazole, oxadiazole, and carboxamide derivatives of artemisinin are highly selective and potent inhibitors of toxoplasma gondii. *Journal of Medicinal Chemistry*. 2010;53(9):3594-601.
21. Li Q, Weina P. Artesunate: The best drug in the treatment of severe and complicated malaria. *Pharmaceuticals*. 2010;3(7):2322-32.
22. Watsierah CA, Ouma C. Access to artemisinin-based combination therapy (act) and quinine in malaria holoendemic regions of western kenya. *Malaria Journal*. 2014;13(1):1-7.
23. Challenger JD, Bruxvoort K, Ghani AC, Okell LC. Assessing the impact of imperfect adherence to artemether-lumefantrine on malaria treatment outcomes using within-host modelling. *Nature Communications*. 2017;8(1):1-9.
24. Premji ZG. Coartem®: The journey to the clinic. *Malaria Journal*. 2009;8(1):1-6.
25. Borrmann S, Sallas WM, Machevo S, González R, Björkman A, Mårtensson A, et al. The effect of food consumption on lumefantrine bioavailability in african children receiving artemether–lumefantrine crushed or dispersible tablets (coartem®) for acute uncomplicated plasmodium falciparum malaria. *Tropical Medicine and International Health*. 2010;15(4):434-41.
26. Fule R, Meer T, Sav A, Amin P. Solubility and dissolution rate enhancement of lumefantrine using hot melt extrusion technology with physicochemical characterisation. *Journal of Pharmaceutical Investigation*. 2013;43(4):305-21.
27. Du Plessis LH, Govender K, Denti P, Wiesner L. In vivo efficacy and bioavailability of lumefantrine: Evaluating the application of pheroid technology. *European Journal of Pharmaceutics and Biopharmaceutics*. 2015;97:68-77.
28. Malaria SEAQA. Artesunate versus quinine for treatment of severe falciparum malaria: A randomised trial. *The Lancet*. 2005;366(9487):717-25.
29. Codd A, Teuscher F, Kyle DE, Cheng Q, Gatton ML. Artemisinin-induced parasite dormancy: A plausible mechanism for treatment failure. *Malaria Journal*. 2011;10(1):1-6.

30. Eldar-Boock A, Blau R, Ryppa C, Baabur-Cohen H, Many A, Vicent MJ, et al. Integrin-targeted nano-sized polymeric systems for paclitaxel conjugation: A comparative study. *Journal of Drug Targeting*. 2017;25(9-10):829-44.
31. Vicent MJ, Duncan R. Polymer conjugates: Nanosized medicines for treating cancer. *Trends in Biotechnology*. 2006;24(1):39-47.
32. Lomkova EA, Chytil P, Janoušková O, Mueller T, Lucas H, Filippov SK, et al. Biodegradable micellar hpma-based polymer–drug conjugates with betulinic acid for passive tumor targeting. *Biomacromolecules*. 2016;17(11):3493-507.
33. Schlupe T, Hwang J, Cheng J, Heidel JD, Bartlett DW, Hollister B, et al. Preclinical efficacy of the camptothecin-polymer conjugate it-101 in multiple cancer models. *Clinical Cancer Research*. 2006;12(5):1606-14.
34. Lv S, Tang Z, Zhang D, Song W, Li M, Lin J, et al. Well-defined polymer-drug conjugate engineered with redox and ph-sensitive release mechanism for efficient delivery of paclitaxel. *Journal of Controlled Release*. 2014;194:220-7.
35. Camacho KM, Kumar S, Menegatti S, Vogus DR, Anselmo AC, Mitragotri S. Synergistic antitumor activity of camptothecin–doxorubicin combinations and their conjugates with hyaluronic acid. *Journal of Controlled Release*. 2015;210:198-207.
36. McClements DJ. Encapsulation, protection, and delivery of bioactive proteins and peptides using nanoparticle and microparticle systems: A review. *Advances in Colloid and Interface Science*. 2018;253:1-22.
37. Prabhu P, Suryavanshi S, Pathak S, Sharma S, Patravale V. Artemether + lumefantrine nanostructured lipid carriers for oral malaria therapy: Enhanced efficacy at reduced dose and dosing frequency. *International Journal of Pharmaceutics*. 2016;511(1):473-87.
38. Larson N, Ghandehari H. Polymeric conjugates for drug delivery. *Chemistry of Materials*. 2012;24(5):840-53.
39. Natfji AA, Osborn HM, Greco F. Feasibility of polymer-drug conjugates for non-cancer applications. *Current Opinion in Colloid & Interface Science*. 2017;31:51-66.
40. Markovsky E, Baabur-Cohen H, Eldar-Boock A, Omer L, Tiram G, Ferber S, et al. Administration, distribution, metabolism and elimination of polymer therapeutics. *Journal of Controlled Release*. 2012;161(2):446-60.
41. Ringsdorf H, editor. Structure and properties of pharmacologically active polymers. *Journal of Polymer Science: Polymer Symposia*. 1975: Wiley Online Library.
42. Mvango S, Matshe WM, Balogun AO, Pilcher LA, Balogun MO. Nanomedicines for malaria chemotherapy: Encapsulation vs. Polymer therapeutics. *Pharmaceutical Research*. 2018;35(12):1-27.



43. Kumar S, Singh RK, Sharma R, Murthy R, Bhardwaj T. Design, synthesis and evaluation of antimalarial potential of polyphosphazene linked combination therapy of primaquine and dihydroartemisinin. *European Journal of Pharmaceutical Sciences*. 2015;66:123-37.
44. Fortuin L, Leshabane M, Pfukwa R, Coertzen D, Birkholtz L-M, Klumperman B. Facile route to targeted, biodegradable polymeric prodrugs for the delivery of combination therapy for malaria. *ACS Biomaterials Science & Engineering*. 2020;6(11):6217-27.
45. Khandare J, Minko T. Polymer–drug conjugates: Progress in polymeric prodrugs. *Progress in Polymer Science*. 2006;31(4):359-97.
46. Cammarata CR, Hughes ME, Ofner III CM. Carbodiimide induced cross-linking, ligand addition, and degradation in gelatin. *Molecular Pharmaceutics*. 2015;12(3):783-93.
47. Thorek DL, Elias eR, Tsourkas A. Comparative analysis of nanoparticle-antibody conjugations: Carbodiimide versus click chemistry. *Molecular Imaging*. 2009;8(4):7290.2009.00021.
48. Ho G-J, Emerson KM, Mathre DJ, Shuman RF, Grabowski EJ. Carbodiimide-mediated amide formation in a two-phase system. A high-yield and low-racemization procedure for peptide synthesis. *The Journal of Organic Chemistry*. 1995;60(11):3569-70.
49. Ferry AI, Malik GI, Guinchard X, Větvička Vc, Crich D. Synthesis and evaluation of di- and trimeric hydroxylamine-based  $\beta$ -(1 $\rightarrow$ 3)-glucan mimetics. *Journal of the American Chemical Society*. 2014;136(42):14852-7.
50. Parrott MC, Finniss M, Luft JC, Pandya A, Gullapalli A, Napier ME, et al. Incorporation and controlled release of silyl ether prodrugs from print nanoparticles. *Journal of the American Chemical Society*. 2012;134(18):7978-82.
51. Chu KS, Finniss MC, Schorzman AN, Kuijter JL, Luft JC, Bowerman CJ, et al. Particle replication in nonwetting templates nanoparticles with tumor selective alkyl silyl ether docetaxel prodrug reduces toxicity. *Nano Letters*. 2014;14(3):1472-6.
52. Kawai F. Microbial degradation of polyethers. *Applied Microbiology and Biotechnology*. 2002;58(1):30-8.
53. Cornella J, Zarate C, Martin R. Metal-catalyzed activation of ethers via C–O bond cleavage: A new strategy for molecular diversity. *Chemical Society Reviews*. 2014;43(23):8081-97.
54. Jasiukaitytė-Grojzdek E, Huš M, Grilc M, Likožar B. Acid-catalysed  $\alpha$ -o-4 aryl-ether bond cleavage in methanol/(aqueous) ethanol: Understanding depolymerisation of a lignin model compound during organosolv pretreatment. *Scientific Reports*. 2020;10(1):1-12.
55. Zhang S, Bryant DA. The tricarboxylic acid cycle in cyanobacteria. *Science*. 2011;334(6062):1551-3.

56. Buwalda SJ, Dijkstra PJ, Calucci L, Forte C, Feijen J. Influence of amide versus ester linkages on the properties of eight-armed peg-pla star block copolymer hydrogels. *Biomacromolecules*. 2010;11(1):224-32.
57. Snape TJ, Astles AM, Davies J. Understanding the chemical basis of drug stability and degradation. *Pharmaceutical Journal*. 2010;285(7622):416-7.
58. D'Souza AJM, Topp EM. Release from polymeric prodrugs: Linkages and their degradation. *Journal of Pharmaceutical Sciences*. 2004;93(8):1962-79.
59. Singer JW, De Vries P, Bhatt R, Tulinsky J, Klein P, Li C, et al. Conjugation of camptothecins to poly-(l-glutamic acid). *Annals of the New York Academy of Sciences*. 2000;922(1):136-50.
60. Rudmann DG, Alston JT, Hanson JC, Heidel S. High molecular weight polyethylene glycol cellular distribution and peg-associated cytoplasmic vacuolation is molecular weight dependent and does not require conjugation to proteins. *Toxicologic Pathology*. 2013;41(7):970-83.
61. Liu G, Li Y, Yang L, Wei Y, Wang X, Wang Z, et al. Cytotoxicity study of polyethylene glycol derivatives. *RSC Advances*. 2017;7(30):18252-9.
62. Nino-Pariente A, J Nebot V, J Vicent M. Relevant physicochemical descriptors of "soft nanomedicines" to bypass biological barriers. *Current Pharmaceutical Design*. 2016;22(9):1274-91.
63. Huang L, Lizak PS, Jayewardene AL, Marzan F, Lee M-NT, Aweeka FT. A modified method for determination of lumefantrine in human plasma by hplc-uv and combination of protein precipitation and solid-phase extraction: Application to a pharmacokinetic study. *Analytical Chemistry Insights - SAGE Journals*. 2010:5.
64. Bakar NA, Klonis N, Hanssen E, Chan C, Tilley L. Digestive-vacuole genesis and endocytic processes in the early intraerythrocytic stages of plasmodium falciparum. *Journal of Cell Science*. 2010;123(3):441-50.
65. Parmoon G, Mohammadi Nafchi A, Pirdashti M. Density, viscosity, refractive index and excess properties of binary and ternary solutions of poly (ethylene glycol), sulfate salts and water at 298.15 k. *Physical Chemistry Research*. 2019;7(4):859-84.
66. Basistyj V, Bukhtoyarova A, Vasil'ev E, Shelkovnikov V. Monomers with a high refraction index based on acryloyl derivatives of spirocyclic piperidin-4-one thioacetals. *Optics and Spectroscopy*. 2018;125(1):82-7.
67. Claessens A, Affara M, Assefa SA, Kwiatkowski DP, Conway DJ. Culture adaptation of malaria parasites selects for convergent loss-of-function mutants. *Scientific Reports*. 2017;7(1):1-8.

68. Ararat-Sarria M, Prado CC, Camargo M, Ospina LT, Camargo PA, Curtidor H, et al. Sexual forms obtained in a continuous in vitro cultured colombian strain of plasmodium falciparum (fcb2). *Malaria Journal*. 2020;19(1):1-13.
69. Tilley L, Dixon MW, Kirk K. The plasmodium falciparum-infected red blood cell. *The International Journal of Biochemistry & Cell Biology*. 2011;43(6):839-42.
70. Brecher G, Schneiderman M. A time-saving device for the counting of reticulocytes. *American Journal of Clinical Pathology*. 1950;20(11\_ts):1079-83.
71. Steck TL. The organization of proteins in the human red blood cell membrane: A review. *The Journal of Cell Biology*. 1974;62(1):1-19.
72. Smith AS, Nowak RB, Zhou S, Giannetto M, Gokhin DS, Papoin J, et al. Myosin iia interacts with the spectrin-actin membrane skeleton to control red blood cell membrane curvature and deformability. *Proceedings of the National Academy of Sciences*. 2018;115(19):E4377-E85.
73. Mosmann T. Rapid colorimetric assay for cellular growth and survival: Application to proliferation and cytotoxicity assays. *Journal of Immunological Methods*. 1983;65(1-2):55-63.
74. McGaw LJ, Van der Merwe D, Eloff J. In vitro anthelmintic, antibacterial and cytotoxic effects of extracts from plants used in south african ethnoveterinary medicine. *The Veterinary Journal*. 2007;173(2):366-72.
75. Cooke BM, Mohandas N, Coppel RL. The malaria-infected red blood cell: Structural and functional changes. *Advances in Parasitology*. 2001; 50: 1-86.
76. Moxon CA, Grau GE, Craig AG. Malaria: Modification of the red blood cell and consequences in the human host. *British Journal of Haematology*. 2011;154(6):670-9.
77. Goodyer ID, Pouvelle B, Schneider TG, Trelka DP, Taraschi TF. Characterization of macromolecular transport pathways in malaria-infected erythrocytes. *Molecular and Biochemical Parasitology*. 1997;87(1):13-28.
78. Biagini GA, Ward SA, Bray PG. Malaria parasite transporters as a drug-delivery strategy. *Trends in Parasitology*. 2005;21(7):299-301.
79. Webster R, Elliott V, Park BK, Walker D, Hankin M, Taupin P. Peg and peg conjugates toxicity: Towards an understanding of the toxicity of peg and its relevance to pegylated biologicals. *PEGylated Protein Drugs: Basic Science and Clinical Applications*. 2009:127-46.
80. World Health Organization. World malaria report 2021. 2021.
81. Dagen M. History of malaria and its treatment. *Antimalarial Agents*. 2020: 1-48.

# Appendix



Faculty of Health Sciences

**Institution:** The Research Ethics Committee, Faculty Health Sciences, University of Pretoria complies with ICH-GCP guidelines and has US Federal wide Assurance.

- FWA 00002567, Approved dd 22 May 2002 and Expires 03/20/2022.
- IORG #: IORG0001762 OMB No. 0990-0279 Approved for use through February 28, 2022 and Expires: 03/04/2023.

## Faculty of Health Sciences Research Ethics Committee

13 August 2021

### Approval Certificate Annual Renewal

Dear Mr WMR Matshe

**Ethics Reference No.:** 202/2019

**Title:** Synthesis, characterization & in vitro analyses of lumefantrine-based pharmacologically active polymer for the treatment of severe malaria

The Annual Renewal as supported by documents received between 2021-07-27 and 2021-08-11 for your research, was approved by the Faculty of Health Sciences Research Ethics Committee on 2021-08-11 as resolved by its quorate meeting.

Please note the following about your ethics approval:

- Renewal of ethics approval is valid for 1 year, subsequent annual renewal will become due on 2022-08-13.
- Please remember to use your protocol number (202/2019 ) on any documents or correspondence with the Research Ethics Committee regarding your research.
- Please note that the Research Ethics Committee may ask further questions, seek additional information, require further modification, monitor the conduct of your research, or suspend or withdraw ethics approval.

Ethics approval is subject to the following:

- The ethics approval is conditional on the research being conducted as stipulated by the details of all documents submitted to the Committee. In the event that a further need arises to change who the investigators are, the methods or any other aspect, such changes must be submitted as an Amendment for approval by the Committee.

We wish you the best with your research.

Yours sincerely

On behalf of the FHS REC, Dr R Sommers  
MBChB, MMed (Int), MPharmMed, PhD  
Deputy Chairperson of the Faculty of Health Sciences Research Ethics Committee, University of Pretoria

The Faculty of Health Sciences Research Ethics Committee complies with the SA National Act 61 of 2003 as it pertains to health research and the United States Code of Federal Regulations Title 46 and 46. This committee abides by the ethical norms and principles for research, established by the Declaration of Helsinki, the South African Medical Research Council Guidelines as well as the Guidelines for Ethical Research: Principles Structures and Processes, Second Edition 2016 (Department of Health)

Research Ethics Committee  
Room 4-60, Level 4, Tswelopele Building  
University of Pretoria, Private Bag x223  
Gauteng 0001, South Africa  
Tel +27 (0)12 350 3064  
Email: [daep@hsc.behaai@up.ac.za](mailto:daep@hsc.behaai@up.ac.za)  
[www.up.ac.za](http://www.up.ac.za)

Fakulteit Gesondheidswetenskap  
Lefaphala Disaense ka Maphelo



CSIR Research Ethics Committee  
PO Box 395 Pretoria 0001 South Africa  
Tel: +27 12 841 4060  
Fax: +27 12 841 2478  
Email: R&DEthics@csir.co.za

### Permission certificate

19 May 2020

Dear: William Matshe

Title: **Synthesis, characterization & *in vitro* analyses of lumefantrine-based pharmacologically active polymer for the treatment of severe malaria, (Ref: 308/2020).**

---

Thank you for your submission to the CSIR Research Ethics Committee's (REC). Your submission was reviewed electronically by the REC.

The CSIR REC duly notes the University of Pretoria REC's research ethics clearance certificate and grants permission for the study to proceed, subject to the following provisos:

- Even though no sensitive data or personal data of participants is being collected in the study, a short statement on how the integrity of the data will be protected should be provided;
- The PI is requested submit their signed and dated CV; and
- There is no statement on the conflicts of interest provided on the submission. The PI is requested to provide a conflict of interest statement.

Kindly note that you are required to submit **bi-annual progress reports** to the CSIR REC and a **final report** on completion of the research in which you indicate (i) that the research has been completed; (ii) if any new or unexpected ethical issues emerged during the course of the study; and if so, (iii) how these ethical issues were addressed.

We wish you all of the best with your research project.

Kind regards,



Prof David Jacobs  
CSIR REC Chair